ADDIS ABABA UNIVERSITY

COLLEGE OF TECHNOLOGY AND BUILT ENVIRONMENT (CTBE)

School of Electrical and Computer Engineering Master of Science in Power Engineering

Technical & Economical Evaluation of High Temperature Superconducting Cable in Ethiopian Power Grid

(Case Study: 132 kV Kaliti 1 to Black Lion Hospital Transmission Network)

By: Henok Zeberga Benti

Thesis Submitted to the School of Graduate Studies of Addis Ababa University in Partial Fulfillment of the Requirements for the Degree of Master of Science in Power Engineering

Thesis Advisor: Dr. -Ing. Getachew Biru

Jun.2025

Addis Ababa, Ethiopia

ADDIS ABABA UNIVERSITY COLLEGE OF TECHNOLOGY AND BUILT ENVIRONMENT

School of Electrical and Computer Engineering Master of Science in Power Engineering

Technical & Economical Evaluation of High Temperature Superconducting Cable in Ethiopian Grid System

(Case Study: 132 kV Kaliti I to Black Lion Line Transmission line in Addis Ababa Ethiopia)

By: Henok Zeberga Benti

APPROVED BY BOARD OF EXAMINERS

____

Chairman, Department of Graduate Committee — Signature

Getachew Biru (Dr.-Ing)

Advisor — Signature

____

Internal Examiner — Signature

____

External Examiner — Signature

DECLARATION

I, the undersigned, declare that this thesis is my original work and has not been presented before for fulfillment of a degree in this or any other institutions. Further, I have acknowledged all sources and materials used for this thesis work and have cited them in the reference section.

Name: Henok Zeberga   Signature: _________________

Place: Addis Ababa, Ethiopia

Date of submission: ______________.

This thesis work has been submitted for examination with my approval as a university advisor.

Dr.-Ing. Getachew Biru

Advisor's Name   Signature

ACKNOWLEDGMENT

I want to start my heartfelt gratitude from God in his invaluable support in any of my tasks.

The journey of completing this thesis was challenging and I could not have achieved this milestone without the encouragement, expertise, and resources provided by various individuals and organizations (EEP), Especially Mr.Doju Kebede.

Firstly, I would like to extend my deepest appreciation to my supervisor, Dr.-Ing. Getachew Biru, whose support, insightful feedback, and dedication in shaping the direction of my research.

Additionally, I owe special thanks to Mr.Teshome Wakijra co-supervisors, Mr.Ebsa Tesfa, Dr.Kasegn Tekletsadik and Mr.Amare Assefa who offered their time, knowledge, and assistance throughout the thesis.

Lastly, I want to thank my family and friends for their constant encouragement and moral support during this endeavor. Their belief in my abilities gave me the motivation to persevere through any challenges I encountered.

Once again, thank you to all those who contributed to the success of this MSc thesis, expressing my gratitude for the collective efforts and support.

ABSTRACT

In the last three decades, there have been big steps forward and improvements in the creation of prototype HTS cables. This breakthrough opened the door for the current research and development of HTS cables, which have the potential to revolutionize power transmission technology. The global energy sector is now leveraging superconductor technology to drive a major transformation.

Superconducting transmission lines conveniently solve contemporary power distribution. It has large power capacity, better controllability, and thermal independence. Its small outer dimension enables it to be installed in existing underground conduits causing little perturbation to urban electricity networks. By virtue of its low impedance, it also efficiently prevents overheating by diverting current from an overloaded transmission line into the SC cable.

The electric and magnetic field distributions in superconducting devices and the technical and commercial feasibility of HTS cables are investigated in this study. This indicates the reduction of power losses experienced with various scenarios, and the final verdict is that the exchange is technically feasible, but not economically since capital and operational cost payments lead to an absurd conclusion of 27 years for 132 kV and 43 years longer for 33 kV system. The possibility of replacing a 132 kV double-circuit overhead transmission line in Ethiopia's electrical grid with a 132 kV and a 33 kV $YBa_2Cu_3O_7$(YBCO)-based SC along Kalilti I to Black Lion line in Adis Ababa is discussed. Thus outlines the benefits in technology that HTS systems can offer in comparison to conventional lines, particularly in terms of performance, cost, and efficiency of operation.

The study uses advanced modeling software like MATLAB, ANSYS Fluent, and Dig SILENT Power Factory to evaluate the superconductivity and performance of HTS cables under different loading conditions. It reveals that HTS cables require fewer transformers, simplifying system design and enhancing efficiency.

At high demand, HTS power lines have brought unparalleled efficiency (99.35%) that account for a revolution in power transmission. Even at 125% capacity, efficiency holds steady with some minor losses. However, with these advantages, the capital and operating costs of it are still high. The advantages brought by the use of HTS technology-improved grid system, increased capacity, and sustainability-make it a strong contender for modern energy systems. Further development is required in cooling optimization and grid integration to exploit its full advantages, even though HTS technology can sets Ethiopia in a pole position of energy improvement and strongly consolidates the ground for future research and application endeavors.

Keywords: High-Temperature Superconductors (HTS), grid modernization, energy efficiency, cryogenic cooling, Ethiopia power grid, electromagnetic-thermal modeling.

Table of Contents

List of Figure

List of Table

List of Abbreviations

AC	Alternative current
BSCCO	Bismuth Strontium Calcium Copper Oxide
CB	Circuit breaker
CD	Cold Dielectric
CFRP	Carbon Fiber Reinforced Polymer
CLR	Current limiter resistor
DC	Direct current
EAPP	East African power pool
EEP	Ethiopia electric power
FEM	Finite element method
GERD	Grand Ethiopian Renaissance dam
HTS	High temperature superconductor
LIPA	Long Island Power Authority
LIWV	Lightning impulse withstand voltage
LN_2	Liquid Nitrogen
LTS	Low temperature superconductor
MgB_2	Magnesium diboride
MLI	Multilayer superinsulation
MRI	Magnetic Resonance Imaging magnesium diboride
NMR	Nuclear Magnetic Resonance
NR	Nitrile rubber
ODEs	Ordinary differential equations
PD	Partial discharging
PDIE	Partial Discharge Inception Electric field strength
PDIV	Partial discharge inception voltage
PPLP	Poly Propylene Laminated Paper
REBCO	Rare earth Barium Copper Oxide
RRRV	Rate rise of recovery
SC	Superconductor
Sc	Short circuit
SCTL	Superconducting Transmission Line
SiC	Silicon carbide
Tyvek	high-density polyethylene
WD	Warm Dielectric
XLPE	Cross-linked polyethylene insulation
YBCO	Yttrium, bismuth, strontium, copper and oxygen

Chapter One

1. Introduction

1.1 Background

The current issues of the electric power business in the twenty-first century need the development of intelligent energy systems that ensure high efficiency in the generation, transportation, and consumption of electricity. The development of power grid infrastructure and the creation of ring circuits of electric networks increases the complexity of power flow management in power systems and can lead to power system failure.

Power companies around the world are facing many challenges due to the rapid increase in power loads. World energy demand is predicted to increase by almost 50% in the 21st century compared to 2020, and by 2100 to more than triple. Inefficient power grids also lead to pollution, as most electricity in some developing countries is generated by burning coal. Currently, huge transmission burdens are reliant on aging and inadequate conventional power grids, and some developing and sparsely populated countries, particularly in Ethiopia, where adding new power cables is practically effortless due to unlimited underground space. The nature of traditional conductors makes it difficult to improve efficiency without pursuing innovative technology.

The adoption of a high-temperature superconducting cable line allows us to introduce a new regulated electrical connection that is free of these drawbacks. Most wealthy countries are starting and planning to replace the current power system with superior conducting materials that exhibit no resistance when cooled below critical temperatures.

To satisfy future power grid demands, including rising volumes of renewable energy, Ethiopia's current electricity grids need to be updated and expanded to increase flexibility and add new short and long-distance SC lines. From Africa, EAPP, the Grand Renaissance Dam (GERD) is Africa's largest hydroelectric power plant [41]. These and other thesis aim not only to serve their own countries but also to provide power to neighboring countries. However, most conductors used in modern power systems, such as generators, transformers, power lines, cables, and motors, are made of copper or aluminum and have much loss.

The maximum permissible temperature of the electrical insulator limits the transmission capacity of conventional wires. And they have resistance R, which limits the electrical system's thermal performance due to resistive losses.

Transmission line losses represent a considerable challenge to the capacity and economic efficiency of Ethiopia's electrical grid system. Research and various publications from EEU, agencies like Française de Développement (AFD) indicate that these losses can be substantial and give information on grid modernization projects.

Line losses in the Ethiopian grid system reveals a complex situation influenced by various factors. Key Factors are power generation sources are often geographically remote from load centers, Environmental Factors, infrastructure quality, poor maintenance and losses under contingency conditions (N-1 contingencies) revealing variations in losses when individual lines are out of service. Ongoing modernization efforts aim to address these issues and improve grid efficiency.

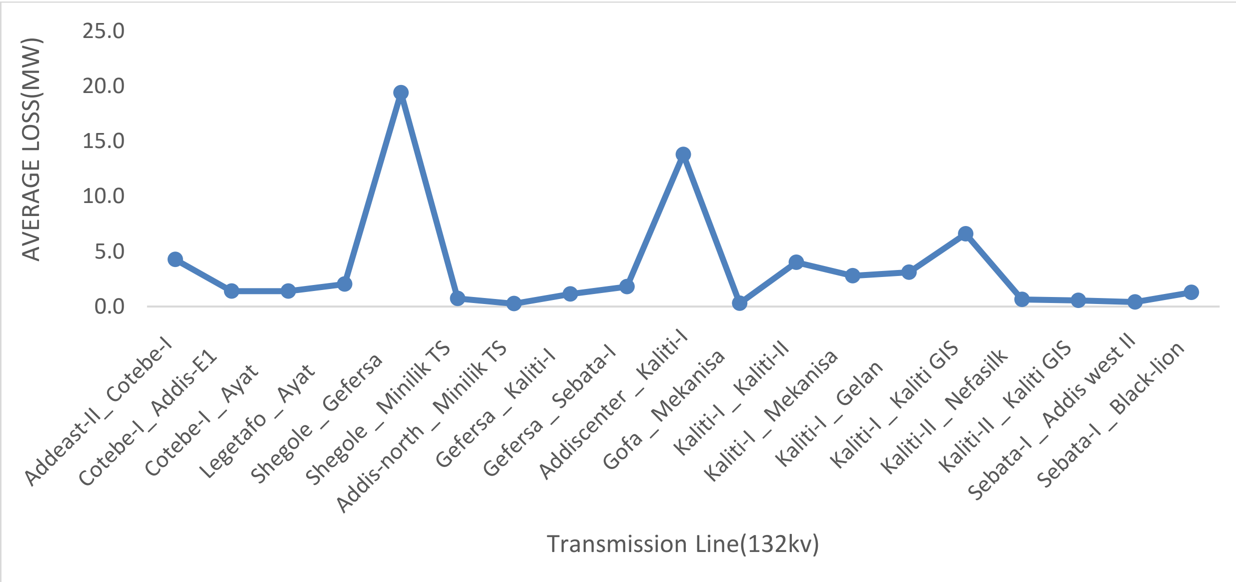

Figure 1.1: Transmission line loss in Ethiopian grid system for selected areas in Addis Ababa

This data set provides insights into the average power losses occurring on the 132 kV transmission line serving Addis Ababa. The data reflects the power lost during power transmission due to resistive losses in the conductors and other factors such as line length, load variation, and environmental conditions. Analyzing this data is critical for understanding the system's performance and identifying areas for improvement.

Addis Ababa, a major load center, receives power from various generation plants, whose transmission lines are affected by seasonal issues. The transmission grid, responsible for transmitting electricity from hydro, wind, solar, and thermal plants, reflects total electricity demand across sectors. Hydropower dominates the energy (over 90%) mix, with wind and solar power also contributing. Technical and non-technical losses remain a concern. Efficient grid management and modernization efforts are essential to minimize these losses.

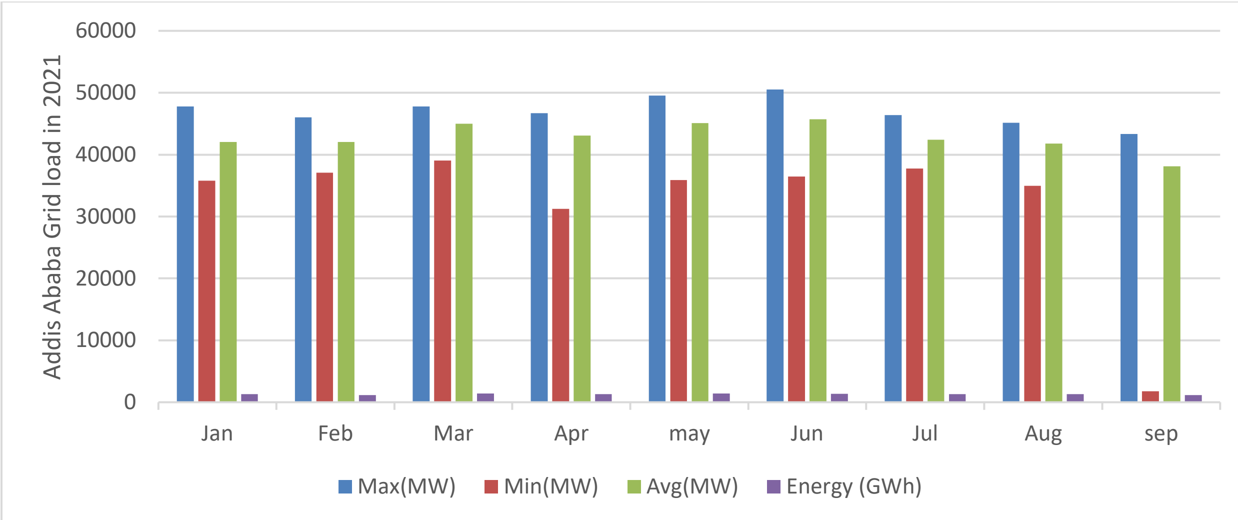

Figure 1.2: Ethiopian transmission line grid load per month in 2021

Addis serves as an important high-load center and faces challenges related to congestion, as well as opportunities for improvement in installation and maintenance practices. The existing power lines currently struggle to deliver or transport the optimal amount of electricity efficiently. Addressing these concerns presents a valuable opportunity to enhance the city's energy infrastructure, ensuring it meets the growing demands of its population and supports sustainable development.

A technology for improving energy efficiency, lossless power transport through superconducting cables, has been discussed for decades. However, the initial concept of using low-temperature superconductors was not competitive due to high cooling requirements. This situation has changed over the past two decades with the advent of commercially available high temperature superconductors. This superconductor has the advantage of requiring only liquid nitrogen for cooling.

Superconducting cables offer increased transmission capacity at current densities of 200 - 3000 A/mm2, compared to 1- 6 A/mm2 for traditional resistive power line wires. This high current density allows for compact designs and allows for as much current to be carried by a cable with a small diameter as a larger cable. Numerous projects have been demonstrated to show technology's technological viability [39].

Table 1.1: Current Density comparison of HTS and copper is based on realistic operating conditions

Type of Conductor	Current Density (A/mm²)
Copper (at 75°C)	~3 - 6 A/mm²
Aluminum (at 75°C)	~1 - 3 A/mm²
YBCO HTS (77 K)	~500 - 3,000 A/mm²
BSCCO HTS (77 K)	~200 - 1,500 A/mm²

1.2 Problem Statement

Ethiopia's electrical transmission lines result in an 5-20% power loss, highlighting the need for superconducting technology to minimize fault occurrences and enhance system capacity, with cost-effective materials accessible for research and production.

To address these challenges, the integration of superconducting transmission lines presents a promising solution and offers a possible option.

- HTS cable provides significant power capacity, reduced controllability, and thermal independence, which makes it a preferred option for engineers because of its compact size and substantial power capabilities.
- The HTS cable's compact design enables the installation of cables in current underground conduits, facilitating the disruption of the urban electricity transmission network.
- characterized by its low impedance, efficiently mitigates overheating by directing current from an overloaded transmission line into the SC cable.

A technical plan for superconducting cables that will replace a 132 kV double circuit line linking a 15.3 km from Kalilti I to Black Lion Line AC transmission line is assessed in this study.

1.3 Objectives

1.3.1 General Objectives

The general objective of this study is to conduct a technical and economic evaluation of implementing high-temperature superconducting transmission cables in the Ethiopian network, with a focus on the electrical characteristics of superconductors.

1.3.2 Specific Objectives

- Modeling a HTS cable to get a precise idea of the electric and magnetic field distributions inside the superconductor
- Design SC cable for particular transmission line in Ethiopia.
- Conduct comparative analysis between the existing power line and the one designed using superconductors.
- Identify the impacts of African environmental conditions on the application of the SC for transmission lines.
- Evaluate the technical performance and implementation of SC in Ethiopia.

1.4 Methodology

This methodology presents a systematic approach for modeling the electromagnetic and thermal behavior of a high-temperature superconductor (HTS) cable. It focuses on integrating the SC cable into an existing power grid and optimizing its performance while balancing technical constraints. The framework combines Multiphysics simulations, and multi-objective optimization to ensure seamless compatibility with grid requirements and enhance operational efficiency.

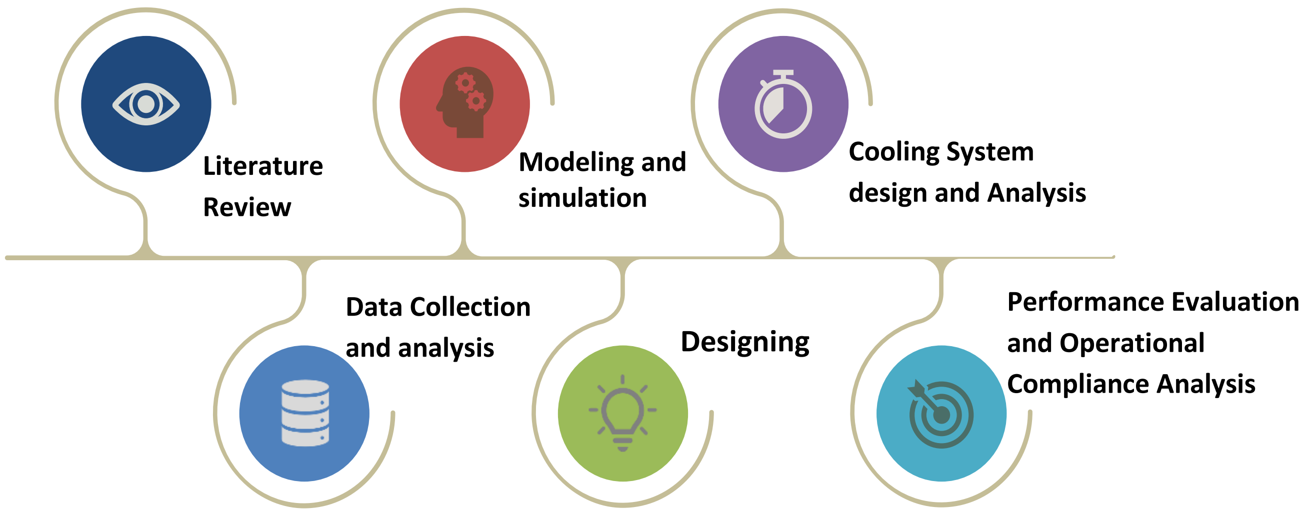

Figure 1.3: Flow chart of the conceptual framework

Literature Review:

The systematic review process begins with clear, focused research questions in superconductors, addressing gaps in current literature. A thorough search of relevant databases, including academic journals and conference proceedings, is crucial to gather a diverse range of studies.

Data Collection and analysis:

The study used data from Ethiopian Electric Power (EEP) and scientific studies to compare existing power lines and superconducting materials. It also analyzed research on grid integration and the impact of superconducting cables, incorporating the latest advancements. The collected data are analyzed in detail and evaluate the significance of the designed system performance from existing one.

Modeling and simulation:

The modeling phase analyzed the technical performance of High-Temperature Superconducting (HTS) cables using MATLAB to model electromagnetic behaviors under various operational scenarios, including load variations, filed, and temperature.

Designing

The design of the HTS cable was completed based on the specific requirements of the selected site. The conventional and HTS-based transmission lines were assessed for feasibility, efficiency, and regulatory compliance within the Ethiopian grid, simulations were carried out using simulation tools (MATLAB and Dig SILENT Power Factory).

Cooling System design and Analysis:

The liquid nitrogen cooling system was designed and analyzed using ANSYS Fluent and MATLAB simulations, considering temperature gradient, superconducting state, and pressure drop for effective nitrogen flow.

Performance Evaluation and Operational Compliance Analysis

The study analyzed SC transmission cables in Ethiopia's power grid context, evaluating compliance with national standards, environmental constraints, and operational efficiency, focusing on power loss reduction, magnetic field penetration, and heat leakage impact.

In conclusion, the analysis of the results has provided valuable insights, resulting in important conclusions and actionable recommendations that can greatly shape the next steps.

1.5 Scope of Study

The study will focus on the technical evaluation of using superconductor's transmission line. The performance of this line will be analyzed in terms of efficiency and current capacities, power loss. Modeling of current and magnetic field distribution inside the superconducting cable is analyzed in detail. A comparative study with the existing line will be done and the amount of power savings will be calculated to prove the technical viability of this system.

1.6 Expected Outcomes

The document will provide a comprehensive, evidence-based roadmap for deploying HTS cables in Ethiopia, balancing technical innovation with practical grid integration. It aims to bridge the gap between theoretical simulations and real-world implementation, offering actionable insights to policymakers, utilities, and researchers working on modernizing power infrastructure in developing economies. And expected to Analyze electromagnetic field distribution and its effects on superconductivity, minimize resistive and AC losses while maintaining high power transmission efficiency, Ensure stable cooling with liquid nitrogen (LN_2) while considering heat leakage and pressure drop. Ensure smooth integration into existing power systems without causing instability.

1.7 Organization of the study

This thesis is structured into four comprehensive chapters. Each chapter addresses key topics, and summarizes their content as follows:

Chapter 1: provides an introduction that outlines the study's background, articulates the problem statement and clearly defines the objectives and scope. Additionally, it outlines the anticipated outcomes, setting the stage for the significance and impact of the research.

Chapter 2: provides a thorough literature review on Superconductivity and superconducting transmission lines, tracing their evolution and the background of superconducting technology. It highlights the transformative potential of these technologies and their critical role in future innovations, highlighting the importance of superconducting cables in modern electrical systems.

Chapter 3: The complex dynamics of electrical and magnetic distribution in superconducting cables are explored, emphasizing the significance of this knowledge for system potential and technological advancement.

Chapter 4: This chapter presents a detailed design of the SCTL for the 132 kV line connecting Kalilti I to the Black Lion interconnector in Addis Ababa. It covers superconducting cable technology, system layout, cooling design and cost analysis, evaluating its superior performance against conventional lines and detailing simulations and analysis.

Chapter 5: The study's final findings are presented in this chapter, together with important conclusions and practical suggestions for further research.

Chapter Two

2. Theoretical Background and Literature Review

2.1. Evolution of Transmission Lines

The evolution of transmission lines can be traced back to the late 19th century when electricity was first harnessed for commercial use. The first transmission lines were simple overhead wires that were used to transmit power from generating stations to nearby towns and cities. These early transmission lines were often inefficient, and they suffered from significant power losses due to resistance in the wires.

In the early 20th century, engineers began to develop new transmission line technologies that used higher voltages and lower currents. These new transmission lines were able to transmit power over longer distances with less power loss. One of the most significant developments in the evolution of transmission lines was the introduction of alternating current (AC) transmission [25]. AC transmission is more efficient and allows for the use of transformers to step up the voltage for long-distance transmission and then step it down for distribution to homes and businesses. Another important development in the evolution of transmission lines was the use of underground cables. Underground cables are less susceptible to damage from weather and vandalism, and they can be used to transmit power in areas where it is not possible to build overhead lines.

The limitations of standard transmission technologies have spurred research and development in the field of electricity transmission based on higher conductivity and less loss of transmission line.

2.1.1 Conductivity

The conductivity of a material is a measure of its ability to carry electric current. The higher the conductivity, the more current the material can carry. Generally, metals are good conductors of electricity, while non-metals are poor conductors. The best conductors of electricity are silver, copper, and gold. The worst conductors of electricity are rubber, glass, and plastic. The conductivity of a material depends on a number of factors, including the material's atomic structure, the temperature, and the presence of impurities [8].

Seeking more conductivity, less power loss and high current caring capacity material will bring new material to superconductors. The development of superconductors has enabled the construction of transmission lines with significantly higher current carrying capacities than conventional conductors. Superconducting materials have zero electrical resistance, which means that they can carry electricity without losing any power. This makes them ideal for use in transmission lines, as they can reduce the amount of energy that is lost during transmission.

2.1.2 Superconductivity

Superconductivity is the state of matter where electrons band together in such a way that the electrical resistance drops to zero. Being able to conduct electricity without resistance is so appealing, computer processes are significantly limited by the heating from the current running through. If we were able to lose resistance from these processes, we could immediately get a dramatic improvement in computing. And this is only one of the many amazing advances that would be able to access, if only had superconductor they worked at room temperature, but there is a major problem. That don't know why high temperatures.

2.2 Background of Superconductor

In 1908, Dutch physicist Heike Kamerlingh Onnes and his students started performing experiments at low temperatures using liquid helium to study how to turn helium gas into liquefied helium for the first time. This was quite an achievement because helium liquefies at only four degrees above absolute zero. That's -269 degrees Celsius, or -452 degrees Fahrenheit. This is the lowest boiling point of any known material. He later cooled down a sample of mercury to this temperature and ran electricity through it.

Recognizing the importance of this phenomenon, Kamerlingh Onnes named the state “SUPERCONDUCTIVITY” and the temperature at which the material achieves this state is called “the transition temperature”. The first superconductors triggered a great deal of excitement, and he received the 1913 Nobel Prize in Physics for this discovery. It was the electrical engineers wet dream, a future free of electrical resistance [8].

In 1914, he then made a coil of lead wire, froze it to 7.2 Kelvin and pass an electrical current through it. But to his disappointment, the coil lost all its superconducting powers when the magnetic field got to be about as strong as a horseshoe magnet. As it turns out, he proposes that Superconductivity requires not only a low enough temperature but also a low enough magnetic field and a low enough amount of current passing through it-current density.

The material can only maintain superconductivity if all three sit within the parameters. Electrical systems encounter magnetic fields all the time. Kamerling Onnes must have been crushed. He was one of the first scientists who had fallen victim to the sirens of superconductivity and would not be the last. [8]

In fact, this material is such that if you put a current in a superconducting wire in a loop, that current will continue to flow virtually forever with no added voltage or energy source. And superconductors have another seemingly magical feature and that they expel magnetic fields. So, if you put a magnet over a superconductor the magnet will levitate.

- How is this possible?

- How can any material carry current perfectly with no energy loss?

To answer this question, have to dive deep into the subatomic realm, which means to invoke quantum mechanics.

- What is Conductivity?
- Why is it so special and how does quantum mechanics explain it?

While the idea of materials reaching a low resistance at very cold temperatures was rather well accepted, the question was what happens at or close to absolute zero (0)? Lord Kelvin thought that electrons would completely stop and thus the resistance would become infinite. So, when it was first discovered that the materials electrical resistance can become zero at very low temperatures, this was unexpected.

Second major discovery that went under the radar in the late 1920s, The Soviet Ukrainian scientist L.V. Shubnikov, worked at a cryogenic lab in the Netherlands. In 1930 he returned to the Soviet Union and continued his research. There are experiments discovered what are now called type II superconductors. These are quite different from the pure metal superconductors today called Type one [13].

Through them, pioneering science was done in the 1930s. discovered three more superconductors, tantalum at 4.4 K, thorium at 1.4K and Niobium. which has the highest transition temperature yet known at 9.2 Kelvin.

The next big discovery was made in 1933 by Walther Meissner and Robert Ochsenfeld. They found that when a metal is cooled while in a small magnetic field, the flux is spontaneously excluded. Then metal becomes superconductor this is known as the Meissner effect. The discovery figures out that superconductors don't just have zero resistance, but also repel magnetic fields, which was an important step towards understanding what was making this exotic state of matter. This is the principle on which the electric generator operates. But, in a superconductor the induced currents exactly mirror the field that would have otherwise penetrated the superconducting material - causing the magnet to be repulsed [12], [14].

All after this in 1937 Lev Landau proposed theory from phase transitions that could help to explain the transition from a metal to a superconductor, which earned him the 1962 Nobel Prize, but this still didn't explain why superconductor is superconductor. That would have to wait until 1957 to have a concrete idea behind the mechanism.

In subsequent decades other superconducting metals, alloys and compounds were discovered. In 1941 niobium-nitride was found to superconduct at 16 K. In 1953 vanadium-silicon displayed superconductive properties at 17.5 K.

And, in 1962 scientists at Westinghouse developed the first commercial superconducting wire, an alloy of niobium and titanium (NbTi). High-energy, particle-accelerator electromagnets made of copper-clad niobium-titanium were then developed in the 1960s at the Rutherford-Appleton Laboratory in the UK.

In the early 1950s, a pair of scientists, BT Mathias and John Holm, embarked on a systematic search via experimentation. Mathias and Holm systematically moved through the periodic table eventually testing over 5000 compounds. This was how they discovered the A3B superconductors (it's a terrible name) -3 niobium atoms and one atom of either silicon, tin or aluminum. Anyway, these would hold the record for the highest transition temperature, 23K for 28 years [1].

The first widely accepted theoretical understanding of superconductivity was advanced in 1957 John Bardeen, Leon Cooper and John Robert Schrieffer proposed what is now called the BCS theory [10]. They theorized that at cold temperatures in certain materials, electrons with opposite spin and momenta could become coupled together such that they would attract one another rather than repel and would form a new quasi particle called a Cooper pair, which would have zero resistance.

As the temperature rises, there are more and more phonons in the lattice, which will eventually start to give the electrons a large enough momentum kick to break the Cooper pair. However, at higher temperatures and with different superconductor systems, the BCS theory has subsequently become inadequate to fully explain how superconductivity is occurring 10][11].

By 1960, knew that about 35 elements and 1000 different alloys to have shown superconductivity under certain conditions. In 1961, scientists discovered a series of Niobium based alloys that retained their superconductivity in the presence of a stronger magnetic field. These were called high-fields superconductors. And they theoretically allowed us to make large superconducting wires that perform far better than traditional copper ones. Such wires can produce very powerful magnetic fields using very little power. High-field superconductors achieved the original dream of kamerling Onnes many decades ago. but even so, it took the industry until early 1970 to reliably and viably produce superconducting wire. Such superconducting wires eventually became the widely accepted method for producing MRI 's [11].

In 1986, two researchers at an IBM lab in Zurich, Switzerland were collaborating managed to create superconductivity in aceramic material at 35 kelvins [2]. Ceramics are traditionally known to be electrical insulators. After further experiments, the duo produced a ceramic compound of barium, lanthanum, copper and oxygen that achieves superconductivity at 35 Kelvin-a legit breakthroughs.

J. George Bednorz and K.Alex Mueller first kept their results away from even their colleagues and their employer. They decided to first publish their results at a small but reputable German physics journal, apparently because they personally knew its editor. In April 1986, they submitted the paper, which was deliberately given a very disarming title, “Possible High Tc superconductivity in the Ba-La-Cu-O system” [2].

The new ceramics also violated the previously established rules of superconductors. It did not follow the Mathias rules, and not only that, it highlighted a hole in BCS theory. By then, physicists had largely adopted BCS as a reasonably rigorous explanation of superconductivity and because BCS only worked at low temperatures, superconductivity in general was regarded as an exclusively low temperature phenomenon. This discovery heralded a new class of ceramic oxide superconductors with high transition temperatures. Higher than ever before seen, referred to, has “high temperature superconductors, or high-T [3].

Research teams around the world raised to replicate the results. In late November 1986, some two months after publication, the Asahi Shinbun newspaper reported that a team led by Shoji Tanaka of the University of Tokyo had successfully repeated the experiment, confirming the results. A few weeks after that, Paul Chu of the University of Houston replicated the results. Chu’s results made the headlines. More impressively, he believed that there were other materials out there with even higher transition temperatures.

A race for news superconductors soon emerged, with the big line being 77 Kelvin, the temperature of liquid nitrogen. Various groups in Beijing, Tokyo and the US traded papers back and forth.

Then in January 1987, Doctor Chu discovered a superconductor with the transition temperature above 90 Kelvin, breaking the so-called liquid nitrogen barrier. Chu held off publishing for as long as possible as he tried to first patent the material. Finally, in February 1987, he announced his marvelous technical breakthrough. This class of high temperatures superconductors is sometimes called 1-2-3 superconductors because they have one atom of Yttrium, 2 atoms of barium and three atoms of copper. These things are also more generally referred to as **YBCO** superconductors, cuprate superconductors or rare earth cuprate superconductors. Cuprates broke the nitrogen barrier, which meant that can use liquid nitrogen to cool them rather than liquid helium, which is what used before. This has significant cost benefits.

In 2001, a Japanese team discovered an interesting non-cuprate superconductor magnesium diboride. Its transition temperature was 39 Kelvin, far below the cuprates, but at least much higher than the traditional low temperature superconductors. Unfortunately, its behavior was conventional BCS, so a dead end [4].

The next significant high temperature discovery came in February 2008. when Doctor Hideo Hosono reported a fluorine-doped iron-based superconductor with a transition temperature of 26 Kelvin. This opened up a new branch of high temperature superconductors separate from the cuprates. At the outset there was a lot of hope. A few months, another iron super conductor was found with a transition temperature of 56 Kelvin [5]. But progress there has since stalled. And then recently in 2015 a team in Germany published a paper claiming superconductivity in Sulphur hydrides at over 200 Kelvin and high pressure. Interesting, but again nothing that has real world industrial implications. And there have been some questions about superconductivity in these sulfide hydrides [6].

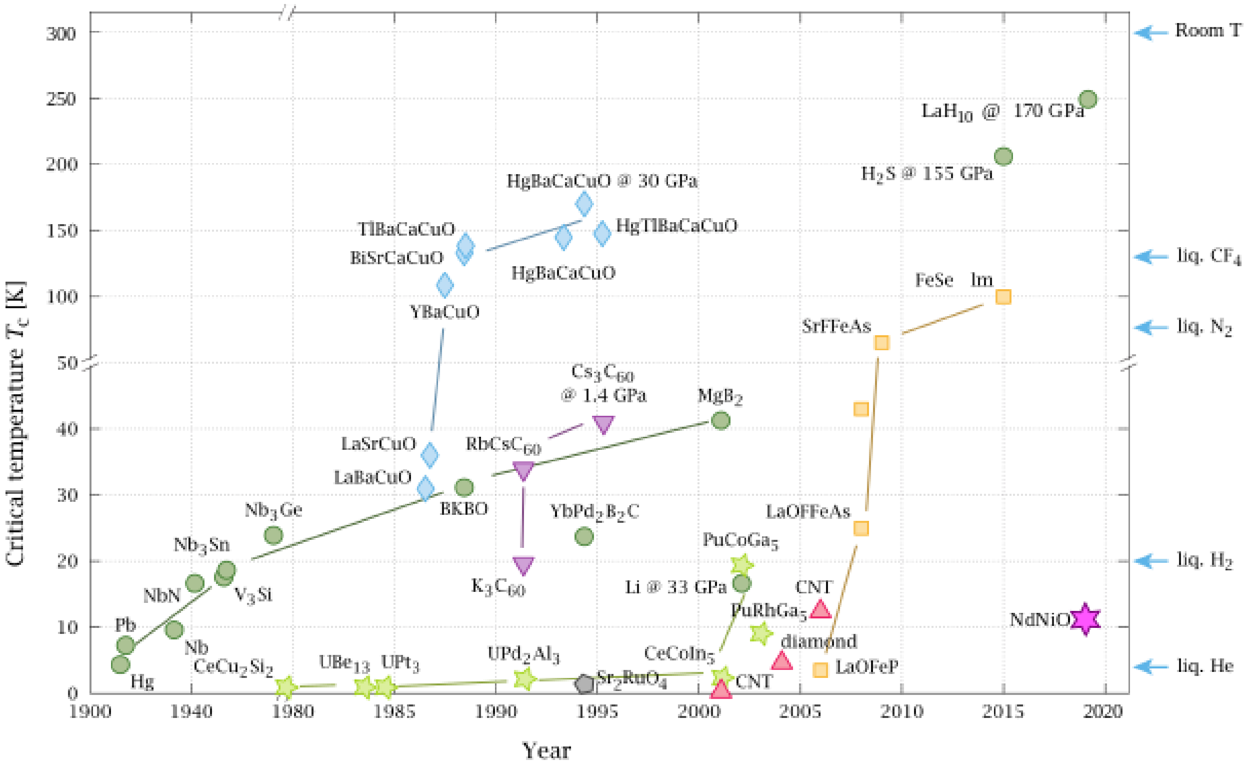

Figure 2.1: Timeline of superconductor discoveries (source: Common figure)

A lot of research is going into this field today. In 2020 the first room temperature superconductor was synthesized. It's a carbonaceous sulfur hydride. Its critical temperature is 15 degrees Celsius, or 59 degrees Fahrenheit. This sounds wonderful, but the caveat is that it requires extreme pressures close to that of the center of the Earth to work, so it's not quite useful for practical applications [7].

The search continues for a room temperature superconductor or even a relatively high temperature superconductor with fewer engineering compromises than they already have.

Recent research in July 2023 Japan scientists announce room temperate-ambient pressure superconductor called LK-99. After that, number of teams claimed that a massive drop in resistance was below the temperature of 127 Celsius, quite hotter than room temperature.

2.2.1 Developments and Advances of HTS Cables

Over a period of over 20 years, significant advances and improvements have been made in the development of prototype HTS cables. This breakthrough paved the way for the current research and development of HTS cables, which have the potential to revolutionize power transmission technology. Since 1969, researchers from Europe, Asia and IBM Research Centers have been designing and developing prototype HTS (High Temperature Superconducting) cables. And in 1992, they demonstrated that they could manufacture SC cables on a scale, thereby reducing overall costs. The success of this test represents a significant advance in the development of HTS cables. The SC cable's dependability and efficiency under high-power and temperature circumstances revealed its potential as a revolutionary power transmission system [36].

In the year 2001, one of the initial efforts on the prototype of HTS cables was made on a 30 meter-long 12.4 kV cable in Georgia, USA. Triaxial SC cable with three-phase terminations was conceived and manufactured. The three concentric superconducting phases are built of BSCCO-2223 HTS tapes separated by layers of cold-dielectric tape. A separate liquid nitrogen stream is used to chill the terminations used in the SC cable tests [18].

A few months later, Italian research group Pirelli Cables tested a 50 meter/115 kV AC HTS cable. A 115 kV high temperature dielectric HTS power line was designed. Goals include achieving a circuit power rating of 400 MVA, increasing performance by 100% in a compact design that can be installed in standard 8-inch pipe, and designing, manufacturing, and testing required for commercial system accessories [19]. Following these prototypes, many studies on AC HTS cables were conducted, although their lengths rarely exceeded 100 meters.

Ultimately, testing was done in Albany, USA, on a 350-meter-long, 34.5 kV HTS cable with an 800 A nominal current. The Bi2223 tapes, which were sintered via a controlled over-pressure technique, were incorporated in the HTS cables. The first cooling procedure was carried out while the SC cable's scattered temperatures were being monitored. On July 20, 2006, the HTS cable system was linked to live network. Since then, the cable has been consistently laid [20].

A 600 m long HTS cable with an operating voltage of 138 kV was then designed, tested and constructed by American Superconductors in Long Island, New York with a capacity of 574 MVA. The first long voltage-carrying high-temperature superconducting power cable using a low-temperature dielectric has been successfully installed on the Long Island Power Authority (LIPA) system [21].

The Ampacity project is one of the most important projects involving the development, manufacture and installation of a 10 kV 40 MVA high temperature superconducting system (HTS) consisting of a residual current limiting device and a 1 km long cable in the city of Essen. Furthermore, it will be the longest HTS cable system ever installed globally [23].

The system connects the medium voltage buses of two substations replacing a conventional high voltage system. The study shows that four out of ten 110/10kV transformer SS were not needed when the 10kV HTS superconductor cable is used. It also allowed for a simpler grid structure and gives an advantage on space requirement. This exhibited a lower overall cost when a grid of 10kV HTS system is used compared to when the conventional 110kV system is implemented thus, it offered a technical and economic advantage [22][37]. The commercial project of HTS Cables by KEPCO in Korea is called the Shingal Project [24].

An economic evaluation proved that the first option of using the HTS Cable was cheaper than the conventional cable option and would further reduce the project cost by as much as 15%.

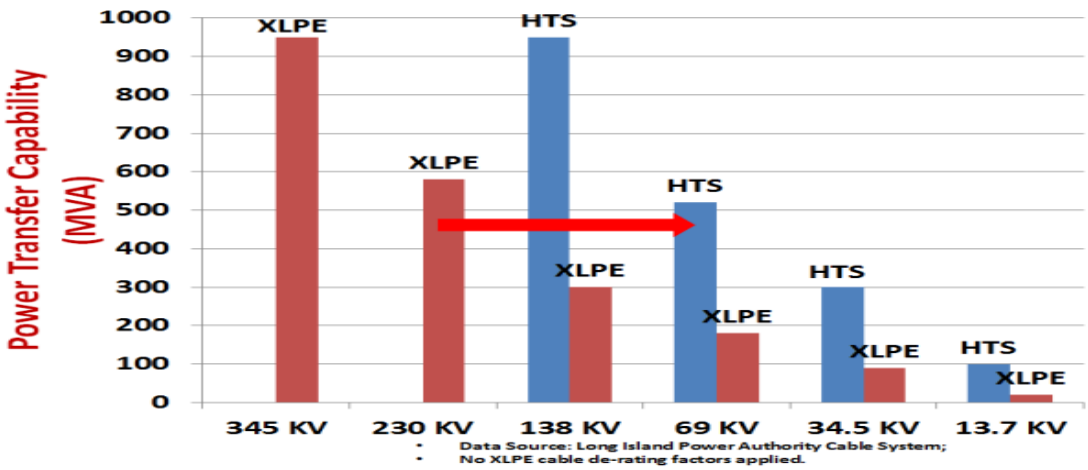

Figure 2.2: The power transmission capacity and voltage level of XLPE cable and HTS cable.

They further mentioned of the planned second HTS cable commercial project in Korea which uses AC 154kV HTS Cable system to provide redundancy on the radial SS and increase the load transfer rate of the distribution which was at 65%. The study shows that construction duration is decreased from 36 months to 12 months since there is no need to construct an underground cable tunnel like in the case where conventional cables are used, rather a small conduit would be good enough [24].

Super Link, a new German project recently launched in Munich, uses a 12 km/110 kV HTS cable, one of the longest HTS cables ever tested [16][25]. It is anticipated that SuperLink will develop into a 12 km link with a voltage of 110 kV and a 500 MW power rating in a closed circuit. The superconducting cable is cooled to - 200ºC using nitrogen, an environmentally safe refrigerant.

D. Kottonau et al in [26] compared a four system 380kV overhead transmission line with a capacity of 6634MVA crossing an urban area over a length of 1.7km with a high voltage superconducting transmission line in terms of corridor width and energy losses. They found that energy loss would be reduced by about 8100MWh per year which translates to a feasible energy loss reduction of approximately 75% when a 380kV SCTL is used instead of conventional
overhead lines which translate to 5% energy saving [27][36].

Researchers have looked into DC cables in addition to AC HTS cables in their studies and projects. Chubu University in Japan launched an experiment in the fall of 2006 utilizing an HTS conductor to create a DC superconducting power transmission line [28]. In 2012, a 1.3 kV and 10 kA DC SC cable was erected by the Chinese Academy of Sciences and the Institute of Electrical Engineering [29][37]. And DC HTS cable was installed in South Korea in 2015. Based on HTS experience, the worldwide standard for HTS AC cables, and the standards for traditional HVDC cables, the qualification test was conducted [30].

Project St. Petersburg took place the 2.5 km long HTS DC cable project with an operating voltage of 20 kV. As part of the national project to deploy a superconducting DC cable with a capacity of 50 MW, 20 kV in St. Petersburg region [31][32]. Dual-circuit cryogenic system with 12 kW at 77 K, rectifier-inverter, automatic process control system, reverse air conditioner (no internal cables) and six SC cable lengths with five connectors and two current leads making up the experiment [40].

In Africa, U. O. Michael and O. Uko in [33] show that Nigeria needs superconductor cables to address the power transmission and distribution problem that is widespread in the country. The application of superconductors would be half the amount of electric power lost by conventional cables.

The Sahara Solar Breeder Project which is to utilize the abundant solar energy in the Sahara would use HTSC to transmit power from the Sahara to Europe if the project would ever be implemented.

Cooling stations would be every 100 kilometers to pump liquid nitrogen coolants through the lines. S. Eliza in [34] says Yamaguchi states that cost of cable for high-temperature superconductor systems is high, but the cost of the coolant (Liquid Nitrogen) is low. Power companies argue that the high cost of SC is covered up by the electrical losses experienced in conventional cables. However, in the proper setting, the energy saved is an advantage to using superconducting lines rather than the conventional lines. A list of most important projects and research on AC/DC HTS cables, adopted from [36][37][41].

Table 2.1: Major HTS Power Transmission Projects Abroad

Area	Project	Voltage (kV)	Current (kA)	Length (m)	Note
US	Albany	34.5	0.8	350	Finished
	Ohio	13.2	3	200	In operation
	LIPA	138	2.4	600	In operation
	Hydra	13.8	4	200	Planned
EU	Denmark	30	0.2	30	Finished
	Amsterdam	50	3	6,000	Planned
	Russia	20	1.4	200	Planned
	Essen	10	2.3	1,000	Planned
China	Yunnan	35	2	33.5	In operation
Korea	GENI	22.9	1.25	410	Planned
	Jeju	154	2.25	1,000	Planned

The development of HTS cables faced several challenges, including the complexity of producing high-quality superconductors, the cost-effectiveness of the technology, and the need for advanced research and development. However, the development of HTS cable was a long and complex process requiring the joint efforts of researchers, engineers and industry experts. The culmination of this joint effort was the result.

2.3 Overview of Superconductivity and Superconducting Cable

The steady increase in electricity consumption and certain constraints in the construction of new transmission and distribution components are forcing the modernization of electricity infrastructure.

Superconductivity is a collection of physical phenomena found in some materials in which electrical resistance disappears like water flowing through a pipe with no obstacles and magnetic flux fields are emitted. Since Heike Kamerlingh Onnes discovered the phenomenon in mercury on April 8, 1908 [8], great progress in the field has occurred. Many other superconducting materials have since been discovered.

Superconductors can be divided into two main groups: Type I superconductors and Type II superconductors, and these two groups behave differently in magnetic fields.

- A type I superconductor are pure metals or metalloids with low critical temperatures and low critical magnetic fields. Which tries to expel magnetic field by setting up shielding currents, a phenomenon called the Meissner effect. When the magnetic field becomes too strong for the shielding current, superconductivity.
- Type II materials, however, are able to maintain superconductivity up to higher field by allowing magnetic flux quanta to penetrate the material, a phenomenon called the Abrikosov effect. Because the electrical current around these flux quanta is circular. They are metallic compounds or alloys with higher critical temperatures and higher critical magnetic fields, also called vortices. By introducing material defects and impurities in the material the material can maintain its superconductivity up to much higher field and current than type I superconductors.

If you expose Superconducting material to a weak magnetic field there will be no field inside the superconductor except for a small region around the boundary, which is known as the Meissner effect. But if you make the magnet stronger, at some point the superconductor doesn't work anymore. The difference between type 1 and type 2 superconductors is how exactly this breakdown occurs. Type 1 superconductors stop working suddenly when the magnet gets too strong.

Can illustrate this behavior using a phase diagram below:

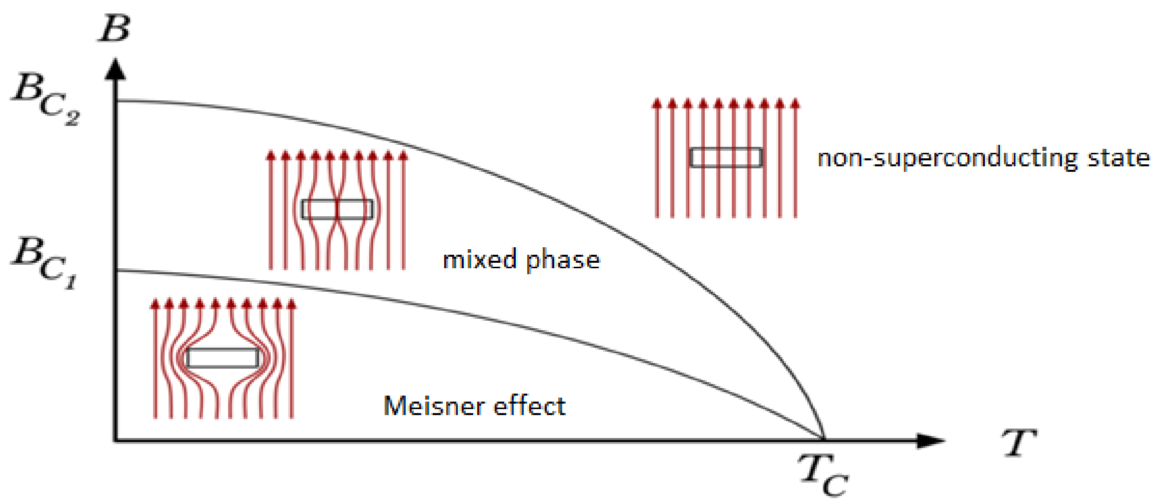

Figure 2.3: phaser diagram of type I and type II superconductor.

The diagram looks like below the first curve are in the so-called Meisner effect which is superconducting. As you can see if we either increase the temperature or the magnetic field above a certain value, we go from the Meisner effect to the non-superconducting one. The currently accepted theory of type 1 superconductors is called the BCS theory. This is a quantum mechanical model where two electrons are supposed to couple to each other forming a so-called Cooper pair. The idea behind this is that all Cooper pairs across the whole material can occupy the same ground state, such that we have a wave function that covers the whole material. As this weight function is not concerned with local obstacles, which means no interaction with the solid, which in turn means no resistance.

For type 2 superconductors have two critical field strengths, take a look at the phase diagram below the first threshold BC_1 in the Meisner effect, which means that the material behaves just like a type one superconductor. After passing this threshold magnetic field vortices can form in the material. Those are small tubes where magnetic flux can travel through the material, if we then increase the magnetic field even more the density of those vortices will increase until we pass the 2^{nd} threshold BC_2, when superconductivity breaks down and the magnetic field can enter the material as usual. The face between BC_1 and BC_2 is called the vortex phase or mixed phase.

Additionally, there is also a mathematical way to distinguish type one from type two superconductors. To demonstrate this, we use the Ginzburg-Landau theory of superconductivity. In the equations of motion of the Ginzburg-landau of theory, two parameters can be identified which both have units of length.

Ginzburg-Landau theory of superconductivity.

$$k = \frac{\lambda}{\varepsilon} \qquad if\ \ 0 < k < \frac{1}{\sqrt{2}} ------------ type\ I$$

$$\text{Else}\ \ k > \frac{1}{\sqrt{2}} ------------ type\ II$$

Where: ε = coherence length, λ = penetration depth, k= Ginzburg-Landau parameter.

If we take the ratio of λ to ε, this dimensionless quantity is usually denoted by Kappa(k) and values between zero and 1 / sqrt 2.

However, when the current density becomes too high, the Lorentz forces on the vortices exceed the pinning forces, resulting in the movement of the flux lines, which causes power dissipation and thus the appearance of resistivity. This effect places an upper limit on the current density flowing through the material, named its critical current density, or, in the case of superconducting wires or cables, their critical current.

The critical values of superconductors are dependent on each other and their mutual dependence are inherent material properties that depend in addition on the various processes that are used to manufacture superconductors. In order to accurately describe an operation point, all three critical values need to be defined. Superconductors must operate in the region defined by three inter-related critical boundaries: critical current (I_c), critical temperature (T_c) and critical magnetic field (H_c).

Critical temperature (T_c)

Electrical resistance of a superconductor normalized to the linear decrease of the normal conducting phase. The transition between normal conducting state and superconducting state is usually steep. Within the normalized values certain thresholds of the electrical resistance are dined (usually 10% and 90%).

Table 2.2: Transition temperature of some high Tc Superconductor alloy

Compound	Tc(k)	Comment
Nb-Ti (Niobium-Titanium)	9.2	LTS, typically cooled with liquid helium. essential for strong magnetic fields. (MRI, fusion reactor)
Nb_3Sn (Niobium-Tin)	18	
$YBa_2Cu_3O_{7-x}$ (YBCO-123)	92	Cuprate Superconductors, widely used in power cables, magnets, and levitation applications.
$Bi_2Sr_2Ca_2Cu_3O_{10+x}$ (Bi-2223)	110	
$HgBa_2Ca_2Cu_3O_{8+x}$ (Hg-1223)	134	
LaH10 (Lanthanum Hydride)	250	Super hydrides, require extremely high pressures (160 – 300 GPa)to exhibit superconductivity, impractical.
CSH (Carbonaceous Sulfur Hydride)	288	

Offering a high critical current density, economical cooling with liquid nitrogen, superior magnetic field tolerance, mechanical robustness, and low AC losses, YBCO is a viable option for high-temperature superconducting grids. These characteristics make it perfect for high-capacity transmission systems and urban settings.

Critical Current

The critical current (I_c): is maximum value of current that can flow through a superconductor with zero resistance at specific magnetic field and temperature levels. The critical current is affected by both temperature and magnetic field magnitude, resulting in a critical surface that is unique to each material. This current-electric field behavior can be modeled in the transition area with a power law dependence.

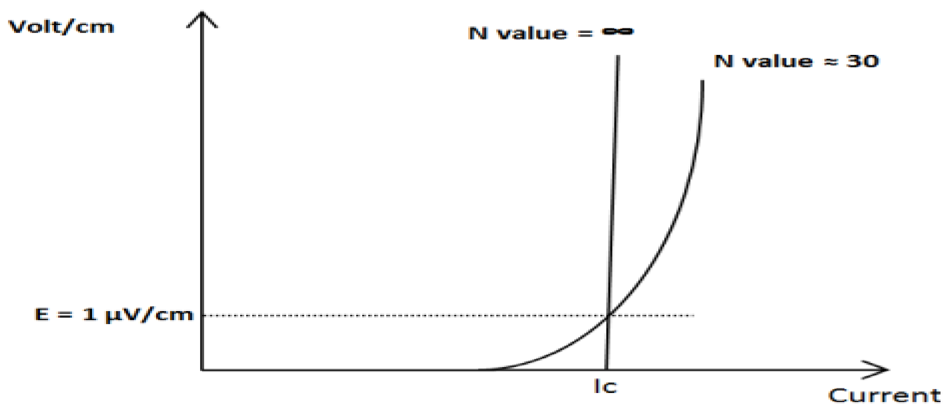

Figure 2.4: The sketch of E-J curves when N = ∞ for Bean Model and N = 30 for practical HTS tape.

$$E = E_c \left(\frac{j}{j_c}\right)^n \tag{2.1}$$

Where: E_c denotes the specified critical electrical field, when E_c = 1 V/cm the critical current is reached in the case of HTS.

- The slope of the phase transition from superconducting to conventional conducting is represented by the exponent n. When possible, the n value is found between E_c and 10 E_c.
- the current carrying capacity of superconducting wires usually include either by the critical current I_c of the wire or by the critical current density J_c.
- The critical current density (J_c) normalizes to the superconducting cross section of the wire:

$$Jc = \frac{I_c}{hts_{area}} \tag{2.2}$$

Critical magnetic field

- The irreversibility field, the superconducting phase limit Bc_2, and the Meisner phase limit Bc_1 are the three unique values. A superconductor can transfer a current to a maximum field, which is described by the irreversibility field Birr. An empirical formula for estimating the irreversibility field B_{irr} is:

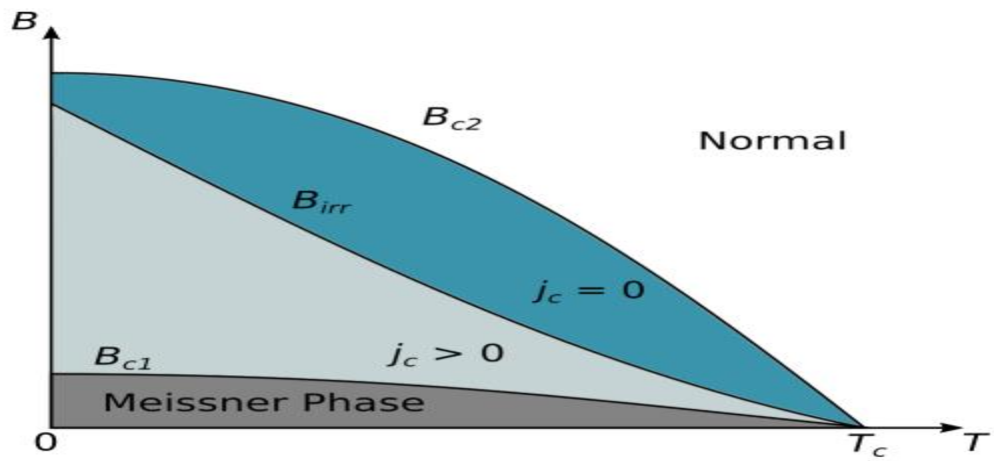

Figure 2.5: Phaser diagram of superconducting devices

$$Birr = Birr(0k)\left(1 - \frac{T}{T_c}\right)^{\alpha} \quad (2.3)$$

Where: T temperature of the material and T_c critical temperature with being α material characteristic

Magnetic field dependence of critical current

In real-world applications, precise determination of the superconductor's critical current necessitates its orientation inside the magnetic field.

$$j_{c(\beta,\theta)} = \frac{j_{c0}}{\left[1 + \sqrt{(k_1.Bcos(\theta+\alpha))^2 + (Bsin(\theta+\alpha))^2/B_k}\right]^{k2}} \quad (2.4)$$

with B_k, k_1 and k_2 being model parameters, j_c the critical current density in self-field, B the magnetic field magnitude, θ the field angle, α the displacement of the critical current peaks from 0°.

Critical current temperature dependence

The resistivity of HTS tape, which is a special kind of tape that conducts electricity very well, is affected by two important things: the critical temperature and the critical current. Mathematically, the critical current density of YBCO tapes is given using the following formula:

$$j_c(T) = j_c(T_{ref})\left(T_{ref}\frac{(T_c - T)^{\alpha}}{(T_c - T_{ref})^{\alpha}}\right) \qquad \text{when } T_{ref} < \mathrm{T} < T_c \tag{2.5}$$

$$= 0 \qquad \text{when } T > T_c$$

where α is 1.5 which is applicable to YBCO and Bi-2223 superconducting material. T_{ref} is the reference temperature, and an operating temperature of 70 K for the HTS cable is used as a reference temperature (ref). 3.5×10^{10} A/m^2, and $T_c = 92$ K is the reference critical current density and critical temperature of the YBCO HTS tape, respectively [54].

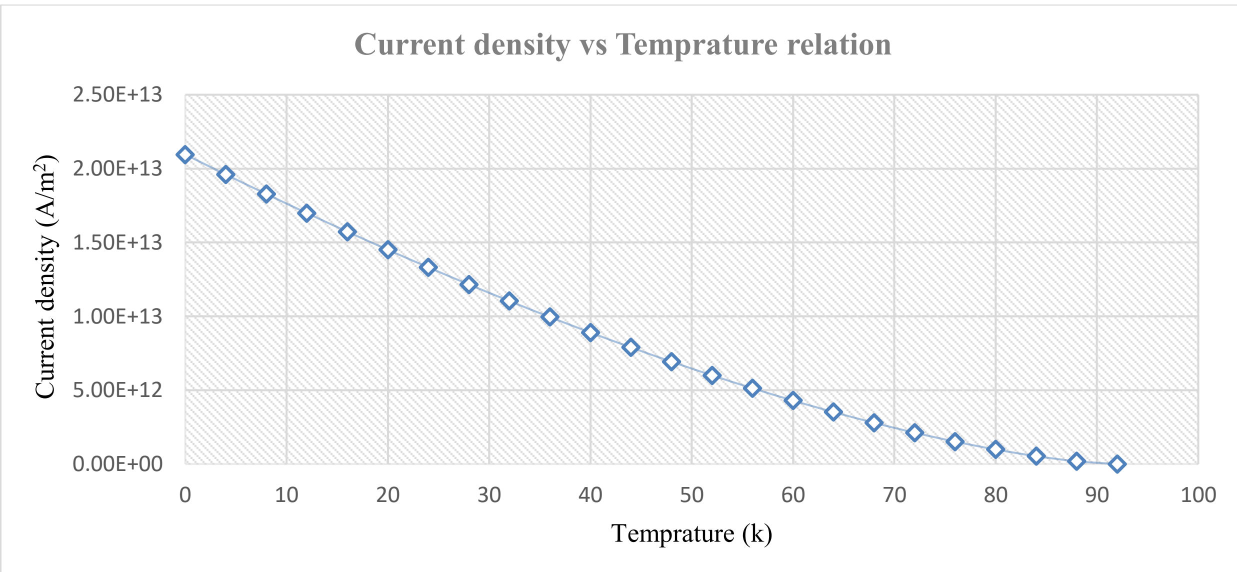

Figure 2.6: Current density and temperature relation of YBCO type superconductor

Critical magnetic field vs temperature dependence

The value of critical field B_c is a function of temperature T *is given by*

$$B_c = B_o\left(1 - \left(\frac{T}{T_c}\right)^2\right) \tag{2.6}$$

2.3.1 How Do Materials Behave as a Superconductor?

Understanding the behavior of superconductors in the presence of magnetic field requires understanding fundamental principles that reveal their remarkable interactions.

1. Electric current generates magnetic field.

2. Magnetic field induces electric current.
3. The electric current created will, in turn, establish a magnetic field that actively opposes the original field.

Applying a magnetic field across anormal material, the induced electric current will somewhat counteract the field, but there is a limit because the resistance of the material will limit the strength of the induced electric current.

But if you apply a magnetic field across a medium with no resistance, the induced electric current can get strong enough to completely cancel out the initial magnetic field. In fact, all free electron in the superconductor will quickly spiral along the magnetic field line and set up vortices of the current at the surface-persistent current. Those little current loops don't take any energy to maintain. They act like a little electromagnet that exactly cancels the incoming magnetic field within the material and call this shielding current.

But why all floating? Let's push together the same pole of a pair of bar magnets and they repel and can think of the surface of the superconductor as being layered with electromagnet. Another way to think about it is that the magnet field lines expelled from the superconductor pile up on the outside, causing an intense magnetic pressure. This effect is nicely described by London equation, figured out by Germany brothers Fritz and Heinz London in 1935. They found that in a material with zero resistance, magnetic fields had to exponentially decay inside it.

$$F_i = -\frac{\alpha_i}{2R^4} R_i \tag{2.7}$$

2.3.2 Classification of Superconducting Material (LTS and HTS)

Low Temperature Superconductors, or LTSs, mostly consist of metal series like NbTi. Most LTS superconductors are too expensive for everyday usage and highly challenging to apply in the industrial field. They require helium cooling below the region of T = 4.2 K.

High Temperature Superconductor (HTS); includes oxide compound materials that are non-metal and belong to the BSCCO and YABCO series. Liquid nitrogen can be used to chill most HTS (T=77 K). It is easier to construct a cooling system for HTS cable because the temperature gradient of the HTS case is significantly less at room temperature than that of the LTS case.

The resistivity of Super tape

The resistivity of the YBCO superconducting tape can be thought of as a special kind of math problem that changes depending on how much electricity is flowing through it and how hot or cold it is.

Phase 1:

The special tape becomes at super state when the applied current I is less than the critical current I_c and the temperature of the HTS tape T is less than the critical value T_c. Resistivity $\rho_0 = 0$ describes this state.

Phase 2:

The YBCO layer quenches when $I > I_c$ and $T < T_c$, causing resistance to appear. The E-J power law describes the superconductor's highly non-linear relationship between current, and voltage and the resistivity of the superconductor can be calculated using:

$$\rho_{hts} = \frac{E_c(T)}{j_c(T)}\left(\frac{j}{j_c(T)}\right)^{n-1} , \qquad I > I_c \;\&\; T < T_c \tag{2.8}$$

where $E_c = 1\mu V/cm$ is the critical electrical field. The N value, which tells us how well the material can handle electricity, is usually between 21 and 30 for YBCO tapes. When too much electricity flows through a superconductor, it can get hot and resistivity of the HTS tape increases exponentially as a function of the current density. This happens because the heat builds up quickly and makes the material hotter.

The equivalent resistance of parallel electrical circuits equation yields the total resistance of the superconductor.

$$R_{sc} = \frac{R_{Hts} * R_{cu}}{R_{Hts} + R_{cu}} \tag{2.9}$$

Where: *RSC* is the total resistance of the SC during phase 2.

Phase 3:

When $T > T_c$ it gets hot, the special layer called YBCO stops being super strong and starts acting like a normal material. The electricity then goes into another layer called copper, which also gets hot. In this case, the special layer is as resistant to electricity as the copper layer, which is a function of the temperature as expressed [53].

$$\rho_{cu} = (0.0084\mathrm{T} - 0.4603) \times 10^{-8} \text{ when } 77\mathrm{K} < \mathrm{T} < 250\mathrm{K} \tag{2.10}$$

2.3.3 Superconducting Cables

The research and development of superconducting cables began in the late 1960s, when low temperature superconducting alloys became available [48], with the motivation for this development in the 1970s and 1980s being the increasing need for transmission systems with high rated power. Latterly on the adding environmental concern about the overhead lines, especially in civil areas made it desirable to find results where lines could transfer large quantities of power.

The power ratings of conventional cables are restricted because of losses in the conductor and dielectric. Naturally cooled 110 kV cables have a transmission capacity range of up to 200 MVA at 400 kV, that range increases to approximately 800 MVA. Using water cooling can raise the levels to 500 MVA at 110 kV and 1500 MVA at 400 kV, for higher power ratings [49].

HTS cable for power transmission has two types of design. The first one is WD (Warm Dielectric Design), which is placed outside of the cryogenic medium while formers, superconductors, and guard layers are inside of the cryogenic fluid. And the alternate bone is CD (Cold dielectric coextensive Design), Electrical sequestration layers of CD HTS lines are kept at cryogenic temperature. In this type of cable, the cooling area is way larger than WD types and this leads to advanced heat cargo and cooling power [13].

2.3.4 SC Tape Technology Types

Working with superconductors over copper or other Ohmic conductors has the primary advantage of allowing for much larger current densities. This allows for the creation of compact and efficient magnets, which is critical for particle accelerators and detectors due to space constraints and power consumption. However, it is also applicable to Magnetic Resonance Imaging (MRI) and Nuclear Magnetic Resonance (NMR) systems.

Three types of high temperature superconductors are commercially available for AC or DC power cables:

- $Bi_2Sr_2Ca_2Cu_3O_{10}$ (BSCCO) with a critical temperature of -160 °C (113 k)
- $YBa_2Cu_3O_7$ (YBCO) with a critical temperature of -180 °C (93 k)
- MgB_2 with a critical temperature of -235 °C (38 k)

Yttrium Barium Copper Oxide, also known as $YBa_2Cu_3O_7x$ or simply YBCO, was found in 1986. YBCO is the first material found to have a critical temperature above 77 K, which is the boiling point of liquid nitrogen. Its critical temperature is 93 K. The upper critical field is dependent on the angle of the magnetic field with respect to the orientation of the crystallographic copper oxide planes because of the highly anisotropic crystal structure of YBCO. According to estimates, the upper critical field is 120 T when the field is perpendicular to these layers, and 240 T when the field is parallel to the copper oxide layers [43].

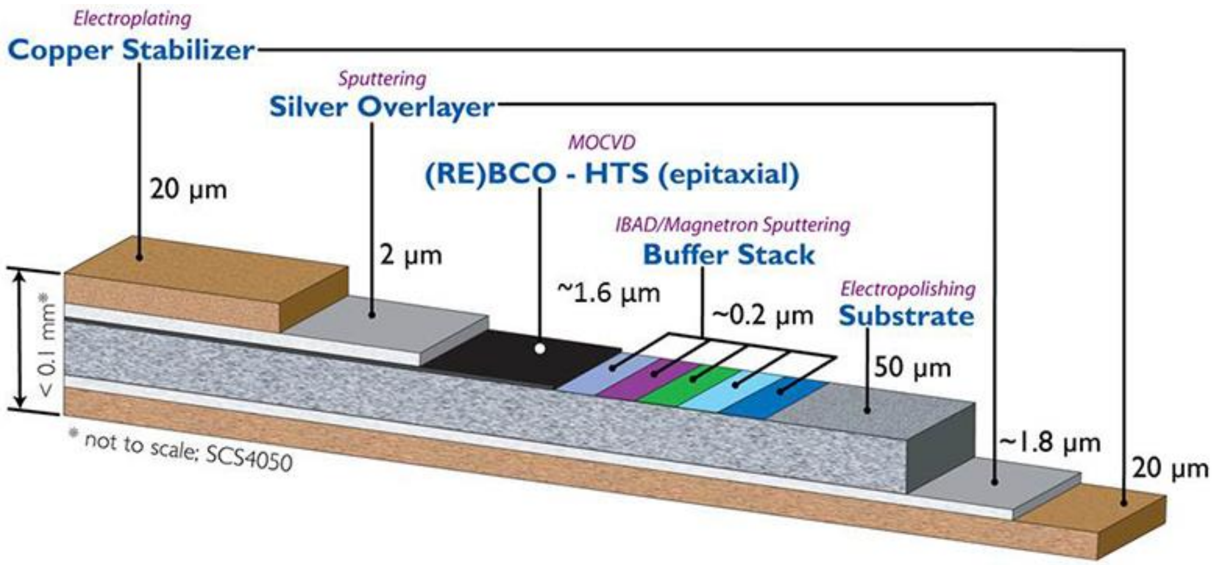

Figure 2.7: Architecture of a standard Superpower 2G YBCO HTS tape.

Bismuth Strontium Calcium Copper Oxide ($Bi_2Sr_2Ca_{n1}Cu_nO_{2n+4+x}$ or BSCCO) is another HTS worth mentioning. In the most common variant, n equals three, and this material is thus known as BSCCO 2223. The critical temperature is 108 K, and the upper critical field is around 200 T. Despite being discovered later than YBCO, it was the first HTS superconductor to be made into practical wires, using a relatively simple Powder in Tube (PIT) method [44]. However, due to the unavoidable use of expensive silver as the tube material, as well as its poor performance in high magnetic fields and temperatures (due to poor vortex pinning), BSCCO is currently a niche product.

Some recent studies have concluded that the affordable superconducting material magnesium diboride (MgB_2) can be a better alternative to HTS SCTL, mainly due to much lower production costs and the abundance of raw materials in nature [51]. MgB_2 displays superconductivity below T=39 K [52].

2.3.5 HTS Components & Enablers

The main components are:

- **HTS tapes or wires**

Superconducting cables have a number of peculiar properties. As an illustration, their current densities are comparable, ranging roughly between 1,000 and 10,000 A/mm². Conversely, the current density of conventional cable systems is lower, ranging from 1 to 5 A/mm². Manufacturers of HT superconductors typically produce their materials in thin strips ranging from 2 mm to 12 mm wide. These tapes, also known as SC tapes or tapes, can be widely used in electrical equipment without much technical effort.

Superconducting Cable Construction

The superconducting cable is composed of the cable core and the line cryostat. The cable core takes part in power transport, electrical isolation, magnetic display and neutral conductor.

HTS shielding layer

HTS shielding is an additional component in cable design. This HTS shield helps in protecting the cable from external magnetic fields especially when the electrical separation of the single conductor cable is cooled. It also increases current carrying capacity using multiple layers of superconducting SC tape. In the three-phase concentric SC cables, when the load is balanced and symmetric, magnetic fields cancel each other thus an additional shielding layer is not a requirement.

Table 2.3: Types of SC cable and application

	Single Conductor Cable	**Three wire Cable**	**Three phase concentric cable**
Voltage Level	High and extra high voltage	Medium to high voltage	Medium to high voltage
Dielectric Medium	Warm & cold	Cold	Cold
SC requirement for three phases	Similar to 3-wire cable (3 x HTS Conductor + 3 x HTS Shield)	Similar single conductor cable	Least (3 x HTS Conductor)
Cable cryostat for three phases	3 cryostats (3 outer tubes & 3 inner tubes)	1 cryostat (1 outer tube &1 inner tube)	1 cryostat (1 outer tube & 1 inner tube)

Former with regulating layer

The former is an inner tube in the cable structure which performs three functions:

1. It is a mechanical support for other layers used in cable construction.
2. It can also be used to transport liquid nitrogen which acts as the coolant.
3. In the scenario of a short circuit fault, the former takes up some of the short-circuit current such that the thermal stability is assured.

A mix of stainless-steel strips, metal foil and padding (polycarbonate) are used in corrugated internal tube to prevent the distortion and destruction of the superconductor tapes.

- **SC Cooling system**

Engineer must make sure that special SC power cables are kept at the proper temperature in order to use them in our electrical system. Due to the need for a specialized refrigeration system, this can be difficult and expensive. To avoid overheating, we also need to properly design the cables and keep them away from heat sources. Certain parts made especially for this use are used to connect these cables to the power source.

For keeping things cold, it needs to know how much cooling power is needed. This depends on three things: the parts that connect everything together (termination or bushings), the special cable used, and the container (vacuum-jacketed cryostat) that keeps everything cold.

- **Liquid nitrogen (for YBCO)**

Liquid nitrogen is a very cold gas that is used to cool things down. It moves through a loop in a SC cable to keep it cool. It is widely used as a coolant for HTS systems. The main reasons for its popularity include its low boiling point, low density, and non-toxicity. Its permittivity (dielectric constant) is crucial for the design and performance of the HTS system.

There is a pump that makes sure the liquid nitrogen keeps flowing at the right speed and pressure.

- **High voltage insulating material (dielectric)**

Since HTS dielectrics have special characteristics and a high electrical breakdown field strength, they have been thoroughly studied. Nitrile rubber (NR) and silicon carbide (SiC) are two materials with excellent thermoelectric properties that are required for the highly temperature-dependent electrical behavior of HTS dielectrics. Hysteresis is reduced as a result of the dielectric constant decreasing in temperature.

- **Polyethylene sheath**

Polyethylene sheaths are like special coverings that can be used to keep things very cold. They work well because they have a good balance between being effective and not too hard to make. Additionally, increasing the thickness of the sheath can also enhance insulation performance.

- **Cryostat wall**

The cryostat is like a special container that keeps things very cold. Its design and insulation help to control how much heat from the surroundings gets inside. As much heat conductivity as possible must be achieved while preserving the necessary mechanical strength and insulation against low-temperature gas leakage. A variety of materials, including Kapton, Carbon Fiber Reinforced Polymer (CFRP), and Alloy 22, are used in the wall design to maximize the material's strength, insulation, and thermal conductivity.

Typically, the HTS cable cryostat has a flexible double-wall design with multilayer superinsulation (MLI) that is vacuum-jacketed. TN, or the ambient sink temperature, can vary from 245 to 320 K based on the time of year and the location of the HTS cable installation. The kind of dielectric material, wall thickness, surface quality, and material flaws all affect the HTS cryostat wall's design and functionality.

The effective or actual field installation thermal conductivity of the most commercially available vacuum-insulated flexible cryostats, k_{eff} is 0.0008 W/m/K. The amount of heat that can go through the cryostat length L, depends on the temperature of the liquid nitrogen inside Tv, and the sizes of the inner and outer tubes of the cryostat, D_{ci} and D_{co}.

The temperature difference that causes this heat transfer term is typically greater than 220 K for an external thermostat:

$$Q = \frac{2\pi k_{eff} L(T_{\infty} - T_v)}{ln(Dco \;/\; Dci)} \qquad (2.11)$$

To make the cryostat work better, it needs to push the cold stuff hard, which helps take away the heat from the special parts that can conduct electricity well.

SC cable joints and terminations

The terminations are like special connectors that are used to connect a superconducting cable to conventional overhead line or underground cable in electrical system. Terminations at each end of the SC cable have to be able to connect the cable to the electrical system and connect it to a special liquid that keeps it cold. These terminations must be designed very carefully and must work well even when there is a lot of electricity flowing through them and able to withstand tough weather conditions. Inside the terminations, they must change the electricity from the normal temperature of the electrical system to the very cold temperature of the SC cable. But they must do all of this without adding too much extra heat to the cold liquid.

The amount of heat produced at the end of the HTS cable system can be calculated using a formula. This formula takes into account the number of electrical connections and their capacity to handle a certain amount of electricity. Additionally, there is also heat generated from the surrounding environment.

$$Q_{end} = 45 * N_e * I_c + Q_{env} \qquad (2.12)$$

Where: Ne is the electrical connections, Ie is the capacity of the connection in kilo-amperes, with an additional heat load from the environment of Q_{env}.

Joints

A joint is like a special connector that connects two pieces of cable together. It's important because it's not possible to put long pieces of SC cable into a pipe, so we need to join smaller sections.

End Stations, Transformers and Converters

End stations and converters help electricity to travel better from where it is made to where it is used. They can change the electricity to make it stronger or weaker, depending on what is needed.

Chapter Three

3. Modeling of Superconductivity

3.1 Modeling of High Temperature Superconducting Cable

Modelling can assist the analysis of electromagnetic characterization of superconducting materials (bulks, wires, tapes, or composite cables). When superconductors are exposed to AC magnetic fields, high losses due to hysteresis are produced. In order to predict them it is important to have models to calculate the current and field profiles inside the superconductors.

The aim of these MODELING is to present elective numerical models to give a precise idea of the electric and magnetic field distributions inside the superconductor. The current distribution in a superconductor is commonly calculated by solving the Maxwell equations in differential form. In particular this part will focus on modelling high-T superconductors in external AC-magnetic field.

Integral formulations and finite element method (FEM) are tools commonly used for modelling the general physical problem. Whereas the FEM is required for problems of superconductors with finite dimensions and because of the high non-linearity, sometimes it is not too sufficient and requires a large numerical effort. Since the integral formulation needs to be solved in the conductor volume only, an alternative method based on an integral form of Maxwell's equations was developed by E. H. Brandt in 1994. Brandt's methods use Maxwell's equations to find an integral equation for the time derivative of the current density, which is better alternative for modelling HTS device due to their simplicity.

Brandt's formulation applied to superconductors with rectangular cross section and its Numerical simulations of this 2D problems with a E-J power law have been developed. Due to the non-linear behavior of the superconductor properties, the final differential equation obtained is highly non-linear and stiff.

Then by spatial discretization, the integral is converted into a matrix multiplication. The resulting system of ordinary differential equations (ODEs) is numerically integrated in time in order to find the current density. An advantage of this approach is that, unlike in differential formulation, no boundary conditions are needed. The equation, thus, has to be solved only in the superconductor volume. This greatly reduces the number of unknowns. Second, the ODE system can be more easily solved in MATLAB or free alternatives.

In order to study the electromagnetic behavior of a superconductor, Maxwell equations must be solved.

Maxwell's equations in conductors are a set of four equations that describe the behavior of electromagnetic fields. That describe the behavior of magnetic and electric fields. Since the 19th century, when James Clerk Maxwell formulated these equations, their application has proven extremely beneficial to several branches of physics, including electromagnetic, optics, and quantum mechanics.

$\nabla . B = 0$	*Gauss's Law for Magnetic Fields, there are no magnetic monopoles, and the divergence of the magnetic field is zero.*
$\nabla X H = J$	*Ampere's circuital law, this equation represents the exclusion of the magnetic field from the interior of a superconductor. This equation also describes the relationship between the magnetic field and the electric currents that generate it.*
$\nabla X E = -\frac{\partial B}{\partial t}$	*Faraday's Law indicates superconductors exhibit the Meissner effect, expelling magnetic fields, explained by the London equation's relation to field changes.*
$\nabla . E = \frac{\rho}{\varepsilon_o}$	*Gauss's Law for Electric Fields, In superconductors, the charge density ρ is typically zero due to the perfect conductivity. Therefore, Gauss's Law simplifies to: $\nabla \cdot E = 0$*

where E is the electric field, B is flux density, H is the magnetic field, J is the electric current density, $\mu_0 > 0$ is the magnetic permeability of the vacuum, and σ is the electric charge density.

In a superconductor, the magnetic field is excluded from the interior of the material, this means that the magnetic field component of Maxwell's equations is zero inside the superconductor. Additionally, the zero electrical resistance of the superconductor means that the electric field component of Maxwell's equations is also zero inside the material.

To effectively understand the electromagnetic properties of superconducting materials, it is essential to establish a clear relationship between magnetic flux density (B) and the magnetic field (H). This relationship is articulated by the equation $B = \mu_0 H$, where μ_0 denotes the permeability of the superconducting material.

3.1.1 Superconductors in Power Applications

The macroscopic relations of electric field (E) and current density (J) are crucial in understanding the behavior of hard superconductors, which can carry large currents for power applications. The electromagnetic properties are determined by vortex physics, but their behavior can be described through a relationship between E and J.

Various physical models describe the relationship between E and J in superconductors. Initially, Anderson and Kim derived the E(J) relationship based on thermally activated flux creep [72], which correlates the voltage across the superconductor to the speed of the vortices. When an external current passes through a Type-II superconductor, it applies to a Lorentz force on the vortices, resulting in the movement of magnetic flux vortices at a velocity *v*. This motion induces an electric field which is given by:

$$E = Bv \qquad (3.1)$$

Since vortices are pinned at defects, they need thermal activation to move. The probability of vortices jumping over energy barriers is governed by Arrhenius' law:

$$v \propto e^{-\mathrm{U(J)}/KT} \qquad (3.2)$$

where: U(J) is the pinning energy barrier, *k* is Boltzmann's constant and T is temperature.

As the current increases, the force acting on the vortices intensifies, significantly lowering the energy barrier U(J). This reduction makes it easier for the vortices to move. Furthermore, the activation energy U(J) for vortex motion decreases as the current density J approaches and surpasses J_c, facilitating even greater vortex activity. It is often modeled as:

$$U(J) = U_0\left(\frac{(Jc/|J|)^{\alpha}}{\alpha} - 1\right) \qquad (3.3)$$

where: α is a material constant, for the case $\alpha = -1$, corresponds to the thermally activated flux creep relation. As α approaches 0, the expression for $U(|J|) = U_0 \ln(J_c/|J|)$, as indicated in equation (3.8). Here, U_0 denotes the maximum pinning potential energy when the current density J is equal to 0, and J_c is the critical current density.

Using equation (3.1), and the electric field E(J) is proportional to the vortex motion, which depends on the activation energy.

$$\mathrm{E} = E_0^{-\frac{\mathrm{U(J)}}{kT}} \qquad (3.4)$$

And

$$\mathrm{E(J)} = E_c^{\left[\frac{U_0}{KT}\left(\frac{|J|}{J_c}-1\right)\right]} \qquad (3.5)$$

The electric field aligns with *J*, so add a directional term $\frac{J}{|J|}$:

$$\mathrm{E(J)} = \frac{J}{|J|}E_c^{\left[\frac{U_0}{KT}\left(\frac{|J|}{J_c}-1\right)\right]} \qquad (3.6)$$

Where: T is the temperature, and U_0 represents the activation energy of the vortex bundles, which is determined by the specific material. Boltzmann's constant is denoted as k = 1.38064852 times 10^{-23} J/K. E_c is the field, and J_c is the current density at which the electric field magnitude |E| reaches E_c depends on the material used.

The exponential term (3.6) reflects the competition between thermal energy (kT) and pinning strength (U_0), while E_c sets the scale for dissipation. The equation determines how the electric field increases with current in a nonlinear way for superconductors. It explains why superconductors have extremely low resistance below J_c but develop some dissipation when $J > J_c$.

In the mixed state (Type II), when a superconductor is exposed to an external magnetic field, magnetic vortices form within the material. The exponent n is related to the vortex pinning potential and temperature. Unlike Ohmic materials, where the electric field E(J) is directly proportional to the current density J, superconductors demonstrate a power-law relationship between these two variables. typically modeled as:

$$E \propto \left(\frac{|J|}{J_c}\right)^n \tag{3.7}$$

where $n > 1$ represents the nonlinearity of the material.

The electric field E(J) needs to match the direction of the current density vector J. To ensure this alignment, we add a term, $\frac{J}{|J|}$. We also introduce a reference electric field, E_c, to keep the equation consistent. When the current density reaches J_c the electric field E will equal E_c.

$$E(J) = E_c \frac{J}{|J|}\left(\frac{|J|}{J_c}\right)^n \tag{3.8}$$

with $n = U_0/kT$. This power-law E(J) has been found.

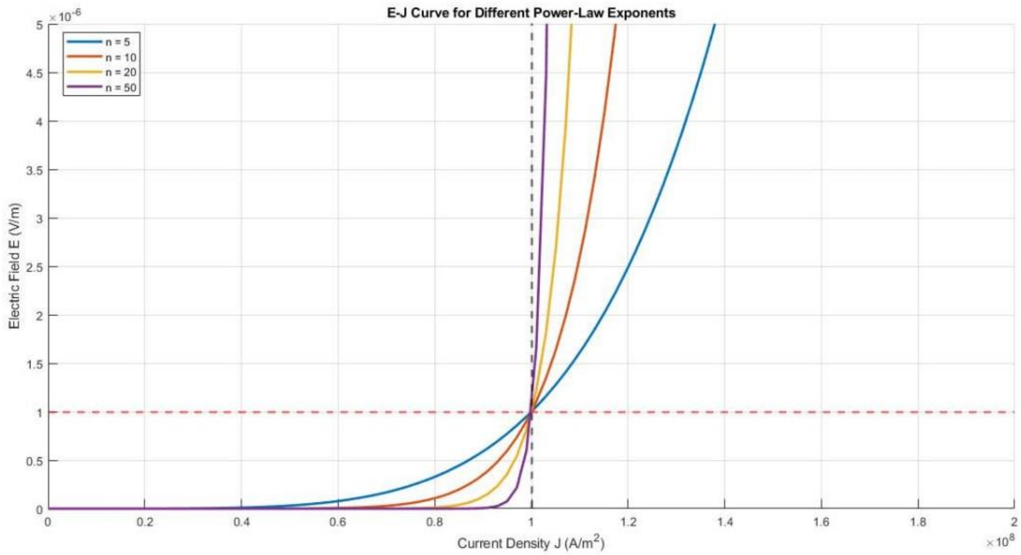

Figure 3.1: The nonlinear E(J) relation of a superconductor which is described by the power law.

Where: $J_c = 1 \times 10^8$ is the critical current density. $E_c = 10^{-6}$ V/m is the electric field when $J = J_c$, and n is the nonlinearity index, which typically ranges from 5 to 50 depending on the materials.

The equation is a phenomenological tool to model the nonlinear electrical behavior of superconductors. When $J < J_c$, the electric field is nearly zero (superconducting state), and $J > J_c$, the electric field increases nonlinearly, causing energy dissipation due to vortex motion. The higher the exponent n, the more sharply the material transitions from the superconducting state to the resistive state.

The simplified relation between electric field intensity and current density in power law depends on the actual temperature. The temperature affects the critical value of the current and the value of the exponent n. which is essential for understanding and optimizing the performance of high-temperature superconductors.

$$\frac{E}{E_c} = \left(\frac{J}{J_c\,(T)}\right)^{n(T)} \tag{3.9}$$

where: E - electric field intensity, V/m,

E_c - is the threshold at which the superconductor transitions, 10^{-6} V/m,

J - Applied current density, A/m^2, J_c - critical current density, A/m^2,

n - is the exponent that varies with material properties and temperature. It affects the steepness of the current-voltage characteristics and is defined for circuit modeling as:

$$n(T) = n_0 \frac{\mathrm{T}}{T_0} \tag{3.10}$$

where: T_0 - reference temperature (K), T - temperature of tape (K),
n_0 - exponent in T_0 temperature (for YBCO n_0 =15 - 50, T_0 = 77 K)

Assuming a homogeneous distribution of current density and electric field intensity, the power-law equation (3.9) for superconductors can be rewritten in terms of voltage u and current I:

$$\frac{\mathrm{u}}{u_c} = \left(\frac{\mathrm{I}}{I_c\,(T)}\right)^{n_0 \frac{\mathrm{T}}{T_0}} \tag{3.11}$$

where: U - Voltage across the superconductor (V), U_c - reference voltage (typically at the critical electric field Ec), I - Transport current, (A), I_c - Temperature-dependent critical current, (A).

By multiplying the components of equation (3.11), we can clearly establish the following important relationship:

$$\frac{\mathrm{U}}{\mathrm{I}} = \frac{U_c}{I_c\,(T)}\left(\frac{\mathrm{I}}{I_c\,(T)}\right)^{n_0 \frac{\mathrm{T}}{T_0}-1} \tag{3.12}$$

Then it can be presented in the form of resistance (U/I) = R:

$$R_{HTS} = \frac{U_c}{I_c\,(T)}\left(\frac{\mathrm{I}}{I_c\,(T)}\right)^{n_0 \frac{\mathrm{T}}{T_0}-1} = R_o\left(\frac{\mathrm{I}}{I_c\,(T)}\right)^{n(T)-1} \tag{3.13}$$

where: R_{HTS} – the resistance of HTS layer, (Ω), R_0 is a scaling factor n(T) controls the transition from superconducting to resistive state.

Here, resistance is defined as a power-law function of current, capturing the dissipative behavior that arises from the motion of magnetic vortices in type-II superconductors when the applied current surpasses the critical current. This behavior is what clearly differentiates superconductors from normal conductors and holds significant implications for their practical applications. The critical current, denoted as $I_c(T)$ in equation (3.13), is effectively represented by a linear relationship:

$$I_c\,(T) = I_{co}\frac{T_c - T}{T_c - T_o} \tag{3.14}$$

where: T_c - critical temperature, K,
I_{co} - critical current in T_0 temperature, A.

By substituting into equation (3.13), can effectively illustrate the relationship in equation (3.14) regarding the critical current Ic(T). This insight lays the groundwork for further analysis.

$$R_{HTS} = \frac{U_c}{I_c}\left(\frac{\mathrm{I}}{I_{co}\,\frac{T_c - T}{T_c - T_o}}\right)^{n_0\frac{\mathrm{T}}{T_0}-1} \quad (3.15)$$

After including the critical electric field intensity, the equation is:

$$R_{HTS} = \frac{E_c * L}{I_c}\left(\frac{\mathrm{I}}{I_{co}\,\frac{T_c - T}{T_c - T_o}}\right)^{n_0\frac{\mathrm{T}}{T_0}-1} \quad (3.16)$$

where: L - length of tape, m.

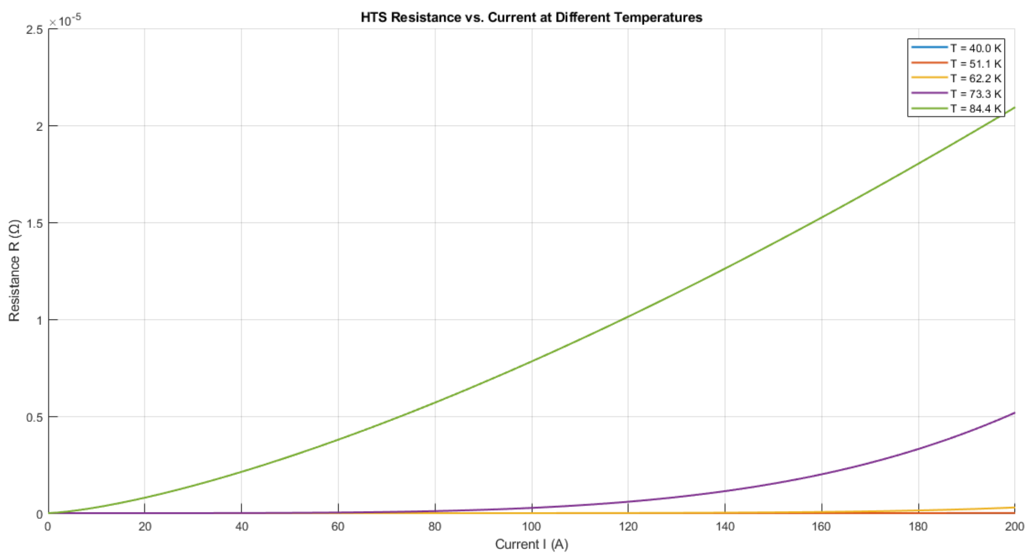

Figure 3.2: The resistance of HTS as a function of current & temperature incorporating critical parameters

At low temperatures (where T is much less than T_c), the SC operates in the SC state with negligible resistance. whereas the temperature close to above T_c, the resistance is significant as the current approaches the critical current I_c.

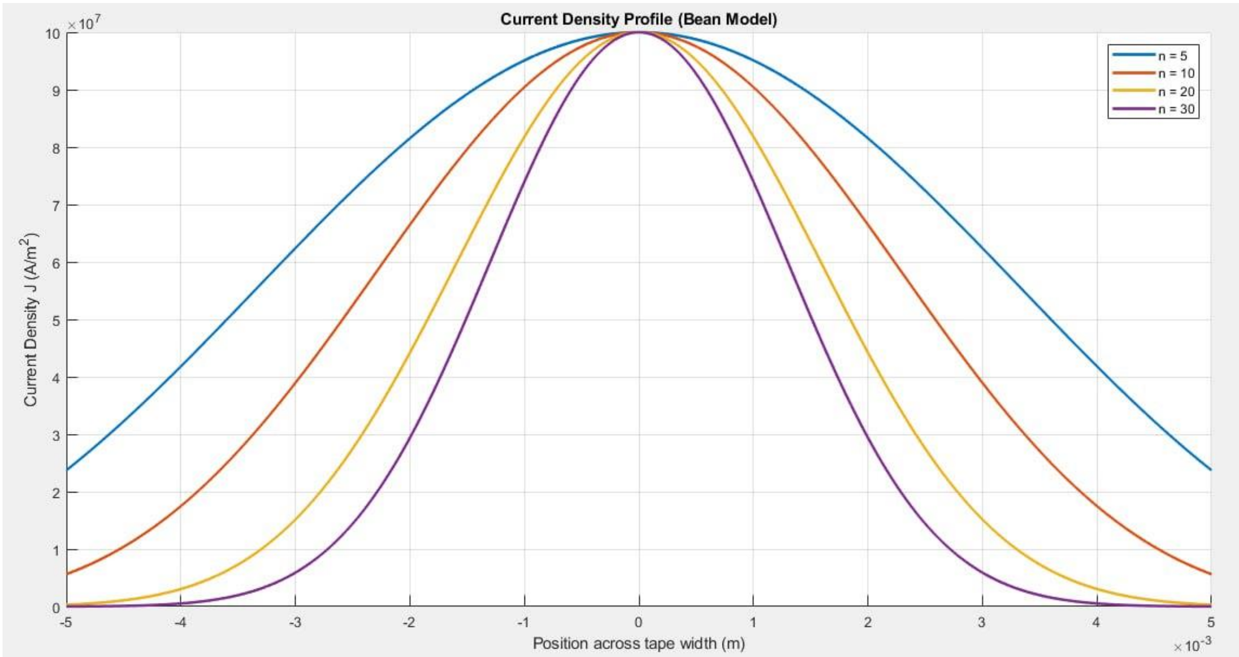

Figure 3.3: Non-uniform current density profile across the width of SC

In HTS tapes, the current density varies across the width due to multiple factors. The self-field effect generates a magnetic field around the tape that decreases critical current density (J_c) near the center, causing current to concentrate toward the edges. Additionally, the Bean Model explains that vortices are pinned in place, but once a certain current threshold is exceeded, they can lead to uneven current distribution, especially as the current-induced Lorentz force is weaker at the edges.

Geometrically, the edges of thin superconducting tapes experience less self-field influence, allowing higher current densities, while localized heating can create hotspots that further impact J_c and current flow. Overall, these effects result in a non-uniform current distribution across the tape. The parameter n in the model determines how sharply the current density decreases from the center toward the edges. It directly affects the inhomogeneity of current distribution across the superconducting tape.

Maxwell equations plus the two laws B-H and E-J are the tool used to calculate the electromagnetic behavior of a superconductor of arbitrary shape when a perpendicular arbitrary magnetic field is applied. Since the current is uniform along the tape axis, then a 2D model of the tape cross section can be used.

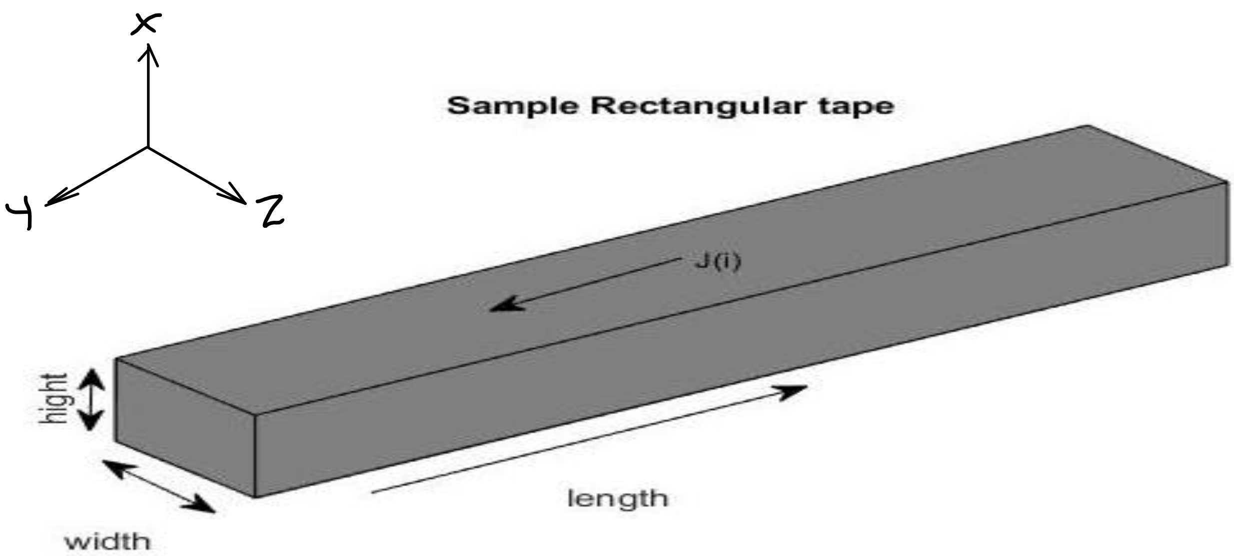

Figure 3.4: Sample rectangular bar geometries.

3.1.2 Brandt's Method

Brandt proposes a 2D model for long superconductors of arbitrary cross-section in perpendicular field which consists on solving the Maxwell equations in an integral form [70]. In that way, it avoids calculating the spatial derivatives and it is not necessary to consider the boundary conditions since the integral equations contain the appropriate differential equations plus the boundary conditions.

The analysis considers a superconductor cross-section placed in the xz-plane and a time dependent applied field B_a in the *y* direction (figure 3.4). This applied field induces current to flow along the y direction, and this current generates a magnetic field *H* without ŷ component.

From $B = \mu_0 H$, can express the magnetic field B using the vector potential A,

$B = \nabla X A$, and neglecting displacement current $\nabla X H = J$ then

Suppose that the superconductor is infinitely long along y. The problem is reduced to 2D in the x-z plane since all quantities are independent of y: Current density: $\mathrm{J} = J_y(\mathrm{x,z})\,\hat{\mathrm{y}}$ and Vector potential: $\mathrm{A} = A_y(\mathrm{x,z})\,\hat{\mathrm{y}}$

The magnetic field is:

$$B = \nabla X A = \left(\frac{\partial A_y}{\partial A_x}, -\frac{\partial A_y}{\partial A_z}, 0\right) \quad (3.17)$$

Substitute $B = \nabla X A$ into $\nabla X B = \mu_0 J = \nabla X(\nabla X A)$ and
Using the vector identity: $\nabla X(\nabla X A) = \nabla(\nabla . A) - \nabla^2 . A$

Choosing the Coulomb gauge ($\nabla . A = 0$): $-\nabla^2 . A = \mu_0 J$ and in 2D (current flowing along y), the vector potential has only a *y*-component A_y, and the equation reduces to:

$$-\nabla^2 . A_y = \mu_0 J_y \tag{3.18}$$

To solve the Poisson equation (3.18), we use Green's function *G*(r, r′), which satisfies:

$$\nabla^2 G(\mathrm{r}, \mathrm{r}') = \delta(\mathrm{r} - \mathrm{r}') \tag{3.19}$$

In 2D polar coordinates, the Laplacian for a radially symmetric function *G*(*ρ*) and for *G* depend only on the distance $\rho=|\mathrm{r}-\mathrm{r}'|$

$$\nabla^2 G = \frac{1}{\rho}\frac{1}{d\rho}\left(\rho \frac{dG}{d\rho}\right) \tag{3.20}$$

$$\int_v \nabla^2 G dA = \int_v \delta(\mathrm{r} - \mathrm{r}') dA = 1 \tag{3.21}$$

Following integration and application into Green's function, a basic solution to a differential equation where the source term is a delta function. its Laplace solution is:

$$G(r, r') = \frac{1}{2\pi} ln(\mathrm{r} - \mathrm{r}') \tag{3.22}$$

3.1.3 Electromagnetic Potentials and Their Relation to the Sources

The electromagnetic problem can be approached through the vector potential, A, which is essential for integral and variational methods. In superconductors, applying the delta function identity aids in solving for the current density, J(r). This allows for the representation of the current density as a sum of delta functions at discrete points, with each point representing a segment of the total current.

$$J(\mathrm{r}) = \int_{\mathrm{V}} \mathrm{d}^2\mathrm{r}' \mathrm{J}(\mathrm{r}')\delta(\mathrm{r} - \mathrm{r}') \tag{3.23}$$

The current density is discretized into localized elements:

$$J(\mathrm{r}) = \sum_{j=1}^{N} J_j \delta(\mathrm{r} - \mathrm{r}') \tag{3.24}$$

Where: J_j is the current density in element *j*, and δ is the Dirac delta function.

Equation (3.23) represents the continuous current density as a superposition of contribution localized at discrete position r′(one of each segment). It is well understood that due to electromagnetic phenomena in superconductors, including self-field effects and flux pinning, the current density is inherently non-uniform across the width w.

The current density J(r) can be expressed as an integral over the entire volume v, using the Dirac delta function δ(r−r′). This formulation indicates that the value of J(r) at a specific point r is obtained by summing the contributions from all possible current sources J(r'). The delta function ensures that only the value at the point where r = r' is considered in the sum.

The vector potential A(r) for a two-dimensional superconducting line carrying a current density J(r′) along the y-axis is from the general solution of equation (3.18) is:

$$A_y(\mathrm{r}) = -\mu_0 \int G(r,r') J_y(\mathrm{r}') \ln|\mathrm{r}-\mathrm{r}'| \mathrm{d}^2 r' \tag{3.25}$$

Combining equations (3.22), (3.23), and (3.29) finds that:

$$\mathrm{A}(\mathrm{r}) = -\frac{\mu_0}{2\pi} \int \mathrm{J}(\mathrm{r}') \ln|\mathrm{r}-\mathrm{r}'| \mathrm{d}^2 r' \tag{3.26}$$

Where: A(r): magnetic vector potential in a 2D superconducting tape subjected to a current density distribution, μ0: Permeability of free space, J(r′): Current density (flowing along ŷ, perpendicular to the cross-section), ln|r−r′|: Green's function for 2D systems describing how current elements contribute to A(r), d^2r': Integration over all current sources.

The conductor is divided in N elements numbered i = 1,2…N, each carrying a uniform current density, J_i over a small area ΔS_j, the integral transforms into a summation. The magnetic vector potential at some point r_i can then be expressed as a linear combination of element current J_i and an external contribution H_{extr}:

$$\mathrm{A}(\mathrm{r}) = -\frac{\mu_0}{2\pi} \sum_{j=1}^{N} J_j \ln|r_i - r_j| \Delta S_j \tag{3.27}$$

The equation can be represented as a matrix equation with a matrix M_{ij}, where the Green's function $\ln|r_i - r_j|$ illustrates the interaction between points r_i and r_j. The matrix M_{ij} is defined for the interaction between the i^{th} point and the j^{th} current element as:

$$M_{ij} = \frac{1}{2\pi} ln|r_i - r_j| \Delta S_j \tag{3.28}$$

The magnetic vector potential at the observation point r_i can be written in matrix form as:

$$A(r_i) = A_{extr} + \frac{\mu_0}{2\pi}\sum_{j=1}^{N} M_{ij}J_j \tag{3.29}$$

where: A is vector of magnetic vector potential values at observation points, H_{extr} is vector representing external contributions, M is m×N matrix representing the interactions between current elements(N) and observation points(m), J is vector of current densities in the current elements.

The contribution from the external magnetic field H_{extr} is chosen such that $\nabla \times H_{extr}$ Closed-form expressions for M and H_{extr} will be derived for several cases. From Maxwell's equations follows that:

$$\frac{\partial A}{\partial t} = -E - \nabla\phi \tag{3.30}$$

Where: The expression ∂J/∂t refers to the evolution of current due to vortex motion and flux flow resistivity, while ∇ϕ represents the electrostatic potential term, which may be trivial.

Taking the time derivative of both sides:

$$\frac{\partial A(r_i)}{\partial t} = \frac{\partial H_{extr}}{\partial t} + \frac{\mu_0}{2\pi}\sum_{j=1}^{N} M_{ij}\frac{\partial J_j}{\partial t} \tag{3.31}$$

Thus, equating with differentiated equation will get:

$$E(r_i) = -\frac{\partial H_{extr}}{\partial t} - \frac{\mu_0}{2\pi}\sum_{j=1}^{N} M_{ij}\frac{\partial J_j}{\partial t} - \nabla\phi \tag{3.32}$$

In type-II superconductors, the relationship between current density (J) and the applied electric field follows a power-law. This means that as the electric field is varied, the current density will change in a predictable, non-linear manner according to this mathematical relation.

By rearranging the terms, it can be rewritten in the form $M_j = f(t, J)$

$$\sum_{j=1}^{N} M_{ij}\frac{\partial J_j}{\partial t} = -\frac{2\pi}{\mu_0}\left(E + \frac{\partial H_{extr}}{\partial t} + \nabla\phi\right) \tag{3.33}$$

One of the various ODE solvers available can be used to numerically integrate the problem in this form. This connects induced electric fields and scalar potentials to time-dependent currents in superconducting components.

Before equation (3.32) can be integrated numerically, the matrix M must be determined. The following section will focus on the integration of the vector potential to obtain M.

3.1.4 YBCO of Superconducting Modelling

YBCO and other HTS compounds possess highly anisotropic and non-linear electromagnetic properties across their dimensions. The performance improvements of the YBCO power cables rely heavily on optimization designs to avoid unnecessary losses. However, such design optimizations can only be achieved with the comprehensive and accurate knowledge of the electromagnetic property distributions across the HTS materials [50]. Therefore, the numeric modelling of the HTS materials' electromagnetic properties become necessary for design optimization research.

In contrast to Brandt's publication, this analysis incorporates discrete geometry from the outset to evade the complications of integral equations. The elements are defined by coordinates a_i, b_i, c_i, and d_i, where i ranges from 1 to N. Each element is characterized by a sheet current density J_i oriented in the y-direction. Focusing on an infinitely long rectangular bar segmented into N elements, each defined by the ranges a < x < b and c < z < d, the bar sustains a uniform current density J in the y-direction. To determine the vector potential, a specific double integral must be computed.

$$A_y(x,z) = -\frac{\mu_0}{2\pi} J \int_c^d \int_a^b \ln\left(\sqrt{(x-x')^2 + (z-z')^2}\right) \mathrm{d}x' \mathrm{d}z' \tag{3.34}$$

where: (a,b) defines the limits in the x′ direction, (c,d) defines the limits in the z′ direction and J is the uniform current density flowing in the y direction.

The **kernel** of the integral is:

$$\ln\left(\sqrt{(x-x')^2 + (z-z')^2}\right) = \frac{1}{2}\ln((x-x')^2 + (z-z')^2) \tag{3.35}$$

where (x, z) is the observation point, and (x′, z′) are coordinates over the rectangular source element *j*.

This expression is evaluated by substituting $u = x - x'$ and $v = z - z'$ and then integrating by parts repeatedly:

$$A_y(x,z) = -\frac{\mu_0 J}{4\pi} \int_{z-c}^{z-d} \int_{x-a}^{x-b} \ln(u^2 + v^2) \mathrm{d}u \mathrm{d}v \tag{3.36}$$

First step 1: Integrate with respect to u:

$\int_{x-a}^{x-b} \ln(u^2 + v^2) du$ and let's denote this integral as F(v,x,z)

Integrate the result from Step 1 with respect to v:

$$A_y(x, z) = -\frac{\mu_0 J}{4\pi} \int_{z-c}^{z-d} \mathrm{F}(\mathrm{v}, \mathrm{x}, \mathrm{z})\, dv \tag{3.37}$$

The integrals are combined and simplified, leading to contributions from the edges of the rectangular bar at $x = a$, b and $z = c$, d.

After simplification, the full antiderivative is:

$$\iint \ln(u^2 + v^2) du\, dv = uv(ln(u^2 + v^2) - 3) + u^2 \tan^{-1}\left(\frac{u}{v}\right) + v^2 \tan^{-1}\left(\frac{u}{v}\right) \tag{3.38}$$

Evaluate the antiderivative at the bounds $u = x - a\ to\ u = x - b\ and\ v = z - c\ to\ v = z - d$

$$A_y(x, z) = -\frac{\mu_0 J}{4\pi} \left[\left[uv(\ln(u^2 + v^2) - 3) + u^2 \tan^{-1}\left(\frac{u}{v}\right) + v^2 \tan^{-1}\left(\frac{u}{v}\right) \right]_{u=x-a}^{x-b} \right]_{v=z-c}^{z-d} \tag{3.39}$$

The values of *matrix* M are thus given by:

$$M_{ij} = -\frac{1}{2} \left[\left[uv(\ln(u^2 + v^2) - 3) + u^2 \tan^{-1}\left(\frac{u}{v}\right) + v^2 \tan^{-1}\left(\frac{u}{v}\right) \right]_{x_i - a_j}^{x_i - b_j} \right]_{z_i - c_j}^{z_i - d_j} \tag{3.40}$$

The coordinates are used to evaluate the vector potential at each element's center: $x_i = (a_i + b_i)/2$ and $z_i = (c_i + d_i)/2$.

To simulate a SC tape in a perpendicular field carrying transport current, the vector potential of the applied axial field can be written as:

$$H_{ext} = -xB_{ext}(t)\hat{y} \qquad and \qquad \nabla\varphi = 0 \tag{3.41}$$

So that the external field (B_{ext})is:

$$B_{ext} = \nabla\, X H_{ext} = B_o sin(\omega t)\hat{z}$$
(3.42)

The vector B_{ext} can be computed by finding a vector potential that satisfies this equation $\nabla \times H_{ext} = B_{ext}$. And for simplicity assuming that, H_{ext} has only z-component. $B_{ext} = A_z(x,t)\hat{y}$ and the external vector potential is $H_{ext} = \frac{B_o}{\omega} cos(\omega t)\hat{x}$

Compute relation from maxwell equation of (3.9) ∂A/∂t:

$$\frac{\partial \text{A}}{\partial t} = \frac{B_o}{\omega} cos(\omega t)\hat{x} = -\text{E} - \nabla\phi \qquad (3.43)$$

Thus,

$$\text{E} = B_o sin(\omega t)\hat{y}$$
(3.44)

The electric field inside the bulk is often assumed small because superconducting material has near-zero resistance. If an electric scalar potential ϕ is present, it accounts for voltage drops due to normal resistive state or induced charge distribution, for full superconducting state ϕ often ignored (no scalar potential variation).

The current distribution is found by numerical time-integration of equation (3.32). Whereas the detail integration was carried out using MATLABs. Integrate the system of ODEs, the time segment's current distribution is given by:

$$J_i(t) = J_i(0) - \frac{2\pi}{\mu_0} \sum_{j=1}^{N} (M^{-1})_{ij}[\text{Et} + B_o sin(\omega t)] \qquad (3.45)$$

If we assume no applied electric E=0 field and J(0) = 0 (initially no current), it simplifies to

$$J_i(t) = -\frac{2\pi B_o}{\omega \mu_0}(M^{-1})_{ij} sin(\omega t)\hat{y} \qquad (3.46)$$

Because the geometry is symmetric in the *xz*-plane and Since H_{ext} and its contribution to the electric field ($-\partial H_{ext}/\partial t$ are odd functions of *y*, the condition of transport current condition is automatically satisfied, and the gradient of the electric potential $\nabla\varphi$ can be set to zero.

This Jacobian indicates how small variations in the integrated equation, which considers both the constant electric field and a time-dependent external field, influence the discrete current value.

The following components transform the Jacobian matrix into a diagonal matrix:

$$\frac{\partial \text{f}_\text{i}}{\partial \text{J}_\text{i}} = -\frac{2\pi}{\mu_o}\frac{\partial \text{E}_\text{i}}{\partial \text{J}_\text{i}} = -\frac{2\pi}{\mu_o}\frac{\text{E}_\text{c} n}{\text{J}_\text{c}}\left|\frac{\text{J}_\text{i}}{\text{J}_\text{c}}\right|^{n-1} \qquad (3.47)$$

When J_c and n are constant, the expression is exact; otherwise, it serves as an approximation of the Jacobian.

It is possible to apply a nonzero transport current to a superconducting sample by using the electric potential gradient ∇φ on the right side of (3.32). Since ∇φ is homogeneous across the strip cross section, it is equal along the other two sides and functions as a voltage source, guaranteeing homogeneity throughout the superconducting strip's cross section.

The voltage source can be operated in a closed loop mode to simulate a current source.

$$\nabla\phi = \gamma(I_{set}(t) - I(t))\hat{y} \tag{3.48}$$

The feedback constant γ is used to control the desired current $I_{set}(t)$ and the actual current I(t), with a value of γ = 100 V/Am resulting in an error less than 0.1% of the amplitude of Iset.

An additional term, $\partial(\nabla\varphi)_i/\partial J_j = \gamma w_j$, is added to the Jacobian matrix, resulting it more complex.

$$\frac{\partial f_i}{\partial J_i} = -\frac{2\pi}{\mu_o}\begin{cases} \dfrac{2\pi}{\mu_o}\dfrac{E_c n}{J_c}\left|\dfrac{J_i}{J_c}\right|^{n-1} + \gamma w_{j,} & i = j \\ \gamma w_j & i \neq j \end{cases} \tag{3.49}$$

With a transport current of $I_{set}(t) = I_o\sin(\omega t)$, the ac loss per cycle is calculated using the dense Jacobian matrix with constant off-diagonal elements.

It is possible to observe the current distribution within SC, while it is simultaneously exposed to an external magnetic field.

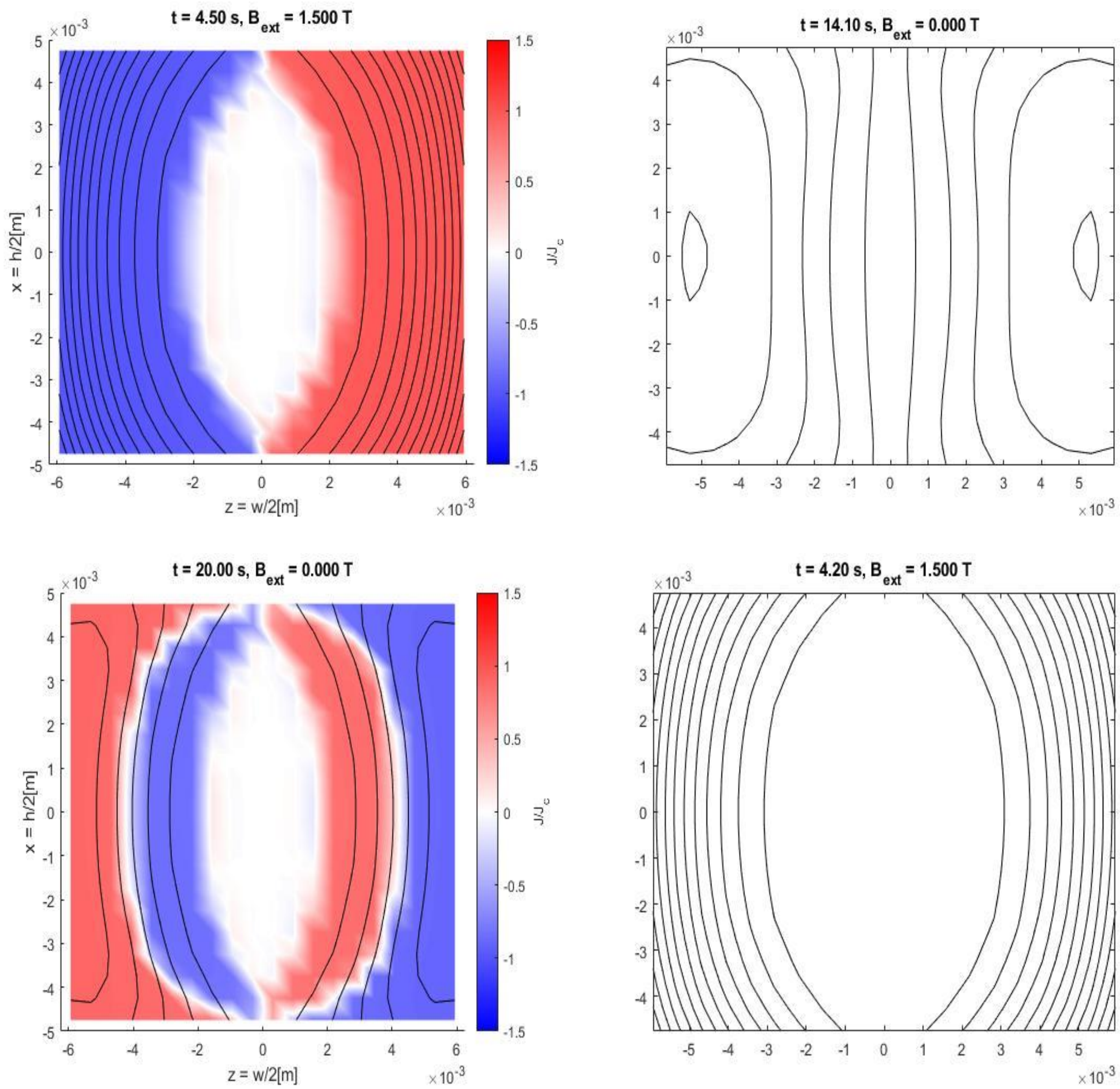

Figure 3.5: Simulation results of current & magnetic field distribution in superconductivity cable

Figure 3.5 illustrates the hysteretic behavior of screening currents and magnetic flux in a superconducting bulk during and after exposure to an external magnetic field. Initially, when the external field is increased, a screening current density $J \approx -J_c$ (which opposes the applied field) flows in the outer region of the superconductor, effectively shielding the interior from flux penetration. As a result, the core remains both current-free and flux-free.

When the external field is reduced back to zero, a reversed screening current $J \approx +J_c$ forms. However, the penetration depth of this current is halved compared to the initial negative current due to a doubled effective change in current density ($\Delta J = 2J_c$). This asymmetry occurs because the positive current layer forms farther from the central axis, which leads to a larger magnetic moment, since the moment scales with the area enclosed by the current loop.

Consequently, even after the external field is removed, the bulk material retains a residual magnetic moment. This phenomenon is characteristic of flux-pinning hysteresis in type-II superconductors. The behavior described aligns with the critical-state model (Bean model), which explains that irreversible flux motion and persistent currents govern the magnetization dynamics.

The magnetic field strength in a high-temperature superconductor (HTS) core is highest at the surface and decreases linearly toward the center, primarily due to the Meissner effect, which causes current to flow only on the surface. As the distance from the HTS core increases, the magnetic field follows an inverse relationship ($B \propto 1/r$). Elevated magnetic fields can amplify AC losses from hysteresis and eddy currents. Moreover, overly strong magnetic fields can negatively affect the critical current density and potentially cause a quench, thus disrupting the superconducting state.

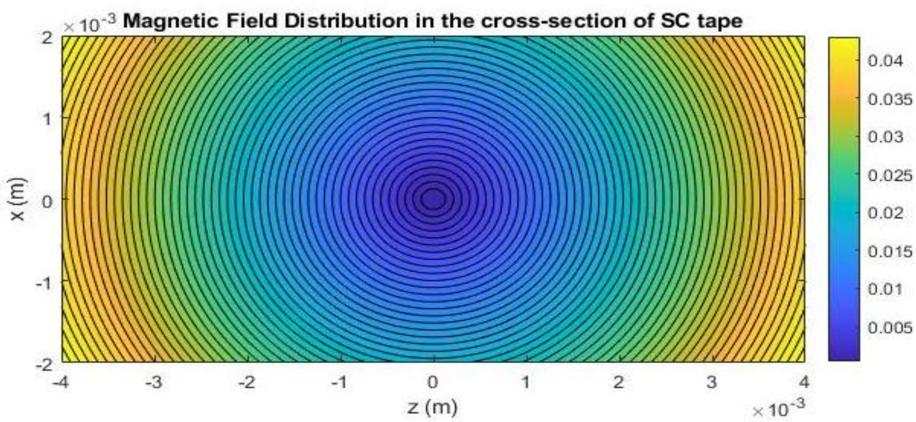

Figure 3.6: The magnetic field in the cross-section of the superconducting cable view

The illustration on figure (3.6) creates a contour plot that visualizes the magnetic field in the cross-section of a superconducting cable. The x and z axes represent spatial coordinates in meters, while the contour lines indicate regions of constant magnetic field strength in Tesla (T). A color bar alongside the plot illustrates the magnitude of magnetic field, with cooler colors (such as blue) indicating lower magnetic field strengths and warmer colors (such as yellow or red) representing higher strengths.

If the AC fields penetrate deeper or are stronger at certain frequencies and current densities, these losses would indeed influence the overall field distribution within and around the HTS cable, potentially deviating from the purely surface-dominated field described for the HTS core in the source

Type-II superconductors (HTS), magnetic fields can enter the material as quantized vortices. Unlike type-I superconductors, the magnetic field is not entirely excluded but instead varies depending on factors such as current density and operational conditions.

The dissipation due to time varying magnetic field is due to the induced current in the SC. The power dissipation per unit volume is given by: $P(t) = \mathrm{J(t)E(t)}$

The overall current density (assuming all segments contribute similarly) is

$$J_i(t) = -\frac{2\pi B_o(t+1)}{\mu_0}\sum_{i,j=1}^{N} (M^{-1})_{ij} sin(\omega t)\hat{y} \tag{3.50}$$

Therefore, the evaluation of the AC loss for superconducting materials can be calculated once **J** is known:

$$P_{AC} = \frac{2\pi {B_o}^2(t+1)}{\mu_0}\sum_{i,j=1}^{N} (M^{-1})_{ij} sin^2(\omega t) \tag{3.51}$$

Where: B_0: Amplitude of the applied magnetic field, t: Thickness of the superconducting tape, μ_0: Permeability of free space, a physical constant, N: Number of superconducting tapes in the system, ω: Angular frequency of the applied AC field

The transient factor (t+1) in this instantaneous formulation would vanish in a steady-state periodic solution once the initial transient has passed. In a system of superconducting tapes exposed to an external alternating magnetic field, it measures the AC losses. When exposed to time-varying magnetic fields, the superconductors' internal magnetic vortices migrate, causing energy dissipation and losses.

The computation was performed for a range of non-linearity index n values. The AC loss of a "hard" superconductor as defined by the critical state model is displayed for comparison (n→∞). For this, Brandt [20] and Zeldov [21] came up with a precise expression.

$$Q = \frac{2\mu_0 {J_c}^2 w^3}{\pi}\left\{\ln\left(\cosh\left(\frac{\pi B_0}{\mu_0 J_c}\right)\right) - \frac{\pi B_0}{2\mu_0 J_c} tanh\left(\frac{\pi B_0}{\mu_0 J_c}\right)\right\} \tag{3.52}$$

Where: Q: Energy loss across one cycle per unit length, $\mu_0 = 4\pi\times10^{-7}$ H/m (permeability of free space), J_c: Critical current density of superconductor (A/m², typically for YBCO at 77 K), B_o: peak external magnetic field amplitude (T, perpendicular to the strip), w: half-width of superconducting strip, cosh and tanh: hyperbolic cosine and tangent functions (parameters controlling field penetration behavior), and $\pi B_o/(\mu_0 J_c)$: normalized magnetic field (field determining the loss behavior).

The numerical result becomes closer to this precise statement as the n-value increases. To convert to power loss (W/m), multiply by the frequency (P= Q × f w/m).

Power dissipation results from the motion of vortices influenced by currents and magnetic fields. According to the critical state model, when the current density exceeds the critical current density J_c, the movement of these vortices begins, which can lead to energy loss. By managing current densities effectively, we can minimize energy loss and enhance the performance of these materials.

Figure 3.7: Simulated power dissipation in a superconducting device.

Figure (3.7) presents the AC power loss data for a superconducting device over a distance of 15.3 km, indicating a low power loss of 0.57297 watts per meter. The analysis examines an external magnetic field of 1.5 T applied in the y-direction, which increases and then decreases at a rate of 0.2 T/s over 5 seconds. The symmetric design of the setup ensures compliance with the zero-transport current condition, which is crucial for the accuracy of the results.

The total loss is measured in watts per meter (W/m) and is essential for the design of cryogenic systems. Moreover, the power curve may display harmonics and nonlinearities due to the E-J power law (n=21), leading to sharper peaks near critical current levels.

Superconductors react to magnetic fields, potentially distorting field lines. Energy loss within these materials can peak when current or field changes are most rapid. If the current density surpasses a critical threshold (J_c), energy dissipation will occur in specific areas, which can be identified in current distribution visualizations. Observing energy loss is possible in a bar experiencing both an external magnetic field and a carried current. The flow of this transport current is governed by adjustments to the gradient of the electrical potential (∇φ).

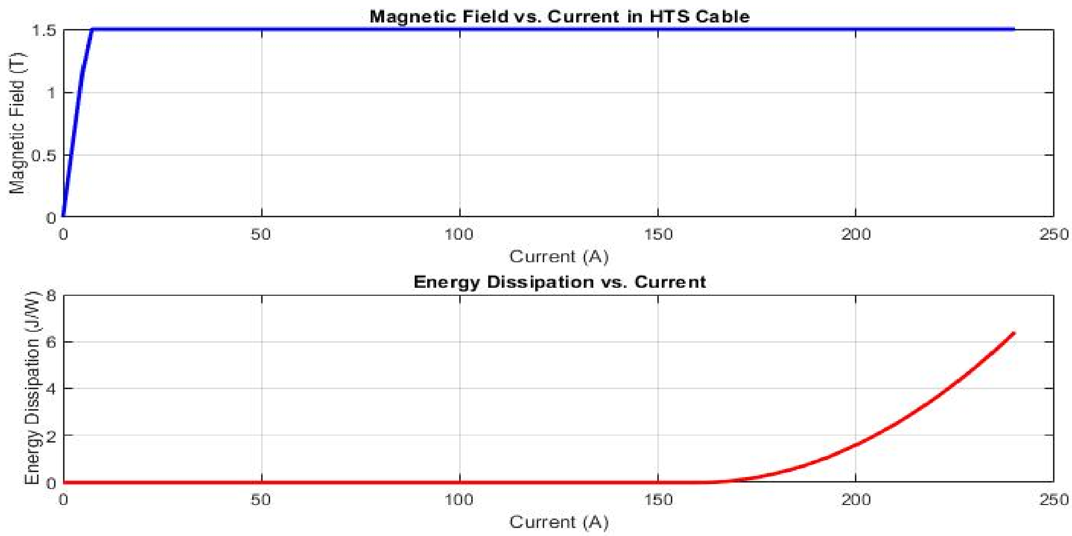

Figure 3.8: The energy dissipation in a SC influenced by the current and the magnetic field.

Magnetic field increases linearly with the current as per the external field limit, which is consistent with the expected Bean critical state model (the higher the current, the stronger the induced magnetic field). At high currents, the magnetic field saturates at B_{extr} (1.5T) indicating that the HTS cable becomes fully penetrated by flux. Flux pinning prevents more flux from entering after that. The curve shows that at high currents, the superconductor perfectly shields the field, but at high currents (> I_c=160A), the flux enters the cable causing energy dissipation.

Chapter Four

4. Conceptual Design of Superconducting Cable Systems for Use in The 132kV grid

The concept design of HTS cable systems emphasizes efficient power transmission in the challenges of integrating with the power grid in a efficient manner and capacity. Important issues include material selection, cooling configurations, and insulation arrangements for performance optimization. The focus would be to replace the current 132 kV AC line with an HTS equivalent and a 33 kV HTS AC cable, which would be the one necessitating higher current for the reduced voltage.

4.1 Site Selection

A technical layout of superconducting cables for use in place of 132 kV double circuit line which connect transmission line total distance is of approximately 15.3 km and spans is from Kalilti I to Black Lion Line.

Section 1: Kalilti I - Addis Center 13.4 km

Section 2: Black Lion Line. 1.9 km

Table 4.1: Planned system line data (conventional line)

Item	Description
Project Name	Addis Center Substation (New)
Current rating	558A
Voltage Level (kV)	132
Equipment	132kV Double Circuit Line
Length	15.3 km
Rating (MVA)	115
Project Detail	Kaliti I - Addis Center Line/Addis Center - Black Lion Line
Tower Configuration	Double
Conductor Type	AAAC
Conductor Size (mm^2)	166
Conductor Code	Ash

4.2 Design Specifications

The process of YBCO AC cable conceptual design is described, especially the importance of defining the operational parameters corresponding to a specific application. The first step is the definition of the specific target application requirements responsible for deriving the operational parameters, which the cable should be able to withstand. The design parameters required to operate YBCO cables *are given in Table 4.2.*

Table 4.2: Designed superconducting line specification

Parameter description	Symbol	Value
Operational current	I_{op}	503 A & 2012 A
Operational voltage	U_{op}	132 kV & 33 kV
Cable length	L	15.3 km
Fault current	I_{fault}	3 kA
Fault duration	T_{fault}	10 sec
Operational temperature	T_{op}	65 to 77 K
Maximum outer diameter	D_{max}	162 mm

4.2.1 Boundary Conditions

The maximum allowable temperature rise during fault propagation is the only boundary condition required to solve the system of equations because of the streamlined design approach. The highest annealing temperature for YBCO is 400 K, at which YBCO does not degrade, to avoid superconductor breakdown during defects [74]. T_{end} = 330 K was chosen as the thesis's maximum temperature during the fault. The Ethiopian environment's impact on temperature makes this conceivable.

The maximum outer diameter was set to 162 mm. This is derived from the fact that larger diameters significantly reduce the amount of cables that fit on standard drums. Therefore, it appeared sensible to limit the diameter to dimensions that are relevant for a full-scale cable.

4.2.2 Temperature and Pressure Profile

The purpose of the coolant is to remove heat that has leaked through the cryostat or was generated due to dissipation. The design of the superconducting cable includes hydraulic, electrical and thermal considerations. Temperature and pressure profiles of a YBCO superconducting cable can be influenced by factors such as the cable geometry, cooling system, and operational parameters.

Table 4.3: Pressure and temperature constraints for the designed lines

Coolant	$Temperature_{in}$	$Temperature_{out}$	$Pressure_{in}$	$Pressure_{out}$
LN_2	65k	77k	25 bar	>5 bar

Liquid nitrogen cooling

Nitrogen can be liquid until the triple point at 63.151 K. With a safety margin against freezing and boiling, the operational temperature range of *YBCO* cables is usually between 67 K and 93 K.

Table 4.4: Fixed point properties of nitrogen

	Temperature (K)	Pressure (MPa)	Density (mol/dm3)
Critical point	126.192	3.34	11.184
Triple point	63.151	0.013	

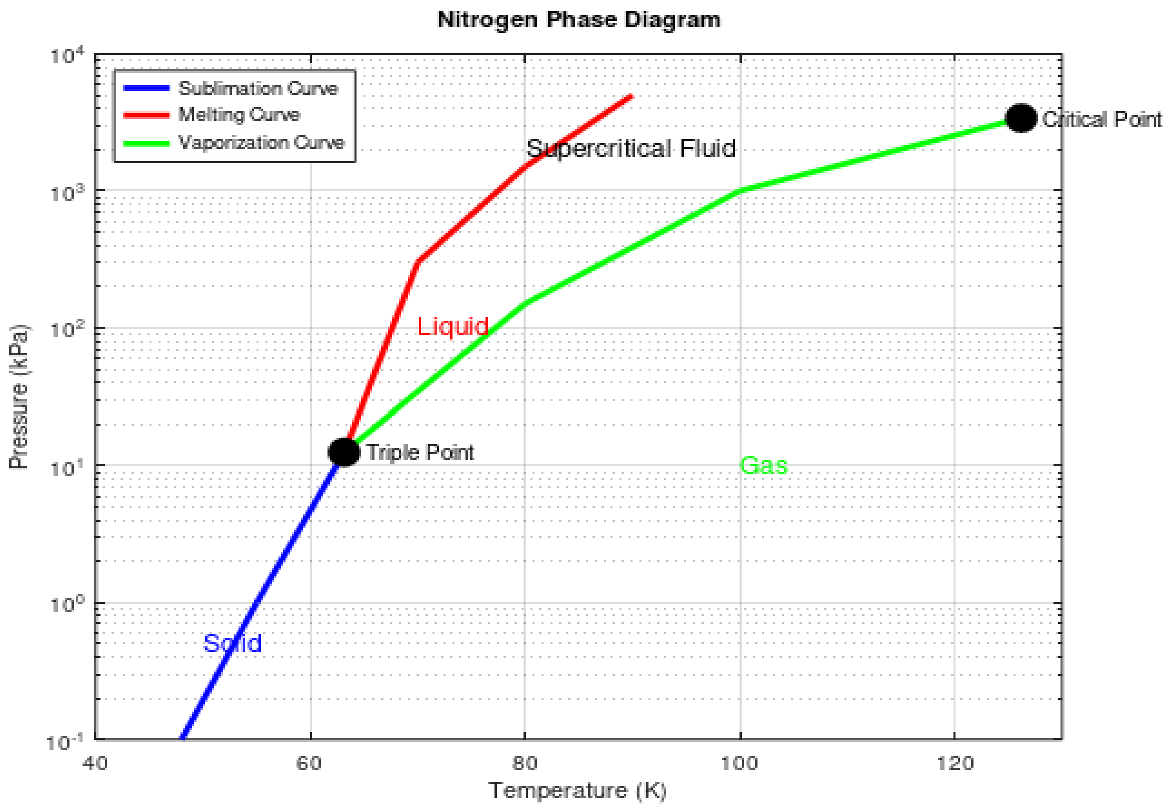

Figure 4.1: Liquid nitrogen phase diagram within the operational range of LN-cooled HTS cables

The static thermal load from the environmental heating depends on the thermal performance of the cryostat used in the system. The HTS cable cryostat typically is a flexible double-wall construction with vacuum-jacketed multilayer superinsulation (MLI). The ambient sink temperature, TN, could range from 245 to 310 k, depending on the geographical location of the HTS cable installation and time of the year [75] [76].

The typical commercially available vacuum-insulated flexible cryostats have an effective or actual field installation thermal conductivity, k_{effc}, of 0.0008 W/m/K. The local heat transfer through the cryostat per unit length can be calculated using below equation and depends on the local LN_2

temperature, Tv, and the cryostat inner and outer tube diameters, D_{ci} and D_{co}. The temperature difference driving this heat-transfer is typically more than 220 K for the outer cryostat:

$$Q = \frac{2\pi * K_{effc} * L * (T_{\infty} - T_v)}{D_{co}/D_{ci}} \quad (4.\ 1)$$

Table 4.5: The local heat transfer through the cryostat for different temperatures

Set T_{∞} =310K, with different T_v	Value (Q in w)	Set T_v =77K, with different T_{∞}	Value (Q in w)
70k	5232.96	280k	4426.2
73k	5167.55	300k	4862.3
75k	5123.94	315k	5189.35
77k	5080.33	320k	5298.37

4.3 Superconducting Cable Build-up

The superconducting cable consists of two main functional components, the cable core and the cryostat line. The cable core performs all electrical functions, such as power transport, electrical insulation, magnetic display and neutral conductor. The line cryostat is used for thermal insulation. The actual coolant flow depends on the cooling concept.

Figure 4.2: HTS cold dielectric cable configuration layout

SC tape former and HTS layer

The reviewed second-generation SC tapes have a layer structure consisting of a metal foil of 50-100 µm thickness as substrate, a buffer layer of various ceramic materials, a superconductor layer of approx. 1 - 2 µm thickness for example of yttrium-barium copper oxide, as well as a thin silver layer and copper stabilization. Width and current density vary depending on manufacturer and are 2 - 12 mm or 250 - 600 A/cm. The SC tapes are wrapped directly next to each other, if possible, without any gap, on the former with compensation layer It is possible to use several layers of the superconducting SC tape to increase the current carrying capacity.

Figure 4.3: Layer structure of Superconducting SC Tape

HTS shield with neutral conductor layer

The protective shield is mounted on the dielectric, which also consists of a superconductor and is used as a return conductor. To completely compensate the magnetic field around the conductor, the superconducting screen is used as a return conductor.

SC cable losses

The high loss inherent in room temperature dielectric cable system can be avoided. This requires that both the conductor and the cable shielding be superconducting. In this case, the shield carries a return current exactly equal to the conductor current and there is no magnetic field external to the outer conductor to cause loss in additional metal components of the assembly.

Cryostat losses

Cryostats are used to reduce heat leakage into the cold, superconducting system. Cryostats operating in the liquid nitrogen region (65K - 77K) are often multi walled vacuum vessels with multi-layer super insulation (MLI) in between. Multi-layer insulation reduces heat transfer by using multiple layers of reflective foil to reduce heat transfer by radiation.

4.3.1 Electrical Insulation of SC Cable

The two dielectrics Polypropylene Laminated Paper (PPLP™, ε_r = 1.78 to 2.20) or high-density polyethylene (Tyvek™, ε_r = 2.25 to 2.35) can be used as electrical insulation material in liquid nitrogen. This study considers exclusively Tyvek™ for the electrical insulation, as the dielectric losses of PPLP™ are greater.

The dielectric is used to keep high-voltage surfaces apart from the grounded potential. Several things can influence how strong a material is before it breaks down, like the type of electrodes, their surface roughness, and the size of the dielectric. Because of this, the reported breakdown strengths can vary quite a bit.

The electric stress of the SC cable can be calculated by

$$E(r) = \frac{U_0}{r.ln\left(\frac{r_{out}}{r_{iner}}\right)} \qquad (4.\ 2)$$

Where: E(r)= Electrical field strength(v/m), U_o Operating voltage(v), r= Radius at the required point ($r = r_{out}$ or $r = r_{iner}$) (m), r_{out} = Outer radius(m), r_{iner} inner radius (m). Two stress values of interest occurred at inner and outer radii, E_{max} at r= $r_{iner}/2$ and Emin at r= $r_{out}/2$. The maximum stress is the controlling parameter in this case.

The equation assumes that both the temperature and the conductivity of the dielectric are uniform throughout. Also, having a lower warm mass inside the cryostat can help to reduce the cool down time for the SC cable.

The testing procedures for HTS cables is for 132 kV and 33 kV power application and the necessity of qualifying the cables to verify proper functionality. The test methods include long term withstand voltage test to evaluate the durability of the insulation and lightning impulse test to evaluate the capability of the HTS cable to withstand the transient voltage.

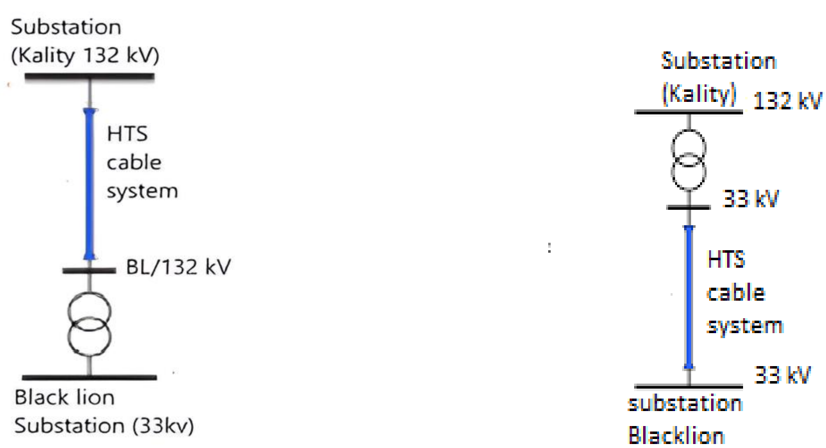

Figure 4.4: layout of designed superconducting cabling system for 132 kV and 33 kV, left to right

The dielectric thickness is calculated to insulate the superconducting cable core from the inner cryostat. The thickness of the electrical insulation layer can be calculated by

$$t = r\left[e^{\left(\frac{S*V}{E*r}\right)} - 1\right] \qquad (4.\ 3)$$

Where:

V = Testing voltage (kV or kV_{rms}), r = Outer radius of high voltage conductor (mm), E = Design electric stress (kV/mm or kV_{rms}/mm)

To ensure that the electric field is greater than the breakdown strength, the safety factor *S* is always larger than one.

Here, the voltage of the HTS cable we have constructed is on both 132 kV & 33 kV, so the AC testing voltage and the impulse testing voltage can be determined by (4.4) and (4.5), respectively. And lifetime coefficient n = 49 suggested by measurement of the *v-t* characteristic of the PDIV for CD specimens [77].

$$V_{test} = \frac{U_0}{\sqrt{3}} * k1 * k \qquad where\ k1 = \left[\frac{service\ life(no\ of\ years)}{testing\ period}\right]^{1/n} \qquad (4.4)$$

$$V_{test,132} = \frac{132}{\sqrt{3}} * 1.1 * \left[\frac{20years*365days/year*24hr/day*60min/hr}{10min}\right]^{1/49}$$

$$V_{test,132kV} = 111.25kV_{rms}$$

$$V_{test,33} = \frac{33}{\sqrt{3}} * 1.1 * \left[\frac{20years * 365days/year * 24hr/day * 60min/hr}{10min}\right]^{1/49}$$

$$V_{test,33kV} = 27.81kV_{rms}$$

Where: U_o = The highest cable operational voltage, K = Tolerance (1.1)

As regards the testing period, [77] requires 0.5 years or more. Hence, as explained below, the long-term voltage withstand test for both 132kV & 33-kV HTS test is scheduled to last 20 years.

Lightning impulse withstands voltage test: This test is done after a long-term voltage withstand test to see how well the power system can handle lightning impulse voltages.

$$V_{imp} = LIWV * K, \qquad V_{imp132kV} = 734kV \ \&\ V_{imp33kV} = 227kV \qquad (4.5)$$

Where; LIWV is the maximum impulse test voltage for device (550kV for 132kV & 170 kV for 33-kV system from Basic Insulation Level (BIL)) [78], K is Correction factor (accounting for altitude, temperature, humidity, etc. for Addis Ababa altitude of 2355m is taken $K_{altitude} = e^{(h/8150)}$)

The pressure of liquid nitrogen in high-temperature superconductor cables usually falls between 0.3 MPa and 1.5 MPa. It's important to avoid partial discharging (PD) in this pressure range since it can really harm the insulation. i.e, the partial discharge inception electric field (PDIE) is 18 kV_{rms}/mm at 0.3 MPa. This value was figured out right above the inner conductor, considering how the insulation's permittivity changes. The PDIV was measured several times and showed an average variation of 1 to 2 kV.

Also, there's a 15% difference in field strength right above the inner conductor due to the different permittivity of high-density polyethylene and liquid nitrogen. To account for tolerances and thickness, the AC design stress is set at 10.5 kV_{rms}/mm [78].

In XLPE cables, electric field design is usually based on the lowest dielectric breakdown stress, set the design value of the lightning impulse stress is E_{imp} = 48 kV/mm [78].

Using equation (4.3), we find that the insulation thickness is 16.9 mm for the 132kV system and 4.77 mm for the 33kV system. However, there is still need to look into how thermal contraction during cooling and mechanical stress during the generation, transport, and installation processes affect the insulation layer. For the 15.3 km length of HTS cables, the insulation thickness is set at 6 mm and 18 mm respective to system voltage.

4.3.2 Geometry of Superconducting Cable

Electrical consideration

Apart from analyzing and computing the design field strengths only, other electrical parameters to be taken under consideration include the current carrying capacity. The choice of the number of HTS SC tapes running in parallel in the cable determines one of the most crucial factors in the electrical design. The width of the HTS SC tapes and the cable core's dimensions decide the geometrically required SC tape quantity. Therefore, some amount of SC tapes has to be lapped around a given diameter's cable.

Current carrying capacity of individual electrical phases depends on the number of SC tapes required electrically. Usually, the geometrically required number of SC tapes (N_{geom}) needs to be equal to or greater than the electrically required number of SC tapes (N_{elec}), that ensures thermal stability, low AC losses, and long-term capability. The geometrical number is calculated as 1.1 times that of electrical which add 10 – 20 % to account for manufacturer tolerance and operational uncertainties.

$$N_{geom} \geq N_{elec}$$

If the condition is not met, the current carrying capacity will be exceeded. One can compute the number of SC tapes needed for each phase beyond which the carrying capacity is exceeded if this condition is not satisfied.

$$N_{ph} = \frac{\hat{\imath}_{r,max}}{KSI * I_c} = \frac{I_{r,max} * \sqrt{2}}{KSI * I_c} \quad (4.\ 6)$$

$$N_{ph} = \frac{2012 * \sqrt{2}}{0.7 * 160}$$

$$N_{ph,33} = 25.41\ tapes\ per\ phase \longrightarrow\ N_{geom} \sim 32\ SC\ tapes$$

$$N_{ph,132} = 6.351\ tapes\ per\ phase \longrightarrow N_{geom} \sim 9\ SC\ tapes,$$

This can be made 16 SC tapes at layer 2 and 16 SC tapes at layer 1, for 33 kV system and 5 SC tapes at layer 2 and 4 SC tapes at layer 1 for 132 kV system, considering safety and shielding layer with the same.

Where: N_{ph33}, N_{ph132} - Number of SC tapes per phase for 33 kV & 132 KV system, $\hat{\imath}_{r,max}$ - Peak value of the rated current (A), $I_{r,max}$ - RMS value of the rated current (A), I_c - Critical current of a SC tape (A), kSI- Safety factor (maximum utilization of the SC tapes up to I_c, margins against thermal, magnetic, or fault conditions)

Each HTS cable system is designed with a safety factor (kSI) between 0.5 and 0.8 to prevent the loss of superconducting properties in SC Tapes due to current surges, especially in Sub-Saharan Africa's unstable electrical networks. It is crucial to remember that the current configuration lacks recommended safeguards against possible short-circuit situations, such as external current limiters or cable designs that are tolerant of short circuits.

Based on the cable's rated current, the conductor's current carrying capacity, and a suitable safety margin, the number of SC tapes (N_{elec}) needed around the cable is determined. The influence of the internal magnetic field makes it difficult to determine the current carrying capacity of a single SC cable. A critical current (I_c) of 160A is chosen for this investigation in order to account for the effects of the magnetic field.

Table 4.6: Geometric and electrical number of SC tapes (per phase)

Nominal diameter of inner tube	Geometric number of SC tapes Layer 1	Geometric number of SC tapes Layer2	Geometric number of SC tapes Total	Electrical number of SC tapes (Minimum)
	N_{1geom}	N_{2geom}	N_{geom}	N_{elec}
DN_36	16	16	32	16
DN_30	4	5	9	4

Individual strips should not have large gaps, as this contributes to a sharp increase in AC losses in the SC cable due to magnetic fields. Considering the three-phase concentric design, the main element determining the design is the geometric factor.

The geometry of an HTS cable is a meticulous engineering process that involves defining the dimensions and arrangement of each component to meet specific performance criteria in electrical, thermal, and mechanical fields. This process considers manufacturing feasibility, installation constraints, and long-term economic viability of the system. The geometry of an HTS cable is not arbitrary, but a precise engineering procedure that ensures the system's long-term economic viability, installation constraints, and manufacturing feasibility. Below is a breakdown of the designed SC for both the 33 kV and 132 kV cable systems.

A conceptual single-core cable is shown below fig:

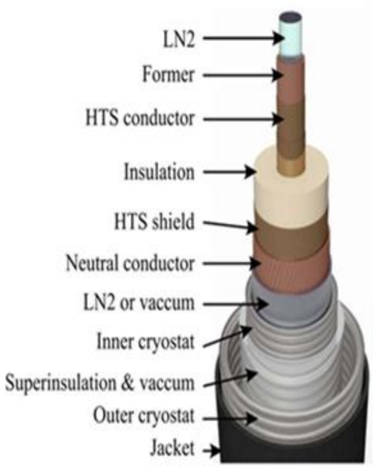

Description	Symbol	Diameter DN_36mm former	Diameter DN_30mm former
Jacket (OD)	$d_{j,o}$	139.6	151.4
Jacket (ID)	$d_{j,i}$	134.2	146.0
Outer cryostat tube (OD)	$d_{cr,o}$	134.2	146.0
Inner cryostat tube (ID)	$d_{cr,i}$	114.4	126.2
Neutral conductor (OD)	$d_{n,o}$	54.6	62.4
HTS screen (OD)	$d_{s,o}$	50.6	58.4
HTS shield (OD)	$d_{sh,o}$	50.2	58.0
Electrical insulation (OD)	$d_{el,o}$	49.8	57.6
HTS conductor (OD)	$d_{c,o}$	42.6	36.0
Former (OD)	$d_{f,o}$	41.0	35.0
Former (ID)	$d_{f,i}$	36.0	30.0

Figure 4.5: Single core corrugated HTS power cable and diameter of the examined cables (ID – Inner diameter, OD – Outer diameter).

The SC cable pertains to HTS winding layer where YBCO tapes are stacked radially around a former. These tapes carry the current (503 A/phase for 132 kV, 2,012 A/phase for 33 kV). The thickness of this multi-layer for both voltage levels is determined, considering the tape requirements with respect to arrangement, based on a triad configuration (three phases in one cryostat, i.e., a single cable housing all three phases). Bounding circle diameter for triad determined as:

$$D_{triad} = \text{spacing} * \left(1 + \frac{1}{\sin{(60)}}\right) \quad (4.7)$$

Superconducting requirement

Determining the conductor layer's required superconducting characteristics is crucial to guaranteeing that it maintains its superconducting characteristics under all operating conditions. This includes considering the combined effects of the critical current of the tapes, twist angle, number of superconducting (SC) tapes, and route length.

The study's assumed angle of shock is 20°, and the geometric relationship between lay angle and route length is as follows.

$$l_{drill} = \frac{\text{L}}{\cos{(\alpha_{drill})}} \qquad (4.\ 8)$$

$$l_{drill} = \frac{15.3}{\cos{(20)}} = 16.28km$$

The length of the SC tape l_{drill} is greater than the route length L(15.3km).

SC tape requirement: electrical phase

The number of superconducting tapes used in each high-temperature superconductor (HTS) layer and the length of the SC tape determine the requirement for superconductors. The following equation is used to find this:

$$l_{L,ges} = 3 * \sum_{I=1}^{NLS} N_{L,i} * L_{drill} \qquad (4.\ 9)$$

$$l_{L,ges} = 3 * \sum_{i=1}^{2} N_{L,i} * L_{drill}$$

$$l_{L,ges,33} = 3 * 16.28(16 + 16) \quad \longrightarrow \quad l_{L,ges,33} = 1562.88\ km$$

$$l_{L,ges,132} = 3 * 16.28(4 + 5) \quad \longrightarrow \quad l_{L,ges,132} = 439.56\ km$$

where: $l_{\text{L,ges}}$ - Superconductor requirement per three-phase system (conductor layer)
N_{LS} - Number of conductor layers, $N_{\text{L,i}}$ - Number of SC tapes per layer
l_{Drill} - Developed SC tape length (km)

The diameter of the inner tube determines how many SC Tapes are used in each layer. The critical current, I_{c}, of the SC tapes indicates their number of layers and current capacity. The width of the SC tape is 4 mm.

The vital electrical insulation is located beneath the protective shielding layer. Because the shielding layer in our high voltage cables has a large diameter, a considerable number of SC tapes must be used. The precise and stable placement of the shield layers is guaranteed by these tapes. In fact, it requires an astounding 102.2 and 28.73 kilometers of superconducting material for every 1-kilometer segment of a three-phase route in 33 kV & 132V system respectively. This emphasizes how crucial it is that we make investments in high-quality materials to ensure our electrical systems operate at their best and are safe.

4.3.3 Electrical Parameter Analysis of HTS Cables

This defines electrical qualities as the amounts of resistance, capacitance, and inductance per unit length. Analytical equations exist for the calculation of these quantities per unit length of the single conductor concept. The superconducting condition results in a very low resistance per unit length, which is $R' < 0.0001$ Ω/km [38].

The inductance per unit length is calculated using Equation (4.10). The first term in the equation describes the inductance based on the lay angle. The third term takes into account the limited thickness of the conductor layer. These two terms have a negligible effect on the total inductance (approximately 5%).

The magnetic field between the conductor and the shield, which is established by the second term in equation (4.10), is the main influencing factor.

$$L = \frac{\mu_o}{4\pi}\tan(\theta_{BL})^2 + \frac{\mu_o}{2\pi}\log\left(\frac{r_{s,i}}{r_{h,o}}\right) + \frac{\mu_o}{2\pi({r_{h,o}}^2 - {r_{h,i}}^2)}\left[\frac{{r_{h,o}}^4 - {r_{h,i}}^4)}{4} + {r_{h,i}}^4\log\left(\frac{r_{h,o}}{r_{h,i}}\right) - {r_{h,in}}^2({r_{h,o}}^2 - {r_{h,i}}^2)\right] \quad (4.10)$$

Where; L - Inductance per unit length (H/km), μ_0 - Magnetic field constants ($4\pi \cdot 10^{-7}$) (V_s/Am), θ_{BL} – pitch angle of inner SC tapes (20°c), $r_{S,i}$ - Internal radius of the shield (0.0292m), $r_{h,i}$ - Internal radius of the conductor (0.0175 m), $r_{h,o}$ - External radius of the conductor (0.018 m)

Since the resistance in an HTS cable is thought to be insignificant in comparison to the inductance, only the inductance is considered. The influence of the inductance is the main focus of this analysis, so contact resistances are disregarded even though they will also have an impact on the current distribution of HTS cable carrying AC transporting current.

$$L = \frac{4\pi * 10^{-7}}{4\pi}\tan(20)^2 + \frac{4\pi * 10^{-7}}{2\pi}\log\left(\frac{0.0292}{0.018}\right) + \frac{4\pi * 10^{-7}}{2\pi(0.018^2 - 0.0175^2)}\left[\frac{0.018^4 - 0.0175^4)}{4} + 0.0175^4\log\left(\frac{0.018}{0.0175}\right) - 0.0175^2(0.018^2 - 0.0175^2)\right]$$

$$the\ total\ inductance\ per\ unit\ length\ is, L = 0.0004204\ mH/km,\ and$$

$$the\ total\ inductance\ , L = 0.0004204\frac{mH}{km} * 15.3km = 0.006432\ mH$$

The formula below can be used to determine the capacitive charging current of the cable when it is operating at an open end:

$$C = \frac{2\pi\varepsilon_r\varepsilon_o}{ln(r_o \,/\, r_i)} \tag{4.11}$$

$$C = \frac{2\pi * 8.8541 * 10^{-12} * 2.3}{ln(0.0292 \,/\, 0.018)}$$

$$line\ capacitance\ per\ unit\ length\ is\ C = 0.2683\ nF/m$$

$$total\ line\ capacitance\ C = 268.3\frac{nF}{km} * 15.3\ km = 4.105\ \mu Farad$$

The SC cable's insulation material experiences dielectric losses, which are brought on by flaws in the electric insulation material. W_d, the dielectric losses can be computed as follows:

$$w_d = \omega C {U_o}^2 tan\delta \tag{4.12}$$

where ω = 2πf, C is the capacitance per unit length, U_o is the rms phase voltage, and tanδ is the loss factor for the actual type of insulation material. It is seen that the dielectric loss is independent of the current and therefore a no-load loss component. For a 132 kV single-core cable the dielectric losses will usually be below 1 W/m phase (typical values are tanδ=0.0002, and ε_r= 2.3, f=50Hz***).***

$$w_d = 2\pi f C {U_o}^2 * 0.001$$

$$w_d = 2\pi * 50 * 0.2683 * 10^{-9} * 132^2 * 0.0002 = 0.2937\ w/m\ phase$$

The capacitive charging current (when the line end is open circuited) of a cable is calculated using the equation below:

$$I_{ch} = \omega\frac{U_N}{\sqrt{3}} * C \tag{4. 13}$$

The charging power of a cable can be calculated with

$$Q_{ch} = \sqrt{3} * U_N * I_{ch} = \omega . {U_o}^2 . C \tag{4. 14}$$

$$I_{ch} = 2\pi * 50 * \frac{132\text{kv}}{\sqrt{3}} * 268.3\ nF/km = 6.42 * 10^{-3} A/km$$

$The\ total\ line\ charging\ current\ is\ I_{ch} = 0.00642\frac{A}{km} * 15.3km = 0.098\ A$, and

$$Q_{ch} = \sqrt{3} * 132kv * 0.098 = 22.4\ kw$$

Where: I_{ch} = capacitive charging current, U_n = nominal voltage, Ω = angular velocity, Q_{ch} = capacitive charging power

At roughly 240 nF/km, XLPE cables provide an impressive capacitance that is only roughly two-thirds of that of conventional cable systems. XLPE cables are a better option for efficiency and performance because of this significant reduction, which results in an amazing reduction of over 65% in the transmission system as a whole.

Table 4.7: Comparison of operating characteristics - line constants of different cables are

Electrical parameters	Overhead line	Underground cable	Super conducting cable
Inductance per unit length L (mH/km)	0.80	0.48	0.13
Capacitance per unit length C (nF/km)	13	230	268
Resistance per unit length R (mΩ/km)	36	7.2	~ 0.0001

4.4 Performance of Heat Transfer and Pressure Drop in SC Cable Former

The cryogenic design of HTS cables is extremely difficult because they must function in particular regions. These cables have to manage heat from multiple sources while maintaining the HTS conductor at a low temperature (65 - 77 K). This is accomplished by using liquid nitrogen (LN_2) as a coolant, which absorbs heat and returns it to the cable. Through conduction and radiation, heat from the surroundings can enter the conductor area. The dielectric may also allow for a small amount of electrical energy to dissipate. Because liquid nitrogen has a density of roughly 810 kg/m^3, there is a pressure differential along the coolant columns, particularly when elevation changes occur.

The total pressure drops along the length due to elevation difference is:

$$\Delta P_{elevation} = \rho g \Delta h = 810\frac{kg}{m^3} x\ 9.8\ m/sec^2\ x\ \Delta h = 8.0(\frac{bar}{15.3km})\Delta h \quad (4.15)$$

$$\Delta P_{elevation} = 1.989\ bar$$

Where: $\Delta h = 2109.41$ m elevation at kality and 2359.74 m at black lion.

Controlling flow velocity is crucial for preserving stability and effectiveness in liquid nitrogen cryogenic cooling systems. To guarantee that the HTS cable stays within the safe temperature range of liquid nitrogen (65–77 K) over its length (15.3 km), an analysis must take into consideration pressure drop, the necessary number of cooling stations, and the cooling needs.

Table 4.8: Physical properties of (LN_2) over considered ranges of pressure and temperature

Density (ρ):	810 kg/m3
Dynamic Viscosity (μ):	1.55×10^{-4} Pa\cdotps
Specific Heat (cp):	2,060 J/kg\cdotpK

The coolant absorbs heat as it flows, causing a temperature increase. The mass flow rate required to limit this temperature rise is:

$$\dot{m} = \frac{Q_{\text{total}}}{c_p \cdot \Delta T} \quad (4.16)$$

Where: $\Delta T = 4k$ Assumed temperature margin,

$$Q_{\text{total,132kv}} = 0.5731kw/km * 15.3km = 10.27kw$$

$$Substitute\ Q_{\text{total}} = 10.27kw, cp = 2{,}060\ \frac{J}{kg\backslash cdotpKc}$$

$$\dot{m}, = \frac{10.27kw}{2{,}060 * 4k} \approx 0.623\,kg/s$$

Volumetric flow rate:

$$\dot{V} = \frac{\dot{m}}{\rho} = \frac{0.623\,kg/s}{810kg/m^3} = 0.0007694 \approx 7.694 \times 10^{-4} m^3/s = 0.7L/s \tag{4. 17}$$

flow velocity

$$v = \frac{\dot{V}}{A}, \qquad where\ area:\ A = \pi.\left(\frac{\mathrm{D}}{2}\right)^2 = \pi \cdot \left(\frac{0.04}{2}\right)^2 = 1.257 \times 10^{-3} m^2 \tag{4. 18}$$

$$v = \frac{7.694 \times 10^{-4} m^3/s}{1.257 \times 10^{-3} m^2} \approx 0.612 m/s$$

4.4.1 Pressure Drop

The Darcy-Weisbach equation is used:

$$\Delta P = f \cdot \frac{L}{D} \cdot \frac{\rho v^2}{2} \tag{4. 19}$$

Reynolds Number:

$$Re = \rho \cdot v \cdot \frac{D}{\mu} Re = \frac{810 * 0.612 * 0.04}{1.55 \times 10^{-4}} \approx 127928 \tag{4. 20}$$

The flow is much greater than the turbulent regime (Re > 4000).

Friction Factor:

Using the Blasius correlation for turbulent flow:

$$f = 0.316 \cdot Re^{-0.25} \tag{4. 21}$$

$$f = 0.316 \cdot (127928)^{-25} \approx 0.0167$$

Total Pressure Drop, from equation (4.19:

$$\frac{\Delta P}{\Delta L} = \frac{f}{D} \cdot \frac{\rho v^2}{2}$$

$$\frac{\Delta P}{\Delta L} = \frac{0.0167}{0.04} \cdot \frac{810 * (0.612)^2}{2} \approx 63.33\,Pa = 0.0006333\,bar$$

The total pressure drop ΔP_{total} combines frictional losses and elevation differences.

$$\Delta P_{\text{total}} = \Delta P_{friction} + \Delta P_{elevation} \tag{4. 22}$$

For cryogenics, the maximum permitted pressure drop is 3 bars over 3.9 km, necessitating the installation of four cooling stations.

A pump must be able to handle a flow rate of roughly 0.7 L/s, plus extra capacity for efficiency and safety. The pump must compensate for a 3.9 bar pressure drop by increasing coolant flow over a 15.3 km distance. It must run with a minimum pressure margin of 15-25% to guarantee dependability, which calls for a pump that can manage at least 25 bars for the 3.9 km distance.

According to a certain equation, the average temperature gradient in a cryogenic pipe containing a compressible fluid is estimated to be 8 K, with a temperature decline of 0.5652 K/km.

$$\frac{\Delta T}{\Delta L} = \frac{f}{D} \cdot \frac{v2}{2c_{\text{p}}} + \frac{q}{\dot{m}c_{\text{p}}} \tag{4. 23}$$

Through efficient heat transfer, the cooling unit maintains the proper operating temperature of the superconducting cable by pumping liquid nitrogen through it.

The temperature distribution and flow velocity were determined by simulating a turbulent flow in a liquid nitrogen pipe. The current study's findings can serve as a guide for simulation studies of cryogen pipe flow and liquid nitrogen pipe flow with thermal insulation systems.

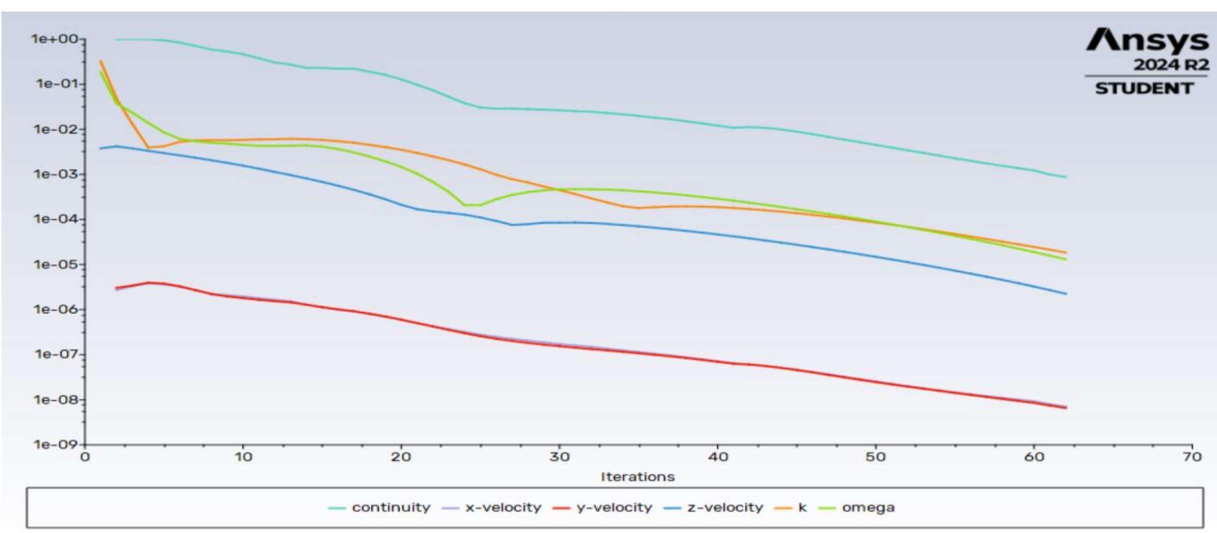

Figure 4.6: Scaled residuals view for flow velocity

Using an inlet speed of 0.612 m/s, Figures 4.6 to 4.9 show how the temperature and velocity vary along the pipe's length (z coordinate) for both the asymmetric line and the wall line.

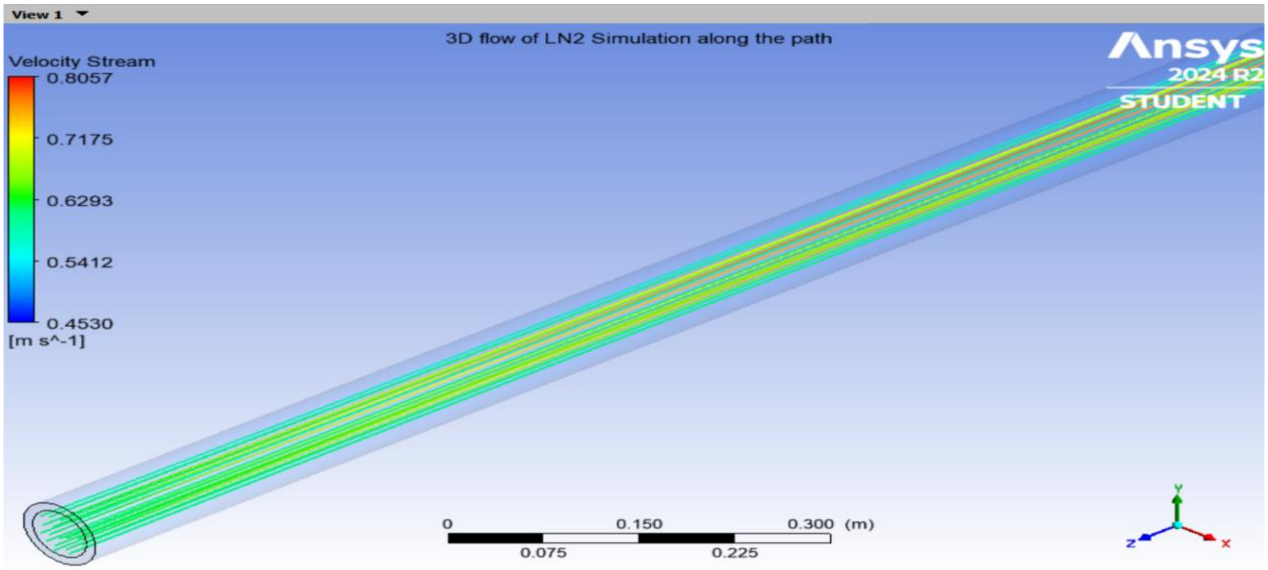

Figure 4.7: Coolant flow velocity stream through pipe view

The asymmetric line velocity gradually increased along the flow pathway from the inlet to the outlet, while the wall line velocity eventually reached zero along the line. Along the pipe's length, the velocity gradient at the asymmetric line also showed an increasing rate.
Due to the no-slip condition at the wall, this observation shows that the velocity at the wall, which is normally impacted by friction and boundary layer effects, reaches zero.

As it travels from the inlet to the outlet, the asymmetric line possibly denoting an off-center line in the pipe sees an increase in velocity, most likely as a result of the evolving flow or modifications in the pressure gradient.

Significant resistance causes fluid layers close to the wall to have zero velocity at the wall and a velocity gradient perpendicular to it. The statement that "the velocity gradient at the asymmetric line increased along the pipe's length" suggests that there is variation in the rate at which velocity changes with distance.

The Joule-Thomson effect, which causes temperature variations from the inlet to the outlet based on pressure changes, is primarily responsible for the increase in temperature along the flow direction. Furthermore, the no-slip boundary condition, a key idea in pipe hydrodynamics, is upheld when the wall line velocity reaches zero.

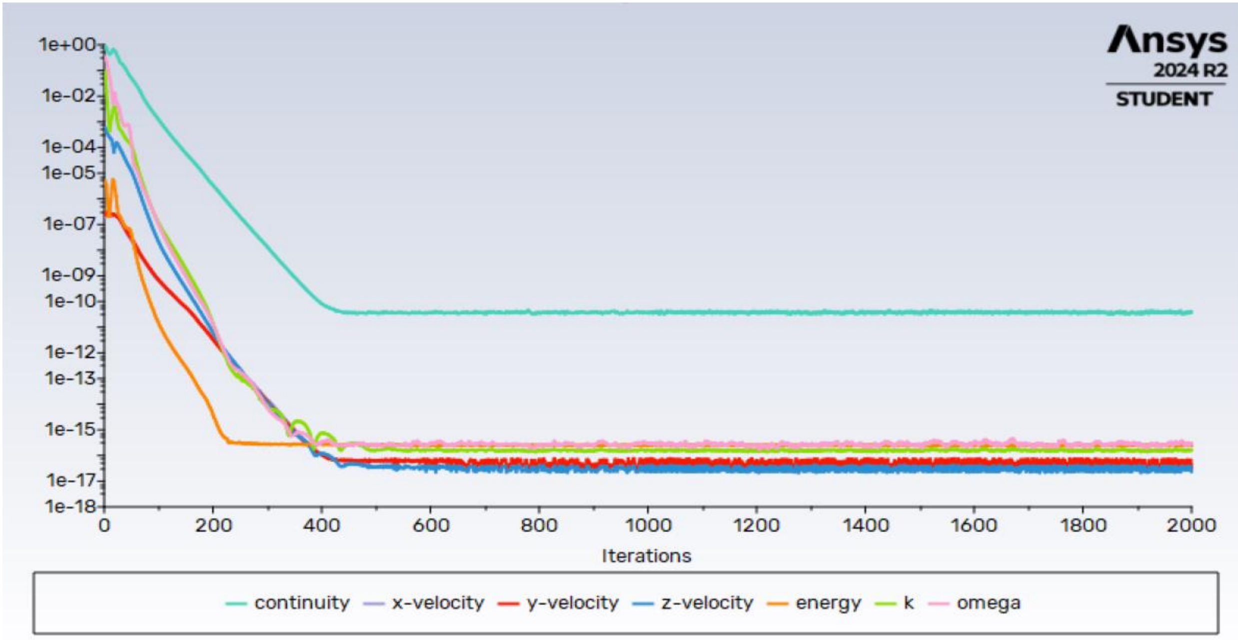

Figure 4.8: Scaled residuals view of the temperature variation

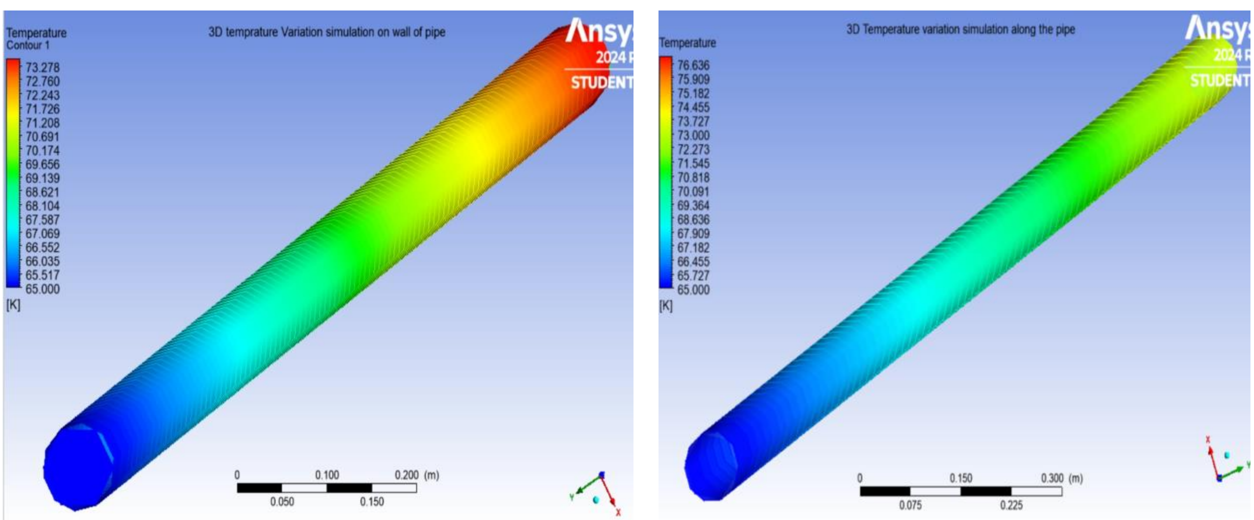

Figure 4.9: Coolant flow temperature variation along the length of pipe

The temperature of the wall is significantly higher than that of the asymmetric line. It takes a higher inlet volume flow rate to keep this temperature constant throughout the flow. Simulations show that the flow temperature stays below the 77 K liquid nitrogen boiling point.

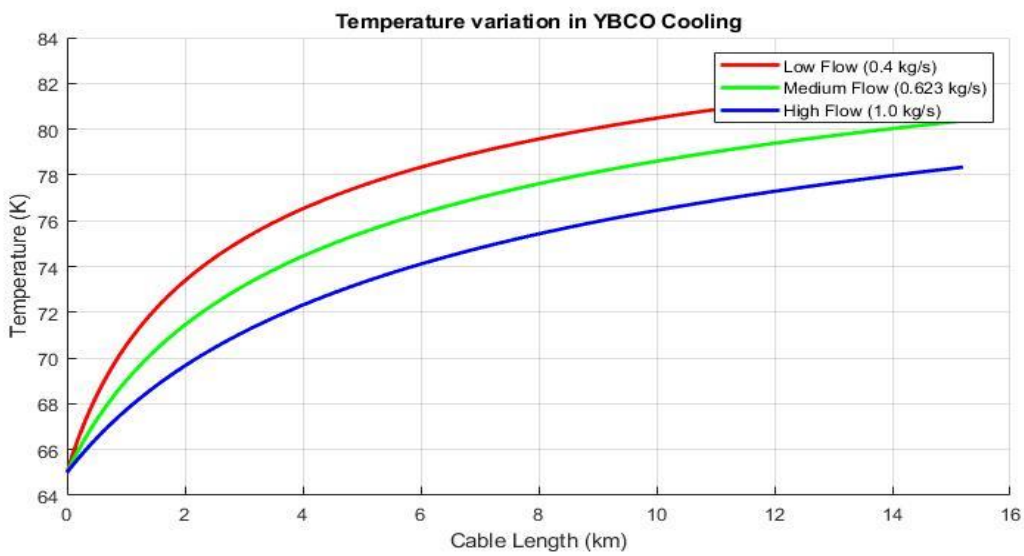

Figure 4.10: Temperature Variation of Liquid Nitrogen in Cryogenic Pipe

The cumulative heat input causes the temperature to rise gradually but a little faster. Because the heat input effect builds up over distance, the increase exhibits a nonlinear trend. The temperature may rise too much and cause the HTS cable to quench if cooling losses are not managed. The superconducting state is lost at temperatures above 77 K, necessitating the use of active cooling or design modifications.

By maintaining a lower temperature, increasing the coolant's flow velocity lessens the chance of the heat transfer system's (HTS) critical temperature being exceeded. Lower flow rates, on the other hand, may cause overheating and call for better thermal insulation to stop heat loss. While friction-induced pressure losses must be controlled, high pressure is necessary to prevent phase change and maintain efficient cooling in a liquid nitrogen superconducting system. Increasing the mass flow rate reduces temperature rise over distances by improving heat absorption, but it also increases pressure drop because of flow resistance.

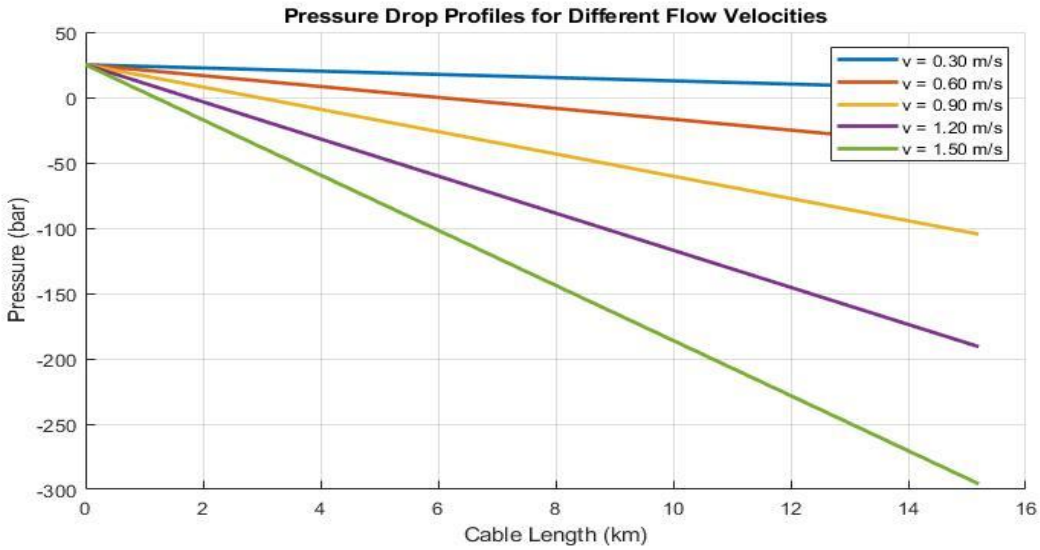

Figure 4.11: Pressure variation along the pipe with different velocity

To maintain liquid stability, the pressure must stay above 2-3 bar, lowering it could cause boiling or cavitation. System stability is provided by lower flow velocities (0.5-0.7 m/s), which minimize pressure losses while maintaining cooling effectiveness. Higher speeds (>1.2 m/s), on the other hand, cause turbulence and a sharp drop in pressure, necessitating careful balancing through pipe diameter optimization.

Variations in fluid density and friction factor have a minor impact on pressure loss rates, but the main trade-off is between pressure retention (which favors lower flow) and cooling performance (which favors higher flow). Because lower flow velocities encourage gradual pressure drops and system stability while higher velocities increase turbulence and pressure losses despite a slight decrease in the friction factor, pipe diameter optimization can help balance cooling efficiency and pressure drop.

4.5 Simulation and Analysis Result

The study here focuses on possibly converting the 132 kV transmission line into a 132 kV HTS cable and a 33 kV HTS cable. It outlines the benefits in the marketplace and in technology that HTS systems can offer in comparison to conventional lines, particularly in terms of performance, cost, efficiency of operation, and environmental sustainability. This kind of analysis aims to highlight the advantages of having HTS cables in future power infrastructure.

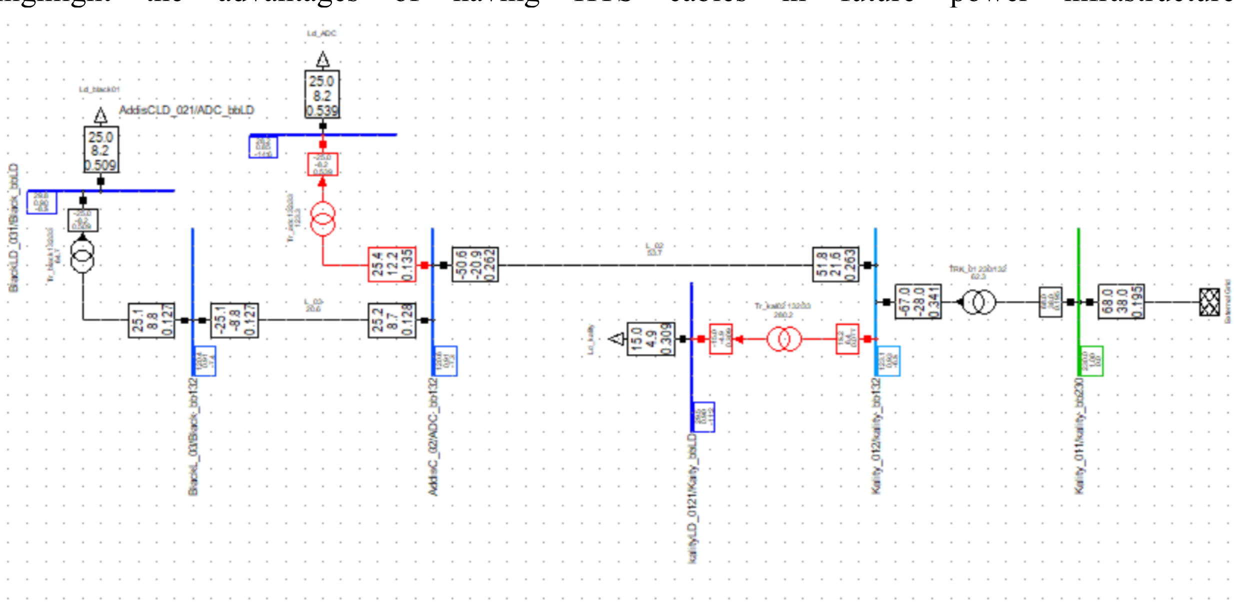

Figure 4.12: Layout of existing transmission line

Table 4.9: The final cable Specifications summary of the designed superconducting cable

Cable parameters	**Symbol**	**Value 33 kV**	**Value 132 kV**
Manufacturer		Superpower	Superpower
No. of layers		2	2
No. of tapes in the inner layer		16	4
No. of tapes in the outer layer		16	5
Capacity (MWA)	S	115	115
Rating voltage (kV)	U_{op}	33	132
Operation current (kA)/phase	I_r	2.012	0.503
Rating current (kA)/phase	I_{op}	11.8	3.52
SC cable structure		Triaxial	triad configured type
Dielectric type		Cold dielectric	Cold dielectric
Operating temperature (K)	T_{op}	65 – 77	65 – 77
YBCO HTS tape critical current	I_c	160 A/tape Superpower	160 A/tape Superpower
YBCO HTS tape thickness (mm)		0.01	0.01
YBCO HTS tape width (mm)	W	4	4
Insulation thickness (mm)	T	6	18
Length of the HTS cable (km)	L	15.3	15.3

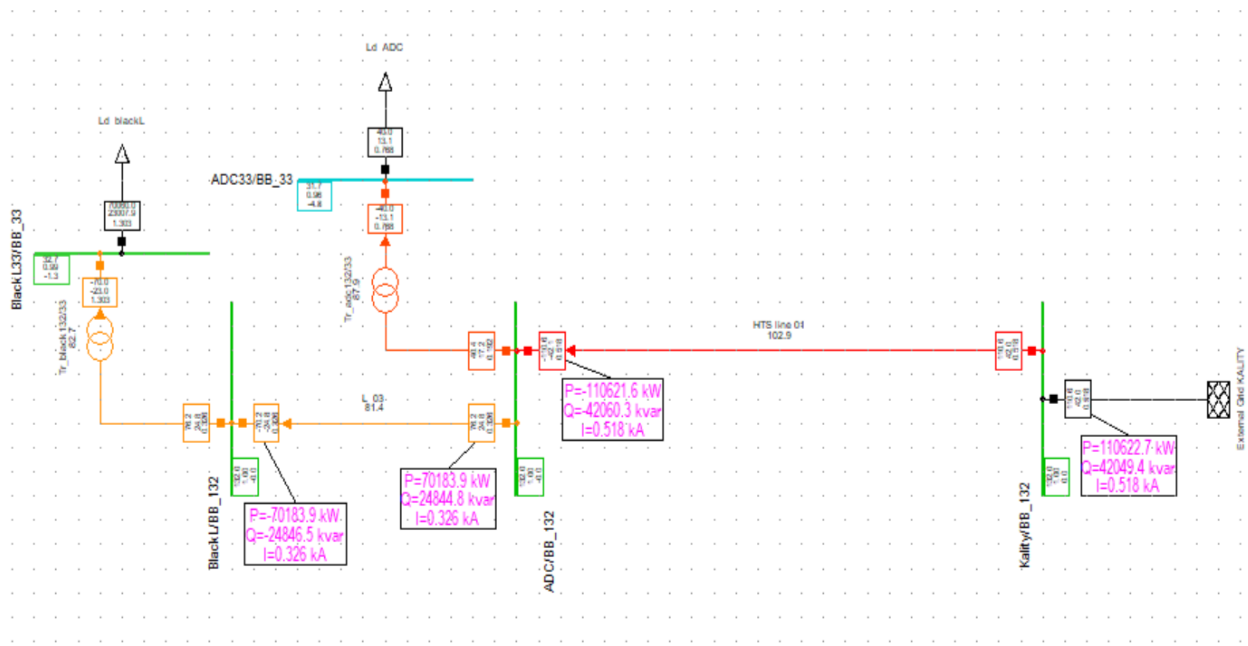

Figure 4.13: Results of designed 132 kV superconducting cabling system

The analysis of the technology indicates that the use of a 132 kV HTS line in transmitting 115 MVA of power has numerous advantages over a conventional 132 kV line. The power losses are reduced significantly as shown in Table 4.10 and are more efficient, with a smaller system topology. Therefore, the HTS technology is a desirable option for modern power transmission, supporting higher performance and a better future. The technical feasibility of replacing to an HTS line from a 132 kV conventional line can be assessed using simulation results with different scenarios. HTS cables have a clear advantage in terms of power losses compared to conventional transmission lines under all loading.

Table 4.10: Grid loss comparison of HTS vs conventional line at different loading conditions

Grid loss at different loading condition

Loading	*Loss for 132 kV Conventional line (MW)*	*Loss for 33 kV HTS (MW)*	*Loss for 132 kV HTS (MW)*
50% of full load	*1.7*	*0.124*	*0.0481*
60% of full load	*2.14*	*0.187*	*0.0502*
75% of full load	*2.95*	*0.321*	*0.0545*
loading 100%	*4.81*	*0.671*	*0.0665*
loading 125%	*7.37*	*1.216*	*0.0857*

The HTS AC losses are very complex and depend on the alternating current, magnetic fields, and specific cable design. There is not one single, universal equation that analytically expresses all

HTS AC losses due to their non-linear behavior, but certain models and empirical relations depend on the cable type, current, and operating conditions. Power loss through HTS AC transmission cables is of another dimension compared to conventional cables as far as the nature of superconductivity is concerned. HTS cables do incur some losses and can be approximated to a sum of transport current loss, magnetization loss, coupling, insulation, and eddy power loss.

The largest fraction for 132 kV system is typically transport loss (0.297 W/m/phase), which is essentially a very nonlinear function of the frequency and current amplitude. And determined by:

$$P_{hys} = \frac{\mu_0 {I_c}^2 f}{\pi}\left[(1-\beta)ln(1-\beta)+\beta-\frac{\beta^2}{2}\right] \qquad (4.\ 24)$$

Where; $\mu_0 = 4\pi\times10^{-7}$ H/m (permeability of free space), P_{hys}: Hysteresis loss per unit length (W/m, usually per phase for 3-phase cables), $\beta = I_t/I_c$: Normalized transport current, where I_t is the RMS current (503 A/phase, 2012 A/phase) and I_c critical current (9 - 32 tapes/phase are required = 600 A - 2080 A)

The line has a significant advantage in terms of power losses over the conventional line for all levels of loading. For instance, at the full load of 100%, the overall power loss of the HTS line's is only 0.0665 at 132 kV and 0.67 MW at 33 kV whereas conventional line is 4.81 MW. This signifies a great reduction in wasted energy, thereby saving on cost and sustainability of the environment. Eddy and coupling losses are discussed in the last section of this paper whereas magnetization losses and insulation losses are discussed in the previous chapter.

The line efficiency is much higher with the HTS line. The low losses result in a larger percentage of transmitted power that reaches the end-use customers, and this is important for grid capability

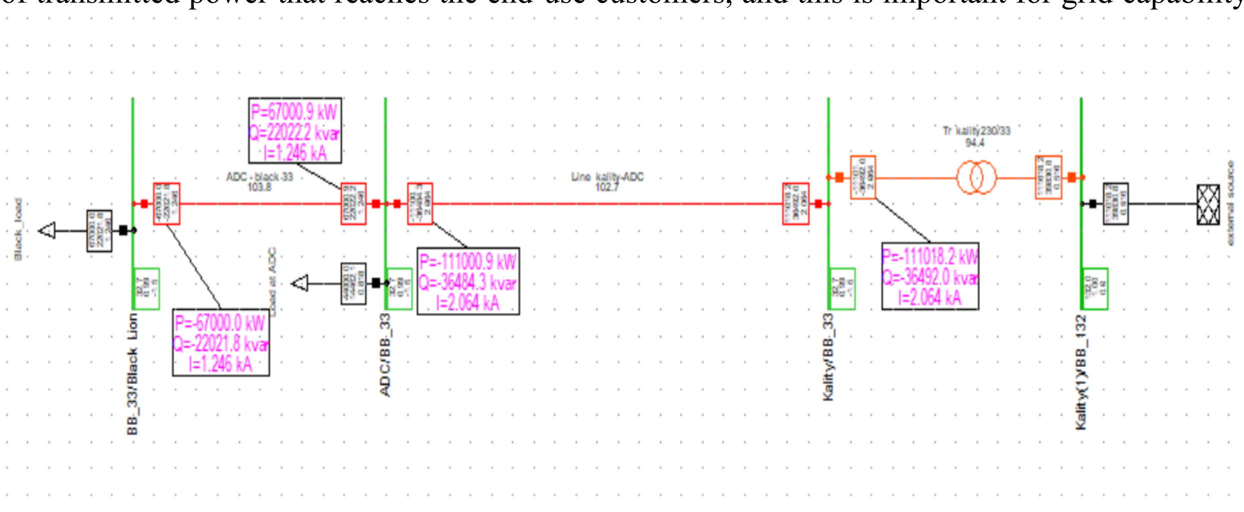

Figure 4.14: Results of designed 33 kV superconducting cabling system

and performance. The HTS line remains efficient even when loaded to 125%, with only a marginal increase in losses (1.216 MW compared with 0.67 MW for 100% loading). This demonstrates that an HTS line can perform well at overloaded conditions.

The Norris ellipse model is dedicated to an ideal single superconducting strip or tape under self-field conditions. Indeed, the model assumes simple geometry and a uniform distribution of current over the area. However, HTS relies on multiple layers of tapes, introducing interlayer coupling and non-uniform current distribution in the presence of applied external magnetic fields. Therefore, empirical scaling has to be used in order to take such complex influences into account.

Conventional power transmission demands high voltage in order to minimize resistive losses incurred at long distances. SC systems, on the other hand, can carry power through the whole distance at lower (line) voltages, without needing to ramp up the system (i.e., 33 kV), leading to lower losses. This is due to the unique property of superconductors, which have near-zero resistance below a specific temperature.

The simplified system design with fewer components reduces transmission system failure points and maintenance needs, resulting in reduced capital cost. However, active cooling or design improvements may be necessary for optimal HTS technology operation. Despite these costs, the potential for efficiency gains and long-term energy savings makes the investment worthwhile.

4.6 Cost Analysis

HTS tapes YBCO are much costlier than traditional conductors because of the specialized ways of making it, less volume production, and complex nature of materials. The market price for HTS wire and tape is around \$150-\$200 per kA-meter, or an equivalent market price of \$24 - \$32 per meter (for a critical current of 160 A) *[80][81][82]*.

The number of SC tapes required determines the current-carrying capacity of the system, which also affects the costs of the SC cable. According to equation (4.8), the number of tapes needed for each phase is nine and thirty-two, resulting in a total of 27 tapes for the 132 kV system and 96 tapes for the 33 kV system. For the designed route, the total length of tape required was calculated to be 439.56 kilometers for the 132 kV system and 1,562.88 kilometers for the 33 kV system.

The total tape cost is:

$$\begin{aligned} for\ 33\ kV &= 1562.88\ km * 160\ A * (\$150\ to\ \$200) per\ kA.m \\ &= (\$37{,}509{,}120\ \ to\ \ \$50{,}012{,}160) \\ for\ 132\ kV &= 439.56\ km * 160\ A * (\$150\ to\ \$200) per\ kA.m \\ &= (\$10{,}549{,}440\ \ to\ \ \$14{,}065{,}920) \end{aligned} \tag{4. 25}$$

Prices for YBCO HTS tapes for power transmission are highly dependent on production volume, technology advancement, and market demand particularly from power transmission. A summary of the situation with pricing is provided below.

Table 4.11: Investment Costs of designed HTS cables

Cost Category/ resources	Number of Units	Per-Unit Cost (USD)	Total Cost (MUSD) along (33kV)	Total Cost (MUSD) along (132kV)	Specifications
HTS Cable (Tape Assembly)	15.3 km		41.1 – 57.012	15.75 – 26.21	YBCO SC tape 4 mm, Ic=160 A, former, PPLP insulation & protective layering
Terminations	2 units	500,000 - 1,000,000	1.0 - 2.0	1.0 - 2.0	cryogenic seals, PPLP/epoxy insulation
Joints	15 (per 1km)	100,000 - 150,000	1.5 - 2.25	1.5 - 2.25	for cable joints ~ 0.1 - 0.5 W heat load
Cooling	15.3 km		9.6 – 17.82	8.85 – 15.2	Vacuum-insulated 1-1.5 W/m heat leak cryostats, LN_2 piping, sensors, refrigerator, Centrifugal pump (>3bar) and control systems.
Fault Current Limiters (FCLs)	2	(67,000 - 133,000) &	1.0 - 2.0	1.5 - 3.0	YBCO-based, 132 kV & 33 kV, 115 MVA, fast response (<1 ms), recovery <1 s
Contingency Reserves		(10–15%) base cost	9.13 - 12.67	6.925 – 11.29	Allocated for unforeseen expenses and project risks.
Engineering & Installation		(5-15) % base cost	10.6 – 17.33	7.2 – 15.2	Covers trenching, ducting, access points, and related infrastructure and encompasses design, modeling, compliance.
Total cost			73.93 - 111.08	42.93 – 75.15	

The yearly expenses and investments are usually used to establish the utility costs of establishing and operating an electric line system. The high installation costs of HTS cables may be difficult to bear. However, there be monetary benefits from higher efficiency and lower energy losses.

Table 4.12: Cooling cost analysis of designed HTS power line

Cooling Device	Per-Unit Cost (MUSD)	Total Cost (MUSD) along length 33 kV	Total Cost (MUSD) along length, 132kV
Cryostats (15.3 km)	0.45 – 1.0	8.0 - 15.3	7.5 – 13
Cryocoolers (4 units)	0.175 – 0.27	0.8 – 1.1	0.75 – 1.0
Pumps (15 kW -25 kW) 8 (with 1 standby for each)	0.05 – 0.09	0.5 – 0.72	0.4 – 0.7
Liquid Nitrogen & Supply (4 tanks)	0.1 – 0.125	0.3 - 0.7	0.2 – 0.5
Total Cooling System	-	9.6 – 17.82	8.85 – 15.2

Cooling cost (closed loop): This cost breakdown is verified against the scaling of LIPA, Ampacity, and other HTS projects and is estimated using industry ratios.

Cooling station = 4 stations (every 4 km) with cooling capacity of 1kW for each

Pricing trends for HTS power transmission wires and cables with 2G YBCO are influenced by tape fabrication advancements, economies of scale, and high-tech sector demand. Firms like TEVA, Bruker, SuperPower, AMSC, Sumitomo Electric, Nexans, and SCSC have established expertise in supplying these materials for practical power transmission applications.

***Note**: Costs are aligned from multiple real-world HTS projects [80][81][82][83]* [84].

Table 4.13: Annual Operational Costs for designed HTS Power Line

Cost Category	Annual Cost (MUSD)/year	Description and Cost Basis
Liquid Nitrogen (LN_2) Supply	0.779 - 1.7	4 LN_2 tanks manage 33 - 45 kW heat load, Cost: \$0.13 - \$0.50/L.
Monitoring & Instrumentation	8,500 - 15,000	sensor calibration, cryocooler servicing, fault detection, Oversight for cooling system,
Personnel & Maintenance	21,000 - 37,000	Annual/monthly inspections, Regular service of pumps, valves, sensors, Annual training on cryogen handling and HV safety
Total	0.8085 - 1.752	

Table 4.14: Investment costs for existing conventional line with a route length of 15.3 km

Resources	Low costs (MUSD)	High costs (MUSD)	Specification
Conventional oner	10.2	15	132 kV three-phase cable systems

It must check the expenses for buying cost of asset equipment, annual maintenance costs, and savings for installation of a conventional power transmission facility at the end to find the payback period.

Annual Power Savings of Innovative Systems Against the Conventional Options

- HTS Power transmitted:
  115 MVA × 0.9 (power factor) = 103.5 MW.
- Energy transmitted:
  103.5 MW × 24 h/day × 365 days/year = 906, 660 MWh/year.
- Conventional line losses:
  13.8 MW or 120, 888 MWh/year.
- Conventional energy value lost:
  120,888 MWh/year × ($0.022 - $0.027)/kWh = ($2,659,540 - $3,263,980) million/year.
- HTS line losses: (132 kV)
  0.0665 MW or 582.54 MWh/year.
- HTS energy lost value: (132 kV)
  582.54 MWh/year × ($0.022 - $0.027)/kWh = ($12,815.88 - 15,728.58)/year.
- Average annual energy savings: (132 kV)
  $2,961,760 – $14,272.23 = $2,947,487.77/year.
- HTS line losses: (33 kV)
  0.671 MW or 5,877.96 MWh/year.
- HTS energy lost value: (33 kV)
  5,877.96 MWh/year × ($0.022 - $0.027)/kWh = ($129,315.12 - 158,704.92)/year.
- Average annual energy savings: (33 kV)
  $2,961,760 – $144,010.02 = $2,817,749.98/year.
- Annual OpEx for HTS: $50,000/year for conventional OpEx,
  additional OpEx = $1.28 million - $50,000 = $1.23 million/year.
- Annual savings: (132 kV) $2.817 - $1.23 = $1.587 million/year.
- Annual savings: (33 kV) $2.947 - $1.23 = $1.717 million/year.

The payback period is calculated as:

$$\text{Payback Period } (132kV) = \frac{\text{Initial Capital Cost}}{\text{Annual Net Cash}} = \frac{\$42.93 \text{ to } \$75.15 \text{ million}}{\$1.587 \text{ million}} \quad (4.\ 26)$$
$$= 27\ to\ 47\ years\ \ for\ 132kV$$

$$\text{Payback Period } (33kV) = \frac{\text{Initial Capital Cost}}{\text{Annual Net Cash}} = \frac{\$73.93 \text{ to } \$111.08 \text{ million}}{\$1.717 \text{ million}} \qquad (4.\ 27)$$
$$= 43\ to\ 64\ years, for\ 33\ kV$$

The high initial cost of investment is undoubtedly a drawback. However, the advantages of continued natures improved capability, increased capacity, and sustainable development make HTS technology an attractive proposition in the modern power system. Transitioning has various advantages concerning energy efficiency and reduced losses; however, these gains will now be offset by complexities and increased initial costing, which are imperative to understand in making such decisions.

HTS technology offers immense potential for transforming power transmission systems built for the future, especially given the continued increase in demand for energy. Realizing very high-efficiency with the technology is expected to result in losses 20 -70% less than conventional lines, hence, being an attractive option for high-capacity low-loss power transmission.

Table 4.15: Summary of Results

Aspect	132 kV Conventional Line	132 kV and 33 kV HTS Line	Implication
Energy Losses	~(4.65-13.3) % of power	~ 0.647% of power	HTS line spares control, diminishing operational costs.
Efficiency	(86.67-95.67% (Limited by conductor & thermal limits)	99.35% (improved capacity without building new lines)	HTS lines guarantee near perfect productivity, progressing framework execution.
system Complexity	Low (mature technology, passive cooling)	High (active cryogenic cooling systems needed)	HTS requires skilled personnel, O&M logistics
Voltage Drop	Significant	Minimal	HTS lowers voltage loss and removes the need for equipment that controls voltage levels.
Environmental Impact	Higher emissions and material usage	Lower emissions and material usage	HTS lines help meet sustainability goals and lessen damage to the environment.
Economics	Capital: \$10.2 - \$15 Operational: around \$50,000	Capital: \$90.7 - \$110.48 million Operational: \$0.8085 - \$1.752 million Payback: 45 – 65.5 years	HTS viable where energy loss reduction is valued over long term, depends on electricity prices.

The power transfer through a 15.3 km HTS transmission system, the findings show that total electrical losses are substantially dependent on the number of superconducting (YBCO) tapes used per phase. At 132 kV, the line current is low, and thus the design can be made more compact with fewer tapes within the acceptable loss limits. In this case, the total AC loss for all phases is approximately 0.8918 W/m. The 33 kV system, on the other hand, has to draw a higher current to transmit the same power, thus requiring a greater number of tapes to distribute effectively the current and avoid quenching. Although the occupied volume and current within the conductor are increased, losses are significantly more, reaching 13.41 W/m. This size of the design also leads to less need for additional equipment that permits transporting a high current in small voltage.

In addition to its compact design and high current capacity of 2013 A per phase, the 33 HTS system offers significant energy savings at low loads. However, compared to the 132 kV HTS system, which has lower energy losses, these advantages are offset by higher expenses and greater cooling needs.

The YBCO-based HTS utility-scale power transmission cables are currently undergoing testing and demonstration after the previous testing phase, which included distances from 100 meters to 2.5 kilometers. The increase in the length of the HTS cable would be a significant boost to the infrastructure.

Hypothetically, exchange is technically feasible but not economically possible because of the enormous operational and capital costs that do not allow a reasonable return. One of the challenges regarding cooling is that one of the most important and hard barriers is data.

Chapter Five

5. Conclusion and Recommendation

5.1 Conclusion

High-temperature superconducting (HTS) cables are emerging as effective alternatives to traditional large-capacity transmission cables, providing improved power transmission with minimal losses. The thesis aims to implement HTS technology in practical applications while promoting its further development.

A study has been developed and analyzed considering the HTS cable designed for integration into the Ethiopian power grid. The technical superiority and economic validity of the HTS cable were rigorously established through electromagnetic-thermal modeling and simulations using MATLAB, ANSYS FLUENT, and Dig SILENT. With various operating conditions, simulations were run on both the conventional and HTS transmission lines. The results of the simulations indicated that the replacement of conventional 132 kV lines with 132 kV HTS and 33 kV HTS cables reduces power losses, increases efficiency, and simplifies system design.

Magnetic field studies show distribution of screening currents and their effects on cable performance thus stressing HTS technology to mitigate energy losses. In-depth investigations into the other thermal and cooling systems reveal the need for maintenance of liquid nitrogen temperatures between 65 K and 77 K for steady superconducting operation. Four cooling stations should be impressed in the 15.3 km stretch. An optimized design based on those specific environmental conditions and load factors in Ethiopia will offer substantial improvements in operation.

The outcome indicates the reduction of power losses experienced with various scenarios, and the final verdict is that the exchange is technically feasible, but not economically since capital and operational cost payments lead to an absurd conclusion of 27 and 43 years longer for 132 kV and 33 kV system respectively. The design is compressed with fewer tapes within the permitted loss (0.8918 W/m) limit due to low line current at 132 kV. However, a 33 kV system requires more tapes to distribute current efficiently and avoid quenching, despite increased loss levels to 13.41 W/m.

Thus, providing a scalable implementation template for phased implementation in major corridors and industrial sites in Addis Ababa. In addition, strategically placed pilot projects and adaptive grid protection systems help to overcome challenges such as high upfront costs and cooling complexity to ensure smooth integration.

Eventually, a regulatory and operation compliance assessment concluded that HTS cables could serve as a plausible substitute for Ethiopia's existing transmission network, if the necessary adjustments to the infrastructure were made. Furthermore, this investigation reveals possibilities for improved grid efficiency and sustainability through the application of HTS technology, thereby laying the groundwork for future uses of superconducting power.

5.2 Recommendation

In the light of this study, the following recommendations have been formulated for facilitating an effective implementation and optimized use of HTS technology.

The ongoing research has included into the electromagnetic and thermal behavior of HTS, particularly considering the critical long-term effects of magnetic field exposure and alternating current (AC) losses in HTS cables. These factors ought to be understood in order to improve the technology and to have an optimum performance of the HTS systems in practical applications. To unlock the immense potential of superconducting technology, Exploring the development of a multifunctional, effective device that operates at room temperature and pressure in a risk-free environment holds the promise of transformative advancements in superconducting technology.

The integration of high-temperature superconducting (HTS) cables must strictly comply with the Ethiopian Electric Power (EEP) standards and regulatory requirements for this integration to be successful. This will entail developing guidelines for fault management and protection schemes that leverage the peculiar electrical characteristics of HTS cables to create a safe and efficient power infrastructure for all.

- To ensure that HTS cables are integrated into energy infrastructure, first test smaller HTS segments for feasibility; assess their suitability for scale-up; and build in-house expertise to facilitate urban and renewable grid initiatives in Ethiopia.
- Examining the line's performance under fault conditions and optimizing the design of its cooling system present valuable opportunities for further research and improvement.

Comprehensive lifecycle cost analyses are crucial for demonstrating the significant long-term savings achieved with our solutions in comparison to conventional cables.

- This approach offers financial advantages and builds stakeholder confidence through reduced losses and lower maintenance costs.

Africa has the potential to transform its role in the deployment of HTS cables, which could greatly enhance energy security, grid resilience, and sustainability. To address all technical and financial hurdles, strategic partnerships, well-planned stages of implementation, and continuous innovation will be needed for the Ethiopian national electrification strategy and that of the continent.

REFERENCES

[1] Electronic structure and Fermi surfaces of the superconductive A3B compounds: A = V, Nb; B = Ga, Ge and Sn, received 30 March 2009, revised 5 May 2009, Accepted 9 May 2009, Available online 18 May 2009.by F. De la Cruz

[2] L. Er-Rakho, C. Michel, J. Provost, B. Raveau. "The Oxides La3-xLnxBa3Cu (II)5-2yCu (III)1+2yO14+y." Journal of Solid-State Chemistry 37 (1981): 151-156.

[3] Bednorz, J.G., Müller, K.A. Possible highTc superconductivity in the Ba-La-Cu-O system. Z. Physik B - Condensed Matter 64, 189–193 (1986). https://doi.org/10.1007/BF01303701

[4] Nagamatsu, J., Nakagawa, N., Muranaka, T. et al. Superconductivity at 39 K in magnesium diboride. Nature 410, 63–64 (2001). https://doi.org/10.1038/35065039

[5] G. Wu, Y.L.Xie, H.Chen, M.Zhong, R.H.Liu, B.C.Shi, Q.J.Li, X.F.Wang, T.Wu, Y.J.Yan, J. J.Ying, X.H.Chen, Superconductivity at 56 K in Samarium-doped SrFeAsF, 5 Nov 2008

[6] Drozdov, A., Eremets, M., Troyan, I. et al. Conventional superconductivity at 203 kelvins at high pressures in the sulfur hydride system. Nature 525, 73–76 (2015). https://doi.org/10.1038/nature14964

[7] Snider, E., Dasenbrock-Gammon, N., McBride, R. et al. RETRACTED ARTICLE: Room-temperature superconductivity in a carbonaceous sulfur hydride. Nature 586, 373–377 (2020). https://doi.org/10.1038/s41586-020-2801-z

[8] Delft, D.A.van and Peter H.Kes. "The discovery of superconductivity." Physics Today 63 (2010): 38-43.

[9] Britannica, The Editors of Encyclopaedia. "BCS theory". Encyclopedia Britannica, 30 May. 2017, https://www.britannica.com/science/BCS-theory. Accessed 9 November 2023.

[10] J. Bardeen, L.N.Cooper*, and J.R.Schrieffer,"Theory of Superconductivity" J.Bardeen, L. N.Cooper, and J.R. Schrieffer Phys. Rev. 108, 1175 – Published 1 December 1957

[11] Gu, C. (2023). The co-production of normal science: A social history of high-temperature superconductivity research in China (1987–2008). Social Studies of Science, 53(1), 81-101. https://doi.org/10.1177/03063127221119215

[12] "Meissner effect | physics". Encyclopedia Britannica. Retrieved 22 April 2017.

[13] Huebener, R.P. The Path to Type-II Superconductivity. Metals 2019, 9, 682. https://doi.org/10.3390/met9060682

[14] Jones, Andrew Zimmerman. "Defining the Meissner Effect in Quantum Physics." ThoughtCo, Apr. 5, 2023, thoughtco.com/meissner-effect-2699258.

[15] Doukas D I 2019 Superconducting transmission systems: review, classification, and technology readiness assessment IEEE Trans. Appl. Supercond. 29 5401205

[16] Prusseit W and Bach R 2021 The Munich superlink project: toughening up city distribution grids with high voltage HTS cables Transform. Mag. 8 38–43

[17] Doukas, Dimitrios I. “Superconducting Transmission Systems: Review, Classification, and Technology Readiness Assessment.” IEEE Transactions on Applied Superconductivity 29 (2019): 1-5.

[18] Gouge M J, Cole M J, Demko J A, Fisher P W, Foster C A, Grabovickic R, Lindsay D T, Lue J W, Roden M L and Tolbert J C 2003 High-temperature superconducting tri-axial power cable Physica C 392 1180–5

[19] Nassi, M. (2000). Latest Developments of HTS Cable Systems in Europe and in the USA. In: Yamashita, T., Tanabe, Ki. (eds) Advances in Superconductivity XII. Springer, Tokyo. https://doi.org/10.1007/978-4-431-66877-0_243

[20] Weber, C.S. & Lee, Ron & Ringo, Steven & Masuda, Takato & Yumura, H. & Moscovic, Jon. (2007). Testing and Demonstration Results of the 350 m Long HTS Cable System Installed in Albany, NY. Applied Superconductivity, IEEE Transactions on. 17. 2038 - 2042. 10.1109/TASC.2007.899828.

[21] Maguire J F, Schmidt F, Bratt S, Welsh T E and Yuan J 2009 Installation and testing results of long island transmission level HTS cable 19 1692–7 IEEE Trans. Appl.Supercond.

[22] P. Cheetham, J. Viquez, L. Graber, C.H. Kim, H. Rodrigo and S.Pamidi, “Novel Design Concept and Demonstration of a Superconducting Gas-Insulated Transmission Line,” Applied Superconductivity, IEEE Transactions, pp 1-4, 2016.

[23] Stemmle, M., et al. "Ampacity project—advanced superconducting 10 kV system replaces conventional 110 kV cable system in city center." Proc. CIGRE. 2014.

[24] L. Chulhyu, S.Hyukchan, W.Youngjin, K.Youngwoong, R.Cheolhwi, P.Minwon and I. Masataka, “Progress of the first commercial project of high-temperature superconducting cables by KEPCO in Korea,” Supercond. Sci. Technol. 33 044006, pp1-9, February 2020.

[25] M. Guarnieri, “The Beginning of Electric Energy Transmission,” IEEE Industrial Electronics Magazine 7 (1): 57–60, Part 1, 2013.

[26] D.Kottonau, E.Shabagin, M. Noe and S. Grohmann, “Opportunities for High Voltage AC Superconducting Cables as Part of New Long-distance Transmission Lines,”IEEE Transactions on Applied Superconductivity, pp 1-5, 2017.

[27] T. Masaru, S.Kenji, F.Yusuke, I.Atsushi, A.Tomoyuki and K.Yusuke, “Energysaving railway systems based on superconducting power transmission”, pp1-30, January,2017.

[28] Hamabe M et al 2013 Status of a 200-meter DC superconducting power transmission cable after cooling cycles IEEE Transactions on Applied Superconductivity 23 3–6

[29] Zhang D et al 2013 Testing results for the cable core of a 360 m/10 kA HTS DC power cable used in the electrolytic aluminum industry IEEE Trans. Appl. Supercond. 23 10–13

[30] Yang B, Kang J, Lee S, Choi C and Moon Y 2015 Qualification test of a 80 kV 500 MW HTS DC cable for applying into real grid IEEE Trans. Appl. Supercond. 25 5402705

[31] HTS DC Transmission Line for Megalopolis Grid Development - Scientific Figure on ResearchGate. Available from: https://www.researchgate.net/figure/HTS-DC-cable-line-installation-in-the-St-Petersburgs-electrical-grid-project_fig1_263604100 [accessed 21 Nov 2023]

[32] Sytnikov, Victor & Bemert, S. & Sergey, Kopylov & Romashov, Maksim & Ryabin, T. & Shakaryan, Gegam & Lobyntsev, V. (2015). Status of HTS cable link project for St. Petersburg Grid. IEEE Transactions on Applied Superconductivity. 25. 1-4. 10.1109/TASC.2014.2373814.

[33] U. O. Michael and O. Uko, “Towards Solving the Problem Of Transmission And Distribution Of Electric Power in Nigeria Via Superconductor Power Cables,” pp 1-9, March 2012.

[34] S. Eliza, “A Green Energy Dream Grows in the Sahara,” Japanese academics plan an energy utopia in the Sahara complete with Superconductors and home brewed silicon photovoltaics, October 2011.

[35] Ryu K S, Jo Y S and Park M 2006 Overview of the development of the advanced power system by the applied superconductivity technologies program in Korea Supercond. Sci. Technol. 19 S102–8

[36] Doukas D I 2019 Superconducting transmission systems: review, classification, and technology readiness assessment IEEE Trans. Appl. Supercond. 29 5401205

[37] Mohammad Yazdani-Asrami et al High temperature superconducting cables and their performance against short circuit faults: current development, challenges, solutions, and future trends2022 Supercond. Sci. Technol. 35 083002

[38] Z. Wang, Z. Lv, P. Yu, Z. Li and B. Wang, "Research Status of High Temperature Superconducting Power Cable," 2022 IEEE International Conference on Electrical Engineering, Big Data and Algorithms (EEBDA), Changchun, China, 2022, pp. 182-186,

[39] Sato KI. High temperature superconductivity: Past, present and future. SEI Technical Review. 2010 Oct; 71:11-6.

[40] Sytnikov V, Kashcheev A, Dubinin M, Karpov V, Ryabin T. Test results of the full-scale HTS transmission cable line (2.4 Km) for the St. Petersburg project. IEEE Transactions on Applied Superconductivity. 2021 Mar 2;31(5):1-5.

[41] Ohya, Masayoshi et al. “Japan’s First Live Power Transmission Using 3-in-One Superconducting Cable (High-Temperature Supercon-ducting Cable Demonstration Project).” (2013).

[42] A.M. Sharaky, K.H. Hamed and A.B.Mohamed, “Model-based optimization for operating the Ethiopian renaissance dam on the Blue Nile River,” pp. 119-148, 2017

[43] M. Y. Sekitani, T and N. Miura, Measurement of the Upper Critical eld of Optimally-Doped Y Ba2Cu3O7 in Megagauss Magnetic Fields,New Journal of Physics, vol. 9, no. 47, pp. 111, 2007.

[44] H. Maeda, Y.Tanaka, M.Fukutumi, and T.Asano, A New High-Tc Oxide Superconductor Without a Rare Earth Element, Japanese Journal of Applied Physics, vol. 27, no. 2, pp. L209L210, 1988.

[45] P. Tixador, Development of Superconducting Power Devices in Europe,Physica C, vol. 470, pp. 971979, 2010

[46] Yazdani-Asrami M, Staines M, Sidorov G, Davies M,Bailey J, Allpress N, Glasson N and Gholamian S A 2019 Fault current limiting HTS transformer with extende

[47] Sadeghi A, Seyyedbarzegar S M and Yazdani-Asrami M 2021 Transient analysis of a 22.9 kV/2 kA HTS cable under short circuit using equivalent circuit model considering di

[48] J. Gerhold, "Power transmission", Handbook of applied superconductivity lOP Publishing Ltd 1998 pp1627-1689

[49] E. Peschke, R. V Olshausen, "Cable systems for high and extra-high voltage", Publicis MCD Verlagl989, pp 178-180.

[50] E.B.Forsyth, R.A.Thomas, "Performance summary of the Brookhaven superconducting power transmission systems", Cryogenics, Vo1.26, 1986, pp.599-614.

[51] Morandi, A., 2015. HTS dc transmission and distribution: concepts, applications and benefits. Superconductor Science and Technology, 28(12), p.123001.

[52] ruzek, C., Ballarino, A., Escamez, G., Giannelli, S., Grilli, F., Lesur, F., Marian, A. and Tropeano, M., 2017. Cable Conductor Design for the High-Power MgB2 DC Superconducting Cable Project of BEST PATHS. IEEE Transactions on Applied Superconductivity, 27(4), pp.1-5

[53] D. Giancoli, Electric Currents and Resistance, New Jersey: Physics for Scientists and Engineers with Modern Physics 2009

[54] S. R. Curras, J. Vina, M. Ruibal et al., "Normal-state resistivity versus critical current in YBa2Cu3O7-delta thin films at high current densities," Physica Superconductivity and Its Applications, vol. 372, pp. 1095-1098, Aug 1, 2002.

[55] Zhang X, Zhong Z, Geng J, Shen B, Ma J, Li C, Zhang H, Dong Q and Coombs T A 2018 Study of critical current and n-values of 2G hts tapes: their magnetic field-angular dependence J. Supercond. Nov. Magn. 31 3847–54

[56] Gapud A A, Feenstra R, Christen D K, Thompson J R and Holesinger T G 2005 Temperature and magnetic field dependence of critical currents in YBCO coated conductors with processing-induced variations in pinning properties IEEE Trans. Appl. Supercond. 15 2578–81

[70] E. H. Brandt and M. Indenbom, "Type-ii-superconductor strip with current in a perpendicular magnetic field," Phys. Rev. B, vol. 48, no. 17, Nov. 1993, Art. no. 12893.

[71] E.Zeldov, J.R.Clem, M.McElfresh, and M.Darwin, "Magnetization and transport currents in thin superconducting films," Phys. Rev. B, vol. 49, no. 14, pp. 9802–9822, Apr. 1994.

[71] W. T. Norris, "Calculation of hysteresis losses in hard superconductors carrying AC: Isolated conductors and edges of thin sheets," J. Phys. D, Appl. Phys., vol. 3, no. 4, pp. 489–507, 1970

[72] Mitchell N. et al. 2008. The ITER magnet system. IEEE Trans. Appl. Supercond. 18(2), 435–440

[73] E. H. Brandt, "Superconductors of finite thickness in a perpendicular magnetic field: Strips and slabs," Phys. Rev. B, vol. 54, no. 6, pp. 4246–4264,1996

[74] M. J. Kim et al. "Determination of maximum permissible temperature rise considering repetitive over-current characteristics of YBCO coated conductors". In: IEEE TRANSACTIONS ON APPLIED SUPERCONDUCTIVITY 18.2 (2008), pp. 660–663. doi:10.1109/TASC.2008.921397.

[75] Fesmire, J. E., Augustynowicz, S. D., & Demko, J. A. (2002a). Thermal insulation performance of flexible piping for use in HTS power cables. In Advances in Cryogenic Engineering (Vol. 47A, pp. 1533e1540). American Institute of Physics.

[76] Fesmire, J. E., Augustynowicz, S. D., & Demko, J. A. (2002b). Overall thermal performance of flexible piping under simulated bending conditions. In Advances in Cryogenic Engineering (Vol. 47A, pp. 1525e1532). American Institute of Physics.

[77] Okubo H, Hazeyama M, Hayakawa N, Honjo S, Masuda T. V-t characteristics of partial discharge

inception in liquid nitrogen/PPLP® composite insulation system for HTS cable.

[78] IEC 60071-1 Insulation co-ordination. Part 1: Definitions, principles and rules.

[79] J. Howe, B.Kehrli, F.Schmidt: "Very Low Impedance Superconductor Cables", A white paper, 2003

[80] NextBigFuture.com - Markets and Future Costs of Superconducting Magnets and Superconducting Wire. (https://www.nextbigfuture.com/2023/09/markets-and-future-costs-of-superconducting-magnets-and-superconducting-wire.html)

[81] Scientific Reports - Development and large volume production of extremely high current density YBa2Cu3O7 superconducting wires for fusion] (Molodyk, A., Samoilenkov, S., Markelov, A. *et al.* Development and large volume production of extremely high current density $YBa_2Cu_3O_7$ superconducting wires for fusion. *Sci Rep* **11**, 2084 (2021). https://doi.org/10.1038/s41598-021-81559-z)

[82] Scientific Reports - Ultra-High Performance, High-Temperature Superconducting Wires via Cost-effective, Scalable, Co-evaporation Process (Kim, HS., Oh, SS., Ha, HS. *et al.* Ultra-High Performance, High-Temperature Superconducting Wires via Cost-effective, Scalable, Co-evaporation Process. *Sci Rep* **4**, 4744 (2014). (https://doi.org/10.1038/srep04744)

[83] Zion Market Research - Global Superconducting Wire Market: Size, Trends, Forecast, 2024-2032] (https://www.zionmarketresearch.com/report/superconducting-wire-market)

[84] Watanabe, Hirofumi & Ivanov, Yury & Chikumoto, Noriko & Takano, Hirohisa & Inoue, Noriyuki & Yamaguchi, Satarou & Ishiyama, Kotaro & Oishi, Zenji & Koshizuka, Hiromi & Watanabe, Michihiko & Masuda, Takato & Hayashi, Kazuhiko & Sawamura, Toru. (2016). Cooling and Liquid Nitrogen Circulation of the 1000 m Class Superconducting DC Power Transmission System in Ishikari. IEEE Transactions on Applied Superconductivity. PP. 1-1. 10.1109/TASC.2016.2642578.

APPENDICES

Appendix A: The key technical parameters, performance characteristics, and specifications of YBCO

Parameter	Typical Values/Description
Superconductor Material	YBCO ($YBa_2Cu_3O_{7-x}$) coated on a flexible substrate (e.g., Hastelloy, stainless steel).
Critical Temperature (T_a)	~90 K (operates at 65–77 K with liquid nitrogen cooling).
Critical Current (I_a)	100–500 A/cm-width (depends on thickness, magnetic field, and temperature).
AC Losses	0.1–1 W/m at 50–60 Hz (lower than conventional cables).
Voltage Rating	30–138 kV (design-dependent).
Current Capacity	3–5 kA (for 40–50 mm width tapes).
Mechanical Strength	Tensile strain tolerance: ≤ 0.4%; Bending radius: 10–30 cm (flexible designs).
Cooling Requirements	Liquid nitrogen (LN_2) at 65–77 K, flow rate: 10–30 L/min for 1 km cable.
Dielectric Insulation	Cryogenic dielectric materials (e.g., PPLP, polypropylene).
Fault Current Tolerance	20–50 kA for 100 ms (requires integrated fault current limiters).

Appendix B: Calculated parameters for the overhead line conductor types(pu)

Bus-Bus			1-2 KI-ADC.	2-3 ADC-BL	1-2 KI-ADC 02.
Voltage (kV)			132	132	132
Conductor			Tiger	Tiger	Tiger
Config. Tower			Single	Single	Single
Cond No.			1	1	1
Positive Sequence	**R**	**pu/km**	0.00149564	0.00149564	0.00149564
	X	**pu/km**	0.00243515	0.00243515	0.00243515
	B	**pu/km**	0.0004669	0.0004669	0.0004669
Zero Sequence	**R0**	**pu/km**	0.0030200	0.0030200	0.0030200
	X0	**pu/km**	0.0068503	0.0068503	0.0068503
	B0	**pu/km**	0.0002881	0.0002881	0.0002881
Thermal rating	**Conductor**	**A**	357	357	357
	Circuit	**A**	357	357	357
		MVA	82	82	82
SIL	**Circuit**	**MW**	44	44	44

Appendix C: Grid Summary of HTS line

```
-------------------------------------------------------------------------------------------------------------------------------
| Grid: kality super        System Stage: kality super    | Study Case: Study Case               | Annex:                  / 1  |
-------------------------------------------------------------------------------------------------------------------------------
|          rated                        Active Reactive Power               |                                                  |
|         Voltage     Bus-voltage        Power   Power   Factor Current Loading|              Additional Data                     |
|          [kV]  [p.u.]    [kV]   [deg]   [MW]   [Mvar]    [-]    [kA]    [%]  |                                                  |
-------------------------------------------------------------------------------------------------------------------------------
|ADC_bb                                                                     |                                                  |
|  ADC_bb3333.00    1.00   32.86   -0.69                                    |                                                  |
|   Cub_1  /Lod      General Load(1)      45.00     14.79   0.95     0.83   |Pl0:     45.00 MW   Ql0:  14.79 Mvar              |
|   Cub_1  /Lne      ADC - black 33       55.00     18.08   0.95     1.02  101.72 |Pv:      0.62 kW   cLod:  0.00 Mvar L:    2.00 km|
|   Cub_1  /Lne      Line_kality-ADC    -100.00    -32.87  -0.95     1.85   92.47 |Pv:     13.85 kW   cLod:  0.00 Mvar L:   13.50 km|
|                                                                           |                                                  |
|Black_bb                                                                   |                                                  |
|  BB_black33.00    1.00   32.86   -0.69                                    |                                                  |
|   Cub_1  /Lod      Black_ld02           55.00     18.08   0.95     1.02   |Pl0:     55.00 MW   Ql0:  18.08 Mvar              |
|   Cub_1  /Lne      ADC - black 33      -55.00    -18.08  -0.95     1.02  101.72 |Pv:      0.62 kW   cLod:  0.00 Mvar L:    2.00 km|
|                                                                           |                                                  |
|Kality_bb01                                                                |                                                  |
|  BB_kality2.00    1.00  230.00    0.00                                    |                                                  |
|   Cub_1  /Xnet     external source     100.01     34.22   0.95     0.27   |Sk": 10000.00 MVA                                 |
|   Cub_1  /Tr2      Tr_kality230/33     100.01     34.22   0.95     0.27   42.28 |Tap:     0.00       Min:      0      Max:     0  |
|                                                                           |                                                  |
|Kality_bb02                                                                |                                                  |
|  Kality_bb3.00    1.00   32.87   -0.69                                    |                                                  |
|   Cub_1  /Lne      Line_kality-ADC     100.01     32.87   0.95     1.85   92.47 |Pv:     13.85 kW   cLod:  0.00 Mvar L:   13.50 km|
|   Cub_1  /Tr2      Tr_kality230/33    -100.01    -32.87  -0.95     1.85   42.28 |Tap:     0.00       Min:      0      Max:     0  |
|                                                                           |                                                  |
-------------------------------------------------------------------------------------------------------------------------------
```

```
-------------------------------------------------------------------------------------------------------------------------------
| Load Flow Calculation                                                                                          Grid Summary |
-------------------------------------------------------------------------------------------------------------------------------
|     AC Load Flow, balanced, positive sequence            |   Automatic Model Adaptation for Convergence          No         |
|     Automatic Tap Adjust of Transformers          No     |   Max. Acceptable Load Flow Error for                            |
|     Consider Reactive Power Limits                No     |     Nodes                                              1.00 kVA  |
|                                                          |     Model Equations                                    0.10 %    |
-------------------------------------------------------------------------------------------------------------------------------
-------------------------------------------------------------------------------------------------------------------------------
| Grid: kality super        System Stage: kality super    | Study Case: Study Case               | Annex:                  / 1  |
-------------------------------------------------------------------------------------------------------------------------------
| Grid: kality super        Summary                                                                                           |
|                                                                                                                             |
| No. of Substations     4         No. of Busbars        4         No. of Terminals      48         No. of Lines           2   |
| No. of 2-w Trfs.       1         No. of 3-w Trfs.      0         No. of syn. Machines  0          No. of asyn.Machines   0   |
| No. of Loads           2         No. of Shunts         0         No. of SVS            0                                     |
|                                                                                                                             |
| Generation           =       0.00  MW          0.00   Mvar      0.00  MVA                                                   |
| External Infeed      =     100.01  MW         34.22   Mvar    105.71  MVA                                                   |
| Inter Grid Flow      =       0.00  MW          0.00   Mvar                                                                  |
| Load P(U)            =     100.00  MW         32.87   Mvar    105.26  MVA                                                   |
| Load P(Un)           =     100.00  MW         32.87   Mvar    105.26  MVA                                                   |
| Load P(Un-U)         =       0.00  MW          0.00   Mvar                                                                  |
| Motor Load           =       0.00  MW          0.00   Mvar      0.00  MVA                                                   |
| Grid Losses          =       0.01  MW          1.35   Mvar                                                                  |
| Line Charging        =                        -0.00   Mvar                                                                  |
| Compensation ind.    =                         0.00   Mvar                                                                  |
| Compensation cap.    =                         0.00   Mvar                                                                  |
|                                                                                                                             |
| Installed Capacity   =       0.00  MW                                                                                       |
| Spinning Reserve     =       0.00  MW                                                                                       |
```

Appendix D: MATLAB Script for Temperature and Pressure Variation in Cryogenic Pipe.

%%%
%%%%%%%% %%%%%%%

```
% MATLAB Code: Cooling System for YBCO HTS Cable, Temperature and
Pressure Variation in Cryogenic Pipe

clc; clear; close all;

% Cable and Cooling System Parameters
L = 15.3e3; % Cable/ cryogenic length (15.3 km)
vsc = 1.55e-4; % dynamic viscosity (pa/cdotps)
k = 6.801; % area elevation and pessure drop safty
dx = 100; % Discretization step (100 m)
N = L/dx; % Number of steps

% Liquid Nitrogen Properties
cp = 2060; % Specific heat capacity (J/kgÂ·K)
rho = 810; % Density of liquid nitrogen (kg/mÂ³)
D = 0.04; % Pipe diameter (m)
vt = 0.612; % Flow velocity (m/s)
P0 = 25e5; % Initial pressure (Pa, 25 bar)
T0 = 65; % Initial temperature (K)

% Range of Flow Velocities for pressure
vp_values = linspace(0.3, 1.5, 5); % Flow velocities from 0.5 m/s to
1.5 m/s

% Define Different Mass Flow Rates for Comparison of temp
mass_flow_rates = [0.4, 0.623, 1.0]; % Low, Medium, High (kg/s)
colors = ['r', 'g', 'b']; % Plot colors

% Temperature Profile Plot
figure; hold on;

for j = 1:length(mass_flow_rates)
    m_dot = mass_flow_rates(j); % Set mass flow rate

    % Initialize Temperature and Pressure Arrays
    T = zeros(1, N);
    P = zeros(1, N);
    T(1) = T0;
    P(1) = P0;

    % Power Dissipation Parameters
    B = 1.5; % Magnetic field strength (T)
    J_c0 = 3.5e9; % Critical current density at 65K (A/mÂ²)
    T_c = 92; % Critical temperature (K)
    n = 3.564; % Empirical factor
    v_f = 1e-7; % Vortex velocity (m/s)
```

```
    f_AC = 50; % AC frequency (Hz)
    C_h = 5e-5; % Hysteresis loss constant (YBCO-specific)
    C_e = 1e-5; % Eddy current loss constant (YBCO-specific)

    % Loop Through Cable Length
    for i = 1:N-1
        % Temperature-Dependent Critical Current
        J_c = J_c0 * (1 - (T(i) / T_c))^n;

        % Loss Calculations (W/m)
        E = v_f * B; % Electric field from vortex motion
        P_flux = J_c * E; % Flux flow loss
        P_hyst = C_h * B^2 * f_AC * (1 - (T(i) / T_c)); % Hysteresis
loss
        P_eddy = C_e * B^2 * f_AC^2 * (1 - (T(i) / T_c)); % Eddy
current loss
        q_loss = P_flux + P_hyst + P_eddy; % Total power loss per
meter

        % Temperature Evolution (Euler method)
        dT = q_loss / (m_dot * cp); % dT per step
        T(i+1) = T(i) + dT * dx;

        % Prevent Temperature Exceeding 100K
        if T(i+1) > 100
            T(i+1) = 100;
        end
    end

    % Plot Temperature Evolution
    figure(1);
    plot((0:N-1) * dx / 1000, T, colors(j), 'LineWidth', 2);

end

% Initialize figure for pressure
figure; hold on;

% Loop over different flow velocities
for v = vp_values
    P = zeros(1, N); % Initialize Pressure Array
    P(1) = 25e5; % Initial pressure (Pa, 25 bar)
    Re = (rho * v * D)/vsc; % determine the Reynolds number
    % Loop Through Cable Length
    for i = 1:N-1

        f = 0.316 * Re^-0.25;  % Empirical velocity-dependent friction
factor

        % Compute Pressure Drop Using Darcy-Weisbach Equation
        dP = -(f / D) * (rho * v^2 / 2) * dx; % Pressure drop per
segment
```

```
        % Update Pressure with a nonlinear adjustment
        P(i+1) = P(i) + dP * (1 + 0.02 * (v - 0.5))*k; % Small
correction for nonlinearity
    end

    % Plot Pressure for each Flow Velocity
    plot((0:N-1) * dx / 1000, P / 1e5, 'LineWidth', 2);
    hold on;
end

%  plot pressure
xlabel('Cable Length (km)');
ylabel('Pressure (bar)');
title('Pressure Drop Profiles for Different Flow Velocities');
legend(arrayfun(@(v) sprintf('v = %.2f m/s', v), vp_values,
'UniformOutput', false));
grid on;

% Final Temperature Plot Formatting
figure(1);
xlabel('Cable Length (km)');
ylabel('Temperature (K)');
title('Temperature variation in YBCO Cooling');
legend('Low Flow (0.4 kg/s)', 'Medium Flow (0.623 kg/s)', 'High Flow
(1.0 kg/s)');
grid on;
```

Appendix E: 132kv Transmission power line loss summary in Addis Ababa

No	Transmission Line Name		AVERAGE LOSS(MW)	AVERAGE LOSS(%)
1	ADDEAST-II	COTEBEI-I	4.3	11.9
2	B.WGN-TP	KALITI1	2.1	5.3
3	COTEBEI-I	ADDIS-E1	1.4	3.2
4	COTEBEI-I	AYAT	1.4	2.5
5	COTEBEI-I	BOLE-LEMI TP	5.9	23.6
6	SULULTA	DANGOTE	0.7	3.0
7	LEGETAFO	AYAT	2.0	3.5
8	LEGETAFO	DEBRE BERHAN	0.7	2.2
9	SHEGOLE	GEFERSA	19.4	65.6
10	SHEGOLE	MINILIK TS	0.7	1.9
11	ADDIS-NORTH	MINILIK TS	0.3	0.8
12	GEFERSA	KALITI1	1.1	5.4
13	GEFERSA	SEBATA -I	1.8	4.0
14	ADDISCENTER	KALITI1	13.8	45.7
15	GOFA	MEKANISA	0.3	1.0
16	KALITI1	KALITI TWO	4.0	11.2
17	KALITI1	KLT.N-TP	1.9	5.7
18	KALITI1	MEKANISA	2.8	7.4
19	KALITI1	YESU	7.6	48.4
20	KALITI1	GELAN	3.1	9.9
21	KALITI1	KALITI GIS	6.6	16.8
22	KALITITWO	NEFASILK	0.7	1.4
23	KALITITWO	KALITI GIS	0.6	1.9
24	MEKANISA	SEBATA -I	1.2	3.1
25	YESU	GELAN	12.8	56.2
26	GELAN	ELALA-TP	6.0	18.6
27	GELAN	DBZT2-TP	18.8	36.3
28	GELAN	KNORIA TEX	0.3	8.7
29	SEBATA-I	ADDIS WEST 2	0.4	0.7
30	SEBATA-I	BLACK-LION	1.3	2.6

Appendix F: The power loss in HTS AC transmission cables fundamental equation

HTS cables incur some losses, can be approximated as the sum of:

$$P_{total} = P_{hys} + P_{magnetization} + P_{coupling} + P_{insulation} + P_{eddy} \qquad (4.\ 8)$$

The primary factor in the HTS layer is typically hysteresis loss, which is non-linear and depends on both the current amplitude and frequency.

$$P_{hys} = \frac{\mu_0 {I_c}^2 \mathrm{f}}{\pi}\left[(1-\beta)ln(1-\beta) + \beta - \frac{\beta^2}{2}\right]$$

Where; $\mu_0 = 4\pi \times 10^{-7}$ H/m (permeability of free space), P_{hys}: Hysteresis loss per unit length (W/m, usually per phase for 3-phase cables), $\beta = I_t/I_c$: Normalized transport current, where I_t is the RMS current (503 A/phase) and I_c critical current (contributing 80 - 90% of the total AC loss)

$$P_{eddy} = \frac{(\omega B_m)^2 d^2}{2\rho}\ .\mathrm{V}$$

Where; ω: Angular frequency, B_m: Peak magnetic field (~0.01 - 0.05 T for YBCO at 503 A), d: Stabilizer thickness (~ 0.1 - 0.2 mm, i.e., copper/silver), ρ: Stabilizer resistivity (~2 × 10^{-8} Ω·m for copper at 77 K), V: Volume per meter of stabilizer.

$$P_{coup} = \frac{\omega^2 \tau {B_m}^2}{2\mu_0}.V_c$$

Where: τ: Coupling time constant (~1 - 10 ms for YBCO), V_c : Coupled volume per meter.

A thorough explanation of insulation loss and magnetization is given in Chapter 3.